



National Library
of Canada

Bibliothèque nationale
du Canada

Canadian Theses Service

Service des thèses canadiennes

Ottawa, Canada
K1A 0N4

NOTICE

The quality of this microform is heavily dependent upon the quality of the original thesis submitted for microfilming. Every effort has been made to ensure the highest quality of reproduction possible.

If pages are missing, contact the university which granted the degree.

Some pages may have indistinct print especially if the original pages were typed with a poor typewriter ribbon or if the university sent us an inferior photocopy.

Reproduction in full or in part of this microform is governed by the Canadian Copyright Act, R.S.C. 1970, c. C-30, and subsequent amendments.

AVIS

La qualité de cette microforme dépend grandement de la qualité de la thèse soumise au microfilmage. Nous avons tout fait pour assurer une qualité supérieure de reproduction.

S'il manque des pages, veuillez communiquer avec l'université qui a conféré le grade.

La qualité d'impression de certaines pages peut laisser à désirer, surtout si les pages originales ont été dactylographiées à l'aide d'un ruban usé ou si l'université nous a fait parvenir une photocopie de qualité inférieure.

La reproduction, même partielle, de cette microforme est soumise à la Loi canadienne sur le droit d'auteur, SRC 1970, c. C-30, et ses amendements subséquents.

THE UNIVERSITY OF ALBERTA
THE ORIGIN OF THE SUPERNORMAL PERIOD IN NEURONAL AND
CARDIAC MEMBRANE MODELS.

BY

EBENEZER NKETIA YAMOAH

A THESIS

SUBMITTED TO THE FACULTY OF GRADUATE STUDIES AND
RESEARCH IN PARTIAL FULFILMENT OF THE REQUIREMENTS
FOR THE DEGREE OF MASTER OF SCIENCE

IN

EXPERIMENTAL SURGERY

DEPARTMENT OF SURGERY

EDMONTON, ALBERTA

SPRING, 1989

Permission has been granted to the National Library of Canada to microfilm this thesis and to lend or sell copies of the film.

The author (copyright owner) has reserved other publication rights, and neither the thesis nor extensive extracts from it may be printed or otherwise reproduced without his/her written permission.

L'autorisation a été accordée à la Bibliothèque nationale du Canada de microfilmer cette thèse et de prêter ou de vendre des exemplaires du film.

L'auteur (titulaire du droit d'auteur) se réserve les autres droits de publication; ni la thèse ni de longs extraits de celle-ci ne doivent être imprimés ou autrement reproduits sans son autorisation écrite.

ISBN 0-315-52775-7

THE UNIVERSITY OF ALBERTA

RELEASE FORM

NAME OF AUTHOR EBENEZER NKETIA YAMOAHI

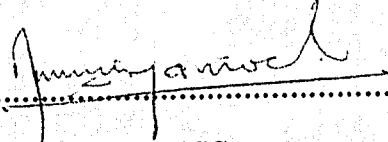
TITLE OF THESIS THE ORIGIN OF THE SUPERNORMAL PERIOD
IN NEURONAL AND CARDIAC MEMBRANE
MODELS.

DEGREE MASTER of SCIENCE.

YEAR THIS DEGREE GRANTED SPRING, 1989.

Permission is hereby granted to THE UNIVERSITY OF
ALBERTA LIBRARY to reproduce single copies of this thesis and to
lend or sell such copies for private, scholarly or scientific research
purposes only.

The author reserves other publication rights, and neither the thesis
nor extensive extracts from it may be printed or otherwise reproduced
without the author's written permission.

(SIGNED) 

PERMANENT ADDRESS:

..... POST OFFICE BOX 8140

..... KUMASI, GHANA

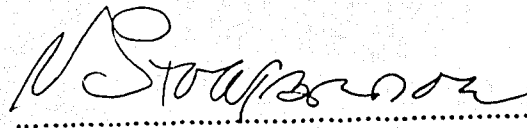
.....

.....

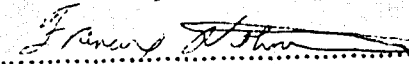
DATEDOctober.....1988

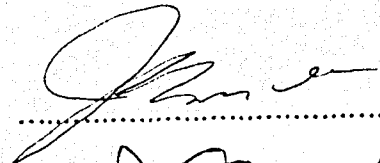
THE UNIVERSITY OF ALBERTA
FACULTY OF GRADUATE STUDIES AND RESEARCH

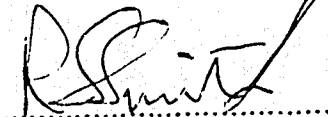
The undersigned certify that they have read, and recommend to the Faculty of Graduate Studies and Research, for acceptance, a thesis entitled THE ORIGIN OF THE SUPERNORMAL PERIOD IN NEURONAL AND CARDIAC MEMBRANE MODELS submitted by EBENEZER NKETIA YAMOAHA in partial fulfillment of the requirements for the degree of MASTER OF SCIENCE in EXPERIMENTAL SURGERY.


.....

Supervisor


.....


.....


.....

Date...12/10/88.....

ABSTRACT

The supernormal period is a time span following an action potential when a stimulus less than the steady state threshold can elicit a second action potential.

A recent report indicates that the Hodgkin and Huxley model for the squid giant axon predicts supernormality and that this results from slow potassium kinetics. The present study was undertaken to determine how common this mechanism was. Models for the crustacean motor neurons, frog myelinated nerve fiber, the ventricle and the Purkinje fiber were studied.

In the crustacean motor neuron model, supernormal excitability resulted from an undershoot of the transient potassium inactivation variable **B** during and following membrane action potential. Prevention of this undershoot in **B** abolished supernormal excitability with no effect on the shape of the action potential. Supernormality in the ventricular model resulted from afterdepolarization, secondary to an undershoot of a potassium current I_{x1} .

The frog myelinated nerve fiber and the Purkinje fiber models did not predict supernormality. However, the Purkinje fiber model showed a region of increased excitability in the refractory period of the membrane which resulted from increased sodium

conductance.

I conclude that supernormality, at least in the models that predict it, results directly or indirectly from an undershoot of a potassium conductance during the repolarization phase of the membrane. The reduction of potassium conductance at a period when the inward currents are back to their steady states means less depolarization is needed to generate a second action potential.

ACKNOWLEDGMENTS

One person alone cannot do all the work that goes into a thesis, and I have had more than my share of help. Norman Stockbridge, my thesis advisor, without his technical and scientific advice, the project never would have gotten off the ground. The other members of my thesis committee, Drs. Wayne Giles, Richard Smith, Frank Witkowski and James Russel provided invaluable advice in their fields of expertise. The thesis itself benefited substantially from the thoughtful reviews of all the thesis committee members.

Even if a student could finish a thesis without the friendship, encouragement, and support of those around him, it would not be worth it. All of my Christian families especially the Paynes and the Dyckerhoffs have made my stay in Edmonton a pleasure. I am also deeply grateful for the support and encouragement that Mrs. Olga Payne has given me. Finally Curtis has provided the encouragement I have needed to get through the final drudgery and frustrations.

Last, but most important, my father has given unfailing support throughout what he calls, an incredibly long academic career. I cannot remember a single time when he questioned the worth of what I was doing, even when I doubted it myself.

This thesis is dedicated to my father Frank Yamoah.

TABLE OF CONTENTS

ABSTRACT.....	i
ACKNOWLEDGMENTS	iii
LIST of FIGURES	vi
ABBREVIATIONS	viii
I. INTRODUCTION and LITERATURE REVIEW	1
<i>Objectives</i>	<i>16</i>
II. METHODS.....	17
<i>A. Numerical Methods</i>	<i>17</i>
<i>B. Threshold Test.....</i>	<i>18</i>
III. RESULTS	20
<i>A. CWM model.....</i>	<i>20</i>
1. <i>Causes of Supernormal excitability</i>	<i>20</i>
2. <i>Effect of repetitive firing on supernormal period</i>	<i>45</i>
<i>B. FH model.....</i>	<i>54</i>
<i>C. BR model.....</i>	<i>61</i>
<i>D. MNT model</i>	<i>75</i>
IV. DISCUSSION	88
<i>A. Supernormal period in the CWM model</i>	<i>88</i>
<i>B. Repetitive stimulation and SNP.....</i>	<i>92</i>
<i>C. FH model</i>	<i>93</i>
<i>D. BR model.....</i>	<i>94</i>
<i>E. MNT model.....</i>	<i>96</i>
<i>F. Future studies.....</i>	<i>99</i>

<i>G. Conclusion</i>	100
VI. REFERENCES	101
V. APPENDIX	113
<i>A. Outline of MAP Program</i>	113
<i>B. CWM model</i>	114
<i>C. FH model</i>	116
<i>D. BR model</i>	118
<i>E. MNT model</i>	120

LIST OF FIGURES

Figure	Page
CWM model.	
1. Placement of electrodes in extracellular recordings	4
2. Membrane action potential for the CWM model.....	22
3. Voltage and time dependent currents in the CWM model.....	24
4. State variables of the conductances in the CWM model	27
5. Time course of the leakage and supernormal period in CWM model	29
6. Assessment of the criteria for threshold.....	32
7. Effect of the Sodium and Leakage currents on the SNP.....	34
8. Effects of I_K on supernormal excitability (I).	37
9. Effects of I_K on supernormal excitability (II).	39
10. Elimination of -B- undershoot removes supernormality.....	41

11. Effect of B- undershoot on the conductance of I_A	44
12. Effect of varying interstimulus intervals on the SNP(I)	47
13. Effect of varying interstimulus intervals on the SNP (II).	49
14. Repetitive firing and the SNP (I).	51
15. Repetitive firing and the SNP (II).	53

FH model

16. Action potential of the FH model and the membrane currents	56
17. Action potential of the FH model and the membrane currents-detail representation.....	58
18. FH model does not exhibit supernormality.....	60

BR model

19. Action potential of the BR model.	63
20. Supernormality in the BR model and	

assessment of threshold test	65
21. Ionic currents in the BR model,	68
22. Effects of I_{Na} and I_s on the SNP,	70
23. Effect of I_{x1} and V_m on supernormality,	72
24. Afterdepolarization causes supernormality in the BR model,	74
MNT model	
25. Action potential of the MNT model and the period of relative excitability,	77
26. Time course of the ionic currents in the MNT model,	80
27. Effect of I_{x1} and I_{x2} on membrane excitability,	82
28. Effect of I_{K2} and I_{sl} on membrane excitability,	84
29. The relative excitability in the MNT model resulted from an increase sodium conductance,	87

ABBREVIATIONS

CWM model

Currents [$\mu\text{A}/\text{cm}^2$]

I_m	Total membrane current
I_{Na}	Sodium current
I_K	Potassium current
I_A	K transient current
I_L	Leakage current

State Variables [unitless]

m	Sodium activation
h	Sodium inactivation
n	Potassium activation- delayed rectifier
A	Transient potassium activation
B	Transient potassium inactivation

Equilibrium potentials [mV]

$E_{Na} = 55$	Sodium equilibrium potential
---------------	------------------------------

$$E_K = -72$$

Potassium equilibrium potential for I_K

$$E_A = -75$$

Potassium equilibrium potential for I_A

$$E_L = -49.402$$

Leakage equilibrium potential

Conductances [mmho/cm²]

$$\overline{g_{Na}} = 120$$

Peak Na conductance

$$\overline{g_K} = 20$$

Peak K conductance (I_K)

$$\overline{g_A} = 47.7$$

Peak K conductance (I_A)

$$g_L = 0.03$$

Leakage conductance

Rate Constants [ms⁻¹]

$$\alpha_m \quad \beta_m$$

$$\alpha_h \quad \beta_h$$

$$\alpha_A \quad \beta_A$$

$$\alpha_B \quad \beta_B$$

$$\alpha_n \quad \beta_n$$

Other variables

$$\Delta t$$

Integration time step [ms]

$$t$$

Simulation time [ms]

$$V_m$$

Membrane potential [mV]

FH model

Currents [$\mu\text{A}/\text{cm}^2$]

I_m	Total membrane current
I_{Na}	Sodium current
I_K	Potassium current
I_P	Nonspecific current
I_L	Leakage current

State Variables [unitless]

m	Sodium activation
h	Sodium inactivation
n	Potassium activation- delayed rectifier
p	Non specific potassium activation

Permeability [cm/s]

$\overline{P_p} = .00054$	Peak nonspecific permeability (I_p)
$\overline{P_K} = .0006$	Peak potassium permeability (I_K)
$\overline{P_{Na}} = .008$	Sodium permeability (I_{Na})

Other constants.

F = 96500

Faradays constant [coul/mol]

R = 8.314

Gas Constant [volt coul/K mol]

Concentrations [mM]

Na_o = 114.5

Sodium extracellular concentration

Na_i = 13.74

Sodium intracellular concentration

K_o = 2.5

Potassium extracellular concentration

K_i = 120

Potassium intracellular concentration

P_o = 114.5

External concentration of non-specific ion

P_i = 13.74

Internal concentration of non-specific ion

BR model

Currents [μ A/cm²]

I_{Na}

Sodium current

I_s

Calcium current

I_{K1}

Potassium current

I_{x1}

Another outward **K⁺** current

State Variables [unitless]

m	Sodium current state variable
h	Sodium current state variable
j	Sodium current state variable
d	Calcium current state variable
f	Calcium current state variable
x_1	Potassium current state variable I_{x1}

Equilibrium potentials [mV]

$E_{Na} = 50$	Sodium equilibrium potential
E_s	Calcium equilibrium potential

Conductances [mmho/cm2]

$\overline{g_{Na}} = 4$	Peak Na conductance [mmho/cm2]
$\overline{g_{Na_c}} = .003$	Leaky Na conductance [mmho/cm2]
$g_s = .09$	Peak Ca conductance [mmho/cm2]

Other variables

Ca_i	Intracellular Ca concentration [mM]
--------	-------------------------------------

MNT model

State variables [unitless]

m	Sodium state variable
h	Sodium state variable
d	Calcium state variable
f	Calcium state variable
q	Chloride state variable
r	Chloride state variable
x_1	Potassium current I_{x1} state variable
x_2	Potassium current I_{x2} state variable

Currents [$\mu\text{A}/\text{cm}^2$]

I_{Na}	Sodium current
I_{si}	Calcium current
I_{qr}	Chloride current
I_{K_2}	Potassium current
I_{x1}	Potassium current
I_{x2}	Potassium current
I_{K_1}	Background potassium current

I_{Na_b}

Background sodium current

I_{Cl_b}

Background Chloride current

Equilibrium Potential [mV]

$E_{Na} = 40.$

Sodium equilibrium potential

$E_{Cl} = -70$

Chloride equilibrium potential

$E_{si} = 70$

Calcium equilibrium potential

Conductances [mmho/cm²]

$\overline{g_{Na}} = 150$

Peak sodium conductance

$\overline{g_{si}} = .8$

Peak calcium conductance

$\overline{g_{qr}} = 2.5$

Peak calcium conductance

$\overline{g_{x_2}} = .385$

Peak potassium conductance

$\overline{g_{cl_b}} = .01$

Leakage conductance

$\overline{g_{Na_b}} = 0.105$

Leakage conductance

Other abbreviations

$g_{K_{Ca}}$

Conductance of calcium activated
potassium channel.

Ca_i

Intracellular calcium.

I. INTRODUCTION and LITERATURE REVIEW

Following the stimulation of a neuron or a muscle fiber with a suprathreshold stimulus (a stimulus which generates an action potential), there is a time span when further stimulation, regardless of strength, cannot elicit a second action potential. This is called the absolute refractory period. Following the absolute refractory period is the relative refractory period; during this period the threshold is increased. However, immediately after the relative refractory period a stimulus smaller than the steady state threshold can elicit a second impulse. This period is known as the **supernormal period (SNP)**. Subsequent to this period, a stimulus greater than or equal to the steady state threshold value will generate an action potential.

The simplest events involved in the generation of a membrane action potential in a space-clamped squid axon are as follows: Depolarization results in an initial increase in sodium conductance. The resulting inward current causes further depolarization and further increases in sodium conductance (sodium activation). Depolarization causes the potassium conductance to increase, but more slowly than the increase in sodium conductance. This outward current, along with the depolarization-dependent inactivation of the sodium current ultimately restores the membrane to its resting potential. The above description is very simplified. More than two ionic currents are involved in the

generation of most action potentials.

The refractory period has been well studied (Hodgkin & Huxley, 1952) and it is understood to result from sodium inactivation as well as potassium activation. The inactivated sodium conductance cannot reactivate until the membrane has repolarized. Until sodium inactivation has been removed, the membrane is absolutely refractory. The potassium conductance turns off slowly following membrane repolarization and the residual outward current is responsible for the relative refractory period.

The term supernormal period was coined by Adrian and Lucas (1912) who described the phenomenon in a nerve-muscle preparation. Later Adrian (1921) observed it in the frog myocardium. Subsequently, Hoff and Nahum (1938) described it in the mammalian ventricular muscle. This period of supernormal excitation has been observed in several kinds of invertebrate (Hodgkin, 1948; Zucker, 1973, 1974; Fuchs & Getting, 1980) and vertebrate (Adrian & Lucas, 1912; Adrian, 1921) nervous systems. In the mammalian central nervous system, this phenomenon has been described in efferents of the caudate nucleus (Kocsis & VanderMaelen, 1979), visual and somatosensory callosal axons (Swadlow & Waxman, 1976; Swadlow, 1985), olfactory peduncle axons (Ferryra-Moyano & Cinelli, 1986, Eng & Kocsis, 1987), fibers of the dorsal hippocampal commissure (Bartesaghi, 1987), parallel fibers in the cerebellum (Gardner-Medwin, 1971; Merrill *et al.*, 1978; Domich *et al.*, 1986), the brainstem (Rompre & Miliarexis, 1987) and lateral Lissauer tract (Merrill *et al.*, 1978). In the mammalian heart, the atrium,

the interatrial fibers (Agha *et al.*, 1972; Childer *et al.*, 1968), the His-Purkinje system (Spear and Moore, 1974; Hoffman & Cranefield, 1976) and the ventricles (Weidmann, 1955b; Goto, 1986 Paleev *et al.*, 1986; Chang, & Prystowsky, 1987) exhibit supernormal excitability.

Prior to the 1940s, direct measurements of the excitability of neurons and the heart were practically non-existent. What little that was known was derived from extracellular and surface electrode recordings. Electrodes were placed on the surface of a nerve-muscle preparation (Adrian, 1912) or, in the case of the heart, electrodes were attached to the myocardium in a way which minimized injury to the underlying tissue (Drury & Andrus, 1924; Lueken & Schutz, 1938).

Figure 1 demonstrates the method used to evaluate membrane excitability. At least four electrodes (S R_1 R_2 R_3) were placed on a nerve fiber or portions of the heart. Through S a specified current stimulus was applied. R_1 - R_3 were unipolar extracellular recording electrodes measuring the local potential with reference to a distant ground electrode (not shown in figure 1). R_1 was positioned close to S to record the local response to the stimulus. R_2 was also positioned within a space constant of S and was used to detect the response which the cells near the stimulation electrode generated.

The conduction time of the response was obtained by observing the difference in activation times between R_2 and R_3 . R_3 is positioned several millimeters away from R_2 . In some studies compartments were built around the electrodes to study localized effects of pH and drugs on

membrane excitability (Adrian, 1921, Schmitt & Erlanger, 1928).

Placement of electrodes in extracellular recordings

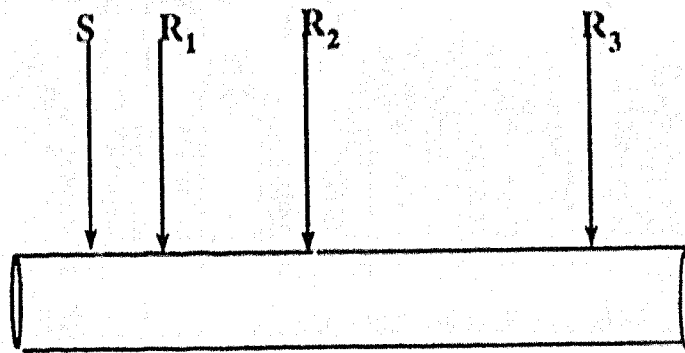


Figure 1. A schematic diagram showing how electrodes were positioned during membrane excitability measurements. S is the stimulating electrode and R_1 records the response to the stimulation. R_1 may be avoided if S is capable of stimulating and recording simultaneously. By recording from R_2 , the apparent threshold potential can be determined. The speed of conduction can be determined from the time taken for the impulse to propagate from R_2 to R_3 and the distance between them.

Most early workers on membrane excitability looked at the velocity of conduction rather than direct measurement of the stimulus magnitude needed to elicit a second impulse after membrane refractoriness. Using extracellular recordings, it was observed that low pH and increased extracellular potassium concentration enhanced membrane excitability as evidenced by increased conduction velocity, whereas high pH had no effect (Adrian, 1921; Schmitt & Erlanger, 1928).

Extracellular recordings gave answers to questions related to the timing and location of supernormal excitability but could not be used to measure the threshold current directly. Recently, intracellular recording has been the main approach to the study of membrane excitability. The same paradigm shown in figure 1 is employed, except that the electrodes are intracellular. Three electrodes are commonly used (Draper & Weidmann, 1951; Spear & Moore, 1974; Hoffman & Cranefield, 1976), since S is capable of stimulating and recording simultaneously. This approach has been more difficult to use on heart preparations than surface stimulation. The main problem arises from unstable electrode penetration due to muscle contraction upon stimulation (Cranefield *et al.*, 1957). Perhaps the most fruitful compromise has been to stimulate with surface electrodes and to record the resulting change in transmembrane potential with one or more intracellular microelectrodes (Hoffman & Cranefield, 1976). If care is taken to avoid distortion of the record of transmembrane potential by longitudinal current, this technique permits a determination of the effects of stimulating current on the transmembrane potential and makes it possible to observe the development of local

responses and propagated action potentials (Hoffman & Cranefield, 1976).

With intracellular electrodes, it has been possible to measure quantitatively the excitability of cells before and immediately after an action potential. Conduction velocities have also been measured accurately. As well, it has been possible to measure the input resistance of the membrane (Spear & Moore, 1974). A change in input resistance, by itself, is an ambiguous indicator of membrane excitability since the change can be in either inward or outward currents.

The SNP has been implicated as playing a physiological role in neural encoding (Kocsis *et al.*, 1979; Raymond & Lettvin, 1978) and in frequency-dependent conduction of action potentials in branched axons (Chung *et al.*, 1970; Kocsis *et al.*, 1979; Zucker *et al.*, 1986; Stockbridge & Stockbridge, 1988; Stockbridge, 1988). Also, Zucker (1973, 1974, 1986) has suggested the possible effects of the SNP on synaptic facilitation. He postulated that repetitive stimulation can cause the smaller axon terminals to become more excitable and that this can cause increased transmitter release.

A variety of results suggests the importance of the SNP in the heart as an explanation for some cardiac arrhythmias, *e.g.* Wolff-Parkinson-White Syndrome (Mark & Langendorf, 1950; McHenry *et al.*, 1966; Cranefield, 1977; Arndorf, 1977; Hoffman & Rosen, 1981). Mark & Langendorf (1950) argued that an abnormality in impulse initiation or conduction could trigger a second impulse propagation independent of the normal rhythm of the heart. *When during an action potential and where*

in the heart can an abnormal impulse be generated? They suggested that the probability of perturbing the rhythm of the heart by initiation of an extra impulse was higher during the SNP than at any other phase of an action potential. They and other authors as well (Hoffman & Cranefield, 1976, Moe *et al.*, 1968; Moe & Anzelevitch, 1987), have suggested that any region of the heart where the SNP has been observed is a potential site for abnormal impulse initiation.

This idea is originally attributable to Schmitt and Erlanger (1928) who performed experiments demonstrating reentry in isolated ventricular tissues. Using a multicompartiment tissue bath, they created segmental refractoriness in strips of turtle ventricle and assessed conduction by monitoring contraction along the various segments of the preparation. Depression of the distal end with high potassium followed by stimulation of the proximal end induced a contraction wave that propagated in the forward direction, giving rise to a contraction wave at the distal site that propagated in the retrograde direction leading to recurrent activation of the proximal end. Their interpretation of this observation was that the high potassium segment caused failure of anterograde conduction of the impulse while impulse conduction succeeded through an adjacent parallel pathway (Schmitt & Erlanger, 1928; Moe *et al.*, 1968; Moe & Anzelevitch, 1987). The successful propagation of an impulse through an adjacent parallel pathway depends on which phase of the membrane excitability the local current meets. If the local current arrives during the phase of membrane refractoriness, then it is unlikely an abnormal impulse would be initiated. However, if the SNP of the incoming impulse is met

by a local current from a branch or parallel fiber, then an abnormal impulse is more likely to be elicited.

Although functional roles of the SNP in nerve and muscle physiology have been suggested, the mechanism of this phenomenon remains somewhat unclear. Attempts have been made to find the causes for supernormal excitability (Stein, 1966; Spear & Moore, 1974; Barrett & Barrett, 1982) but all fall short of determining the actual ionic basis for this phenomenon.

Stein (1966) showed that the SNP was observed only coincident with the afterdepolarization phase of the Hodgkin & Huxley model of the squid axon action potential. Eight years later, Spear and Moore (1974) showed that action potentials in Purkinje fibers from the canine heart which showed a depolarizing afterpotential exhibited supernormality, while regions which had no afterdepolarization (His bundle and ventricle) did not. These findings also suggested that afterdepolarization may be related to the SNP. Perhaps the best attempt that has been made to find the cause of afterdepolarization was the work of Barrett and Barrett (1980). With intracellular recording of the frog sciatic nerve, they observed that altering different ion concentrations did not affect the depolarizing afterpotential. However, the voltage transient evoked by a hyperpolarizing current pulse had a slowly decaying component, and its time constant resembled that of the depolarizing afterpotential. On the basis of this observation, the afterdepolarization was attributed to the capacitive current that flows in the internodal portions of myelinated nerves.

Although these investigators have concluded that the afterdepolarization and the SNP were causally related, the afterdepolarization is not a requirement for supernormality, since there are cases where supernormality is present without an afterdepolarization, *e.g.* in crustacean motor nerves (Zar, 1974).

The inactivation of inward currents and activation of outward currents are responsible for the decreased excitability during the refractory period. The possible causes of enhanced excitability during the SNP are:

- (1) activation of an inward current;
- (2) reduction in the outward current or
- (3) afterdepolarization, possibly secondary to (1) or (2) above.

Recently, the SNP in the squid giant axon model (Hodgkin & Huxley, 1952) has been attributed to the slow kinetics of the delayed rectifier potassium current (Stockbridge, 1988). Stockbridge (1988) reported that the activation variable, n , undershoots its steady state value during the SNP. As a result, the outward current remains below its resting value for a period of time when the membrane potential and inward current variables have returned to their steady state values. As a consequence, there is a larger net inward current within this time span and a lower threshold.

It is unclear whether the recent explanation of the ionic basis for supernormality in the squid axon model applies to other neuron models or to models for cardiac action potentials. Other voltage and time

dependent potassium currents could cause supernormality if they had similar slow kinetics. In particular, the calcium-activated potassium current, whose recovery requires the reduction of the submembrane calcium concentration (Stockbridge, 1988), is a possible candidate. A chloride current with the appropriate kinetics (Owen *et al.*, 1986) could also cause supernormality. Supernormality could result from the afterdepolarization following a membrane action potential (Spear & Moore, 1974). The afterdepolarization might result from one of the suggested causes of supernormality or a prolonged calcium conductance as seen in some ventricles (Beeler & Reuter, 1977).

The study of the SNP and its origin in biological preparations is hindered by the difficulty in maintaining a microelectrode in a neuron or a contracting muscle fiber. This difficulty hinders one's ability to define the exact time span of the SNP and to do any ionic manipulations to document the ionic basis for its occurrence. Biological variation is also a potent problem which makes studies on the SNP difficult. As well, some experimental manipulations are impossible to do, *e.g.* clamping a state variable of an ionic current to its resting value during the course of an action potential (Stockbridge, 1988).

Descriptive equations of the membrane ionic currents of neurons and cardiac muscles have been formulated based on voltage clamp experimental results obtain by many investigators, *e.g.* the Connor, Walter & McKown (CWM, 1977) model for crustacean motor neurons, the Frankenhaeuser & Huxley (FH, 1964) model for frog myelinated axon, the McAllister, Noble & Tsien (MNT, 1975) model for Purkinje fibers,

the Beeler & Reuter (BR, 1977) model for ventricular myocardial fibers, and Noble's (1985) model for atrium and rat ventricular cells.

These models represent an extension of the Hodgkin & Huxley (1952) formalism for the ionic conductances which are functions of voltage and time, although significant new features were added to recreate the shape of the membrane action potential of the respective cell or fiber. Although, quantitative and perhaps qualitative changes in these models may be required as further investigation of the physiology of excitable membranes continues, the present models do recreate many of the electrical phenomena associated with ionic concentration changes, drug effects, shape of the respective action potentials and the changes in threshold following the action potentials (Sharp & Joyner, 1980). One way of studying membrane excitability is to use the formulated models and test for threshold to define the time span of the SNP and to investigate its etiology.

As a prelude to the quantitative description of the ionic currents an insight for the basis of the model would be relevant. The cell membrane is made up of a mosaic layer of a phospholipid bilayer and proteins. By virtue of its impermeability, the bilayer acts like a capacitor and can store electrical charges. Some of the membrane proteins act as ion-specific channels through which ions pass in and out of the cell passively following their electrochemical gradients. There are also protein pumps, some of which are electrogenic. The action of these pumps causes an unequal distribution of ions (charges), which creates a potential across the membrane. Upon stimulation the permeability of the membrane is

perturbed, channels open and ions (mostly sodium and calcium) flow into the cell. Other channels open to cause the efflux of positive charges (mostly potassium ions), ultimately bringing the inside of the membrane back to its negative resting potential.

In consequence of the capacitive nature of the membrane and the ensuing ionic currents, the total membrane current can be represented as the sum of the capacitive current and the total ionic current.

Thus:

$$I_t = C \partial V_m / \partial t + I_i$$

The ionic current can be divided into components carried by various ions. These currents can be classified as inward and outward currents. The inward currents principally are carried by sodium and calcium and the outward currents mostly by potassium. Some of the currents are mixed, *i.e.* carried by two or more ions. The ionic permeability of the membrane could be satisfactorily expressed in terms of conductance (Hodgkin and Huxley, 1952). Taking sodium current (I_{Na}) as an example:

$$I_{Na} = g_{Na}(V_m - E_{Na}).$$

The form of this equation applies to the other components of the ionic current. The formal representation of g_{Na} is:

$$g_{Na} = m^3 h \bar{g}_{Na}.$$

Rate constants for these variables are expressed as:

$$\partial m / \partial t = \alpha_m (1 - m) - \beta_m m,$$

$$\partial h / \partial t = \alpha_h (1 - h) - \beta_h h,$$

where the α 's and β 's are instantaneous functions of voltage. The rate constants are such that m increases with depolarization and thus represents sodium activation, while h decreases with depolarization and thus represents inactivation. Refer to the appendix for the quantitative description of the α s and β s of the state variables of the different ionic currents in the models discussed.

The models selected for the present studies have been listed above. The FH model describes the membrane action potential of frog myelinated nerves. This preparation is important since the idea of supernormality first arose from studying of frog myelinated nerve (Adrian & Lucas, 1912). Adrian (1921), proposed that the existence of a SNP might account for the type of nervous summation in which a series of impulses succeed in passing a region of imperfect conduction whereas a single impulse fails to do so - an observation made in the same preparation (Adrian & Lucas, 1912). Such differential conduction in myelinated nerves may contribute to memory encoding in the central nervous system of vertebrates (Kocsis & VanderMaelen, 1979; Kocsis *et al.*, 1979, Stockbridge, 1988). Presently, there are two models which describe action potentials in myelinated nerves: the Frankenhaeuser & Huxley model for amphibian nerve and the Chiu, Ritchie, Rogart and Stagg (CRRS, 1979) model for rabbit nerve. The CRRS model is based on more recent voltage clamp experiment on myelinated nerves. To date, the frog nerve-muscle preparation is the only case in which the SNP has been described in myelinated nerves. The FH model was therefore studied.

Supernormal excitability of the synaptic terminals of the crayfish motor neuron might be involved in the profound synaptic facilitation recorded at the neuromuscular junction (Zucker, 1974; Zucker *et al.*, 1986). For that reason the causes of the SNP in the CWM model for crustacean motor neuron and the correlation between repetitive firing and the SNP was ascertained.

Supernormal excitability in various regions of the heart is thought to play a role in some aberrant conditions observed in cardiac diseases. Afterdepolarization has been cited as a possible cause of supernormal excitability in the heart (Hoffman & Rosen, 1981) but this has not been shown directly. A detailed description of the mechanism of supernormality could lead to improved antiarrhythmic therapy. For this reason, the BR and the MNT models for ventricular and Purkinje fibers were investigated.

New and improved models appear in the cardiac electrophysiology literature almost every three years (Noble, 1984; Drouhard & Roberge, 1986). Old cardiac models do however, reproduce many gross features of action potential in these tissues and have been used to study drug effects (Sharp & Joyner, 1980) and conducted action potentials (Joyner & Capelle, 1986). Newer models are much more complex and include new currents, the effect of ion concentration changes and electrogenic pumps. As well, some of the names and descriptions of the ionic currents have been modified (Noble, 1984) to suit recent observations. However, looking at simple models to study the excitability of cardiac muscles is a reasonable first step. It will give an idea of what to look for

when more complex models are studied.

The nomenclature and description of the currents discussed in this thesis will be taken solely from the papers describing the models. These may appear different from more recent ideas. However, the older nomenclature has been used for reasons of consistency.

OBJECTIVES

The aims of this project were:

1. To compute action potentials using the neuronal and cardiac models of Connor, Walter and McKown (1977), Frankenhaeuser and Huxley (1964), Beeler and Reuter (1977), and McAllister, Noble and Tsien (1975).
2. To test for threshold following a membrane action potential and observe whether these models do predict supernormal excitability.
3. To determine the ionic current changes which cause the supernormal period in the models which demonstrate it.
4. To find the relationship between supernormal excitability and repetitive firing in the CWM model.

II. METHODS

A. Numerical Methods.

The equations describing the membrane ionic currents discussed in this paper are from the CWM (1977), FH (1964), BR (1977) and MNT (1975) models for crustacean motor neurons, frog (*Xenopus laevis*) myelinated nerve, ventricular and Purkinje fiber membrane action potentials respectively. The equations for each model are presented in the appendix. Basically, all the models represent an extension of the Hodgkin and Huxley (1952) formalism of the ionic conductances which are functions of voltage and time.

Solution of the simultaneous differential equations of the rate constants in each model was carried out with a Sun workstation using a numerical approximation (the Runge-Kutta method). A brief outline of the steps involved in the programs which generate membrane action potentials (Map; Stockbridge 1988) is presented in the appendix. Solutions for the rapid changes in the membrane potential occurring during the action potential were obtained using a time step of integration, Δt , of 0.05 ms. It was found that integration at shorter time steps did not produce an appreciably different result.

A table for the non-time-dependent variables was stored for each V_m in steps of 0.5 mV to speed up the integration (Stockbridge, 1988). All calculations were performed using IEEE double precision floating point arithmetic, which has about 12 significant digits.

To begin the computation in each model, the initial values for the state variables were set. This was done by setting the membrane potential to its resting value, setting state variables to their steady states and adjusting the leakage current so that the net membrane current was zero. All the models were stable at rest except the MNT model for Purkinje fiber action potential which was spontaneously active. Since no meaningful threshold test could be made with a spontaneously active membrane, the conductance $\overline{g_{Na,b}}$ of the leakage current $I_{Na,b}$ (inward background current) was adjusted to maintain a stable resting membrane potential of -80 mV.

The results of the computation were printed out every 0.1 ms. In addition to the membrane potential (V_m), the time (t), the state variables and individual ionic currents were printed out when required. Where appropriate, the ionic currents and the state variables were plotted on different sheets and then superimposed on the action potential plot.

B. Threshold Test

The program used for the threshold test was called th.c (Stockbridge, 1988). The stimulus was a rectangular current pulse of fixed duration. A threshold amplitude was found by a binary search technique which established 2-3 significant digits (Stockbridge, 1988). The criteria for defining an action potential were: a membrane

depolarization of at least 30 mV and positive first and second derivatives of the membrane potential.

The validity of the chosen criteria was tested by another simulation program that presented a second stimulus with a given timing, magnitude and width. The threshold obtained by the th.c program always gave an action potential of suitable amplitude and shape for the second action potential, while a 0.01% reduction in amplitude gave a much smaller response.

The CWM model was used to investigate the effects of repetitive firing on the SNP. This was effected by modifying the th.c program to generate a specified number of action potentials before the threshold test was initiated.

In the models in which the SNP was predicted, the time course of the ionic currents and state variables controlling those conductances were studied and the possible causes of supernormal excitability identified. Each possible candidate was separately assessed, usually by allowing the conditioning action potential to proceed normally. At some point in time prior to the onset of supernormal excitability, the candidate variable was reset to its steady state value and held there until the time came to test for threshold. At that time the variable was allowed to follow its normal course. Usually these changes had small effects on the shape of the late phase of the conditioning action potential. However, some of these changes eliminated supernormal excitability. In a few cases, changes in the variables were not to their steady state values, and these modifications are described where they apply.

III. RESULTS

A. CWM Model

1. Causes of Supernormal excitability.

Figure 2 presents the membrane action potential of crustacean motor neurons with different time scales (top and bottom traces). The resting membrane potential was -68 mV and the spike amplitude was about 100 mV. Detailed examination of the action potential waveform in the top panel showed a long phase of afterhyperpolarization following the spike. Recovery of the membrane potential to its resting level took about 30-40 ms. A more detailed representation of the rapidly changing phase of the spike waveform is shown in the bottom panel.

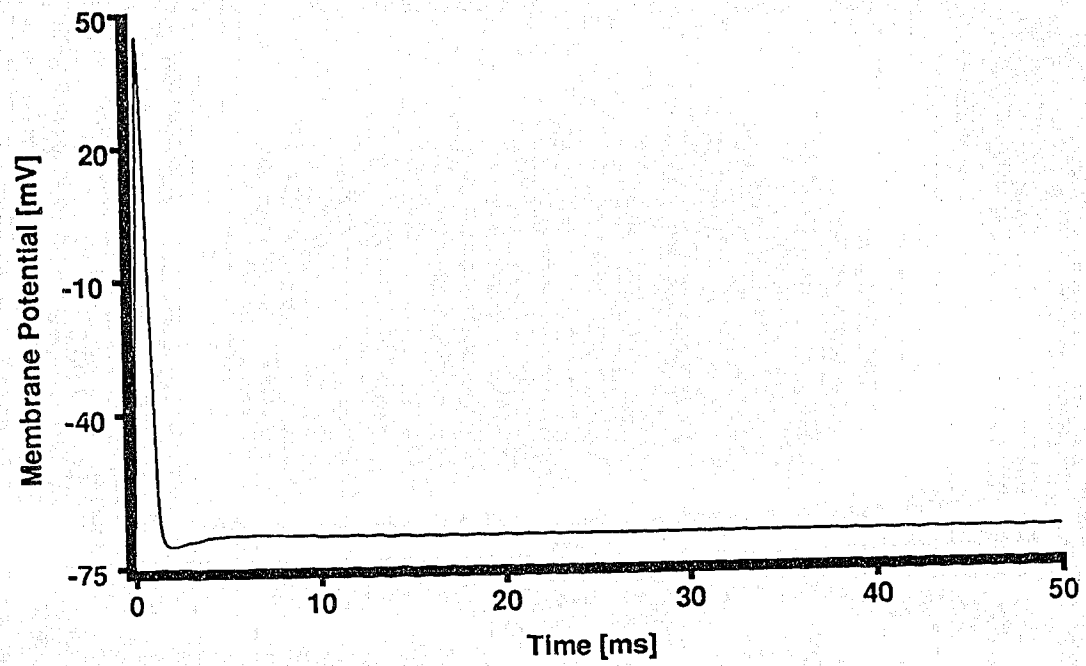
Shown in the top panel of figure 3 is the time course of the sodium current. The initial abrupt increase in the sodium current generated the spike of the action potential, and the activation state variable m rose much faster than the inactivation state variable h fell (see figure 3). Within about 0.5 ms however, the decrease in h was sufficient to reduce I_{Na} drastically, and in about 0.5 ms, the current settled to the steady state.

Next to the I_{Na} , the second current to turn on was the transient potassium current (I_A) which is presented in the bottom trace of figure 3. This current undershot its steady state value during the

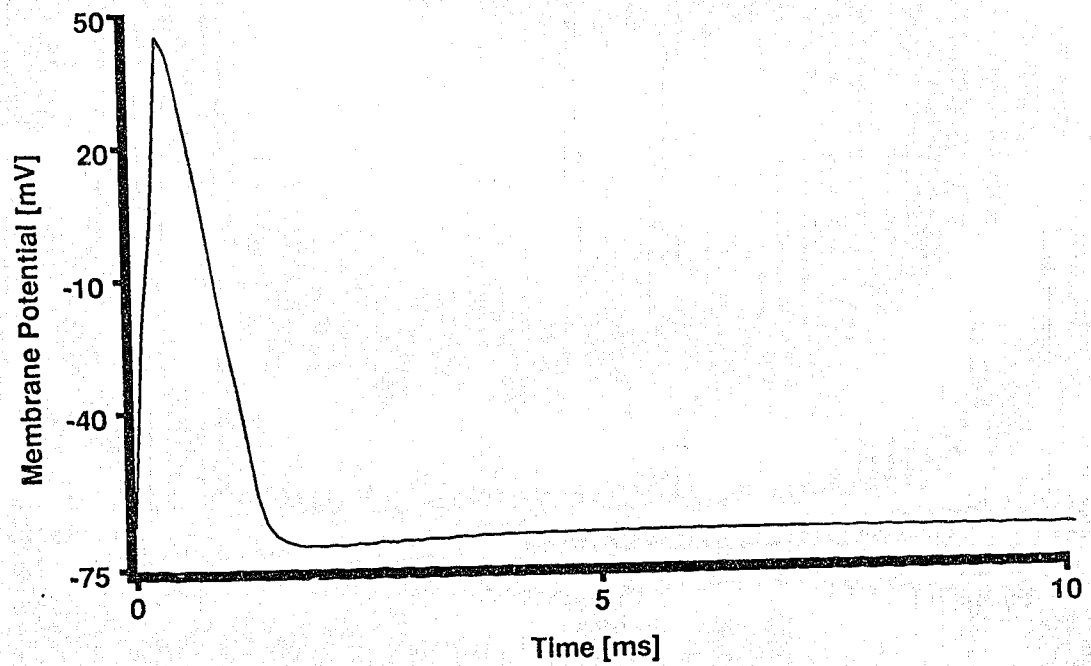
Membrane action potential for the CWM model.

FIGURE 2. The top trace shows the membrane action potential obtained with the Connor, Walter and McKown model for 50 ms time course. The lower trace shows a 10 ms time course of the same action potential showing the shape in more detail. The resting membrane potential was -68 mV and the action potential had an amplitude of over 100 mV. The action potential was generated with a current pulse of 0.1 ms duration. The shape closely resembles that in the CWM, 1977 paper. Note the long afterhyperpolarization which is obvious in the lower trace.

Action Potential [CWM]

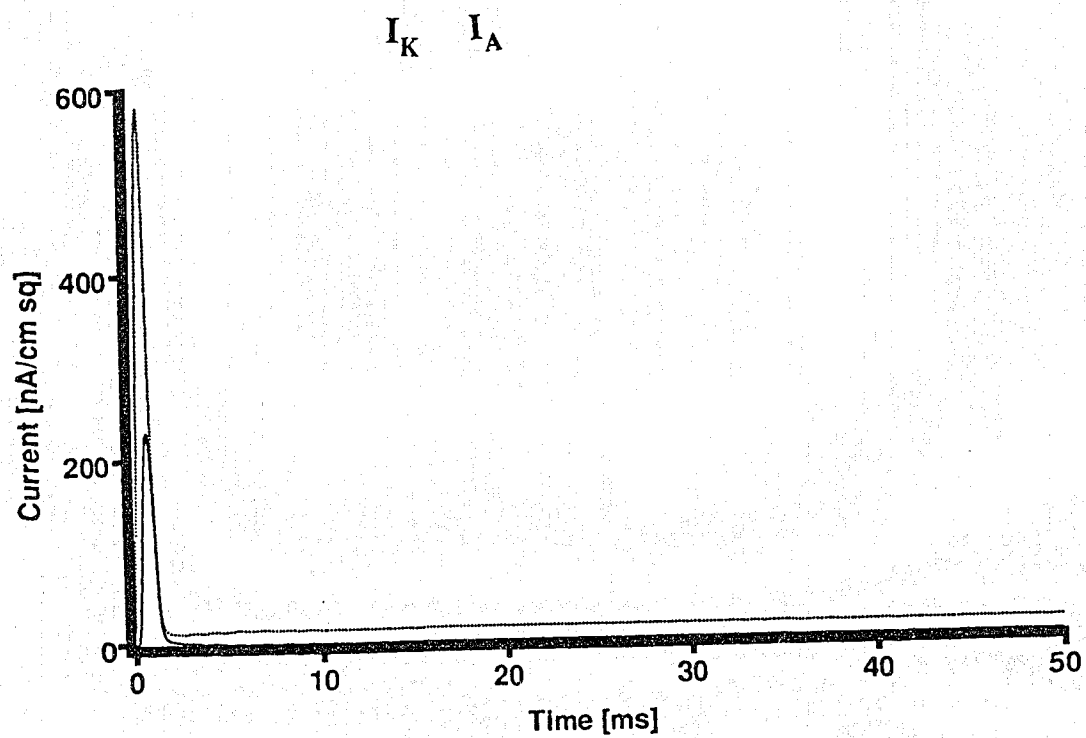
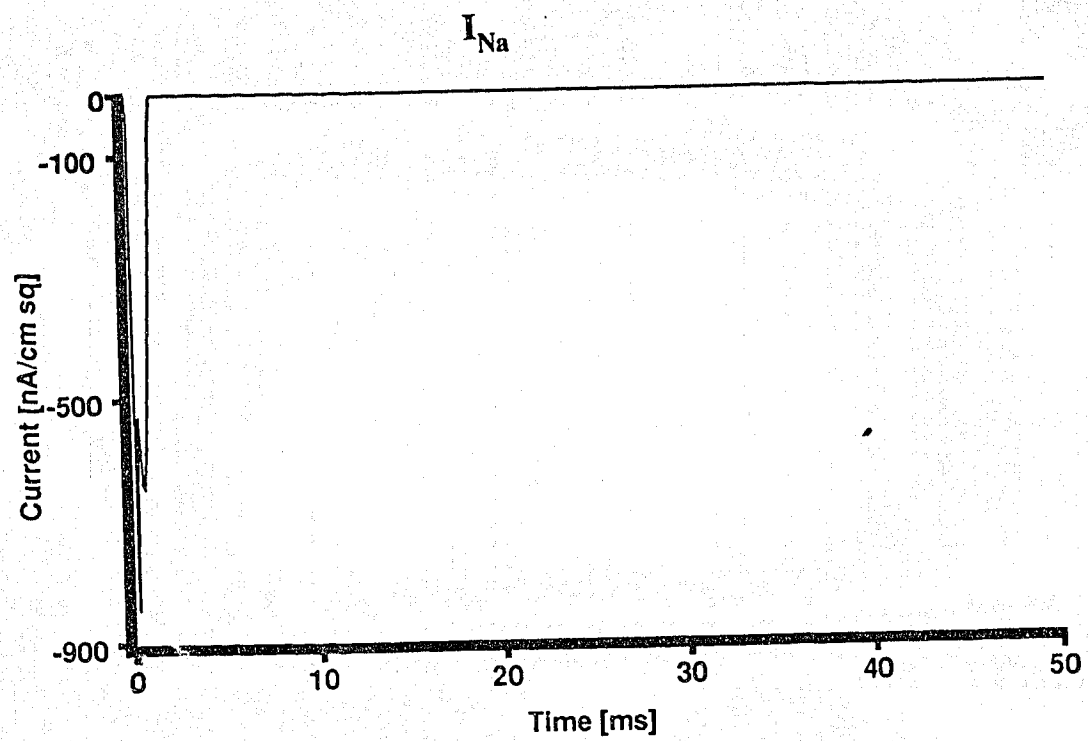


Action Potential [CWM]



Voltage and time dependent currents in the CWM model.

FIGURE 3. Top trace shows the sodium current. The sodium current (I_{Na}) increased abruptly and peaked twice before settling to its steady state. The effect of the I_{Na} on the membrane potential lasted for less than 2 ms. Shown on the lower trace are the two outward currents I_K (delayed rectifier potassium current)- solid line, and I_A (transient potassium current) in broken line. The I_A rose fairly early while I_K was rather delayed. Both currents fell to their steady states at the same time. However, there was a slight undershoot of I_A before it came back to its resting level.



afterhyperpolarization.

A similar undershoot of the potassium current has been shown previously to be the cause for supernormal excitability in the squid axon model (Stockbridge, 1988). However, in the squid axon model, the decrease in the potassium current was a result of an undershoot of the delayed rectifier conductance. The delayed rectifier in the CWM model did not exhibit such undershoot, as shown in the bottom trace of figure 3. Examination of the transient potassium conductance (g_{Na}) provided the reason for the undershoot. At about two milliseconds after the initiation of an action potential, there was a progressive decrease in the activation state variable **A** while the inactivation variable **B** undershot its steady state (figure 4, bottom trace). The result of this was that the conductance factor A^3B undershot the steady state (shown figure 9).

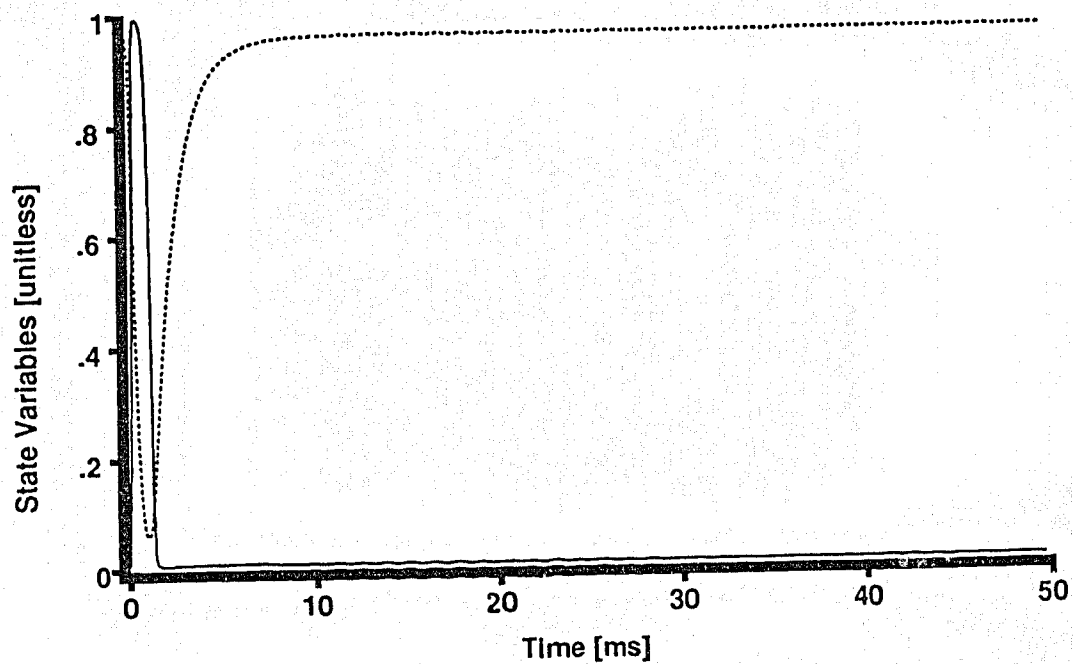
Presented on the upper trace of figure 5 is the leakage current (I_L). As expected, its shape resembled that of the action potential. The bottom trace of figure 5 shows results of the excitability determination, beginning 1 ms after the initiation of the conditioning action potential. The threshold for each test time was normalized by dividing the computed threshold by the steady state threshold (340.97 nA/cm²). These normalized values were plotted as relative threshold versus time.

A supernormal period was predicted by the CWM model. The SNP began about 2 ms after the initial stimulus and followed a period of relative refractoriness. Paradoxically, the SNP occurred during the membrane after hyperpolarization, when one would expect to be further

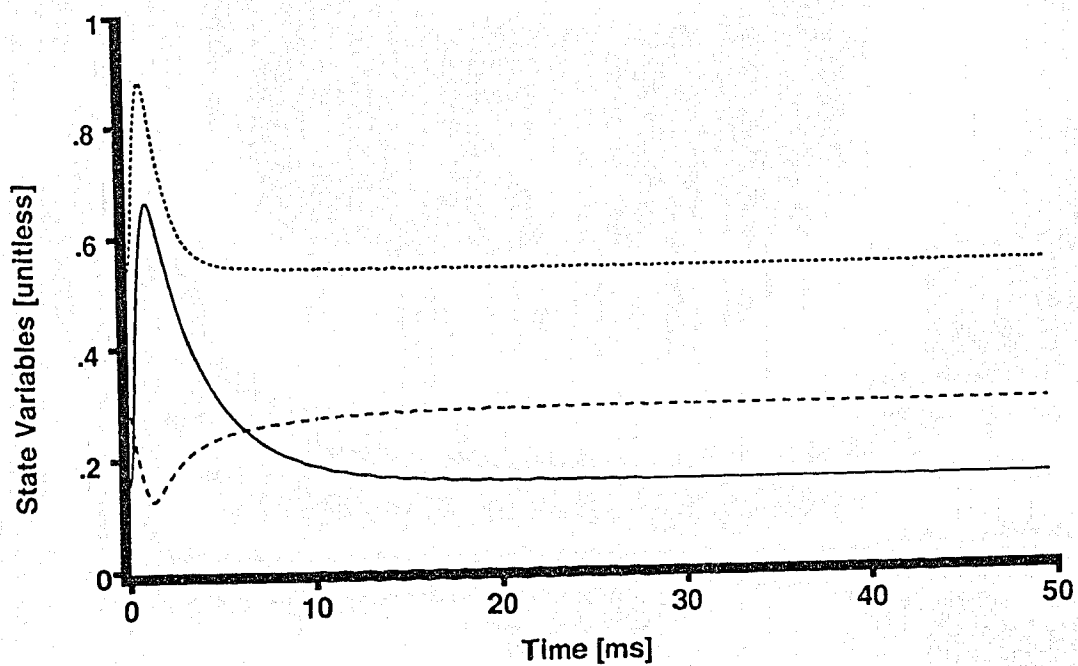
State variables of the conductances in the CWM model.

FIGURE 4. The state variables of all the currents were computed. Shown on the top trace is the sodium current state variables **m** (solid line) and **h** (broken line). The two crossings of **m** and **h** resulted in the double peak of I_{Na} . The solid line in the lower trace represents the time course of the **n** (solid line), **A** (fine dashed line) and **B** (coarse dashed line) variables for the outward currents, I_K and I_A . Note that the undershoot of the **B** variable lasted for about 40 ms before settling at its steady state.

State Variables [m,h]

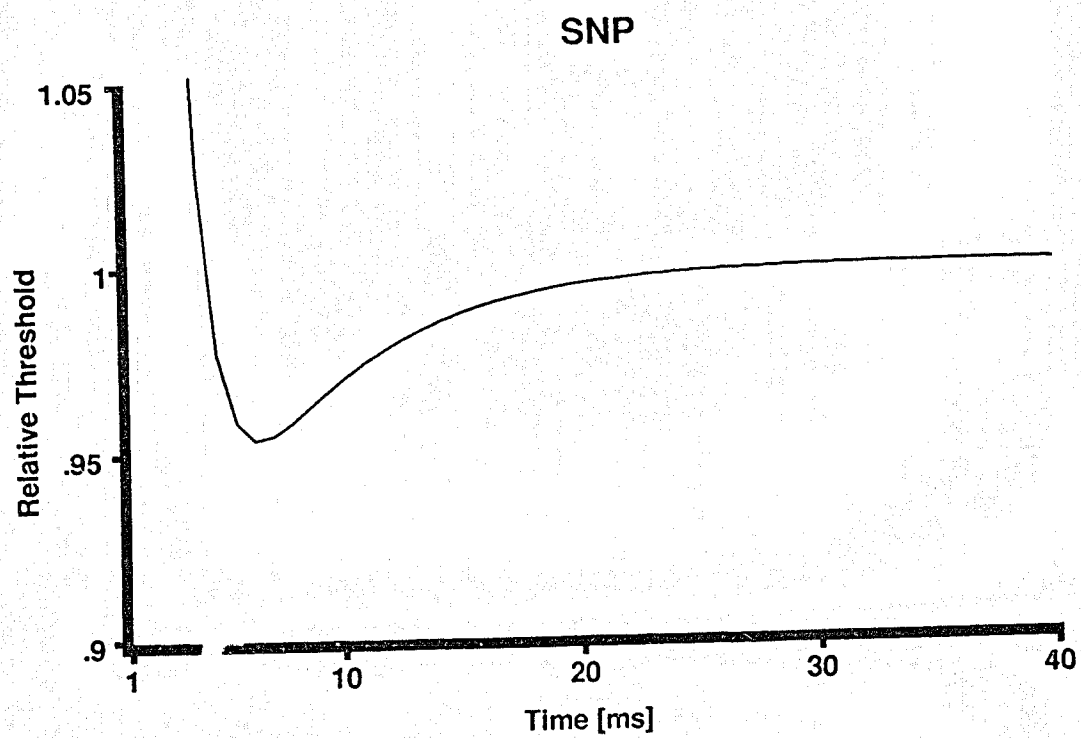
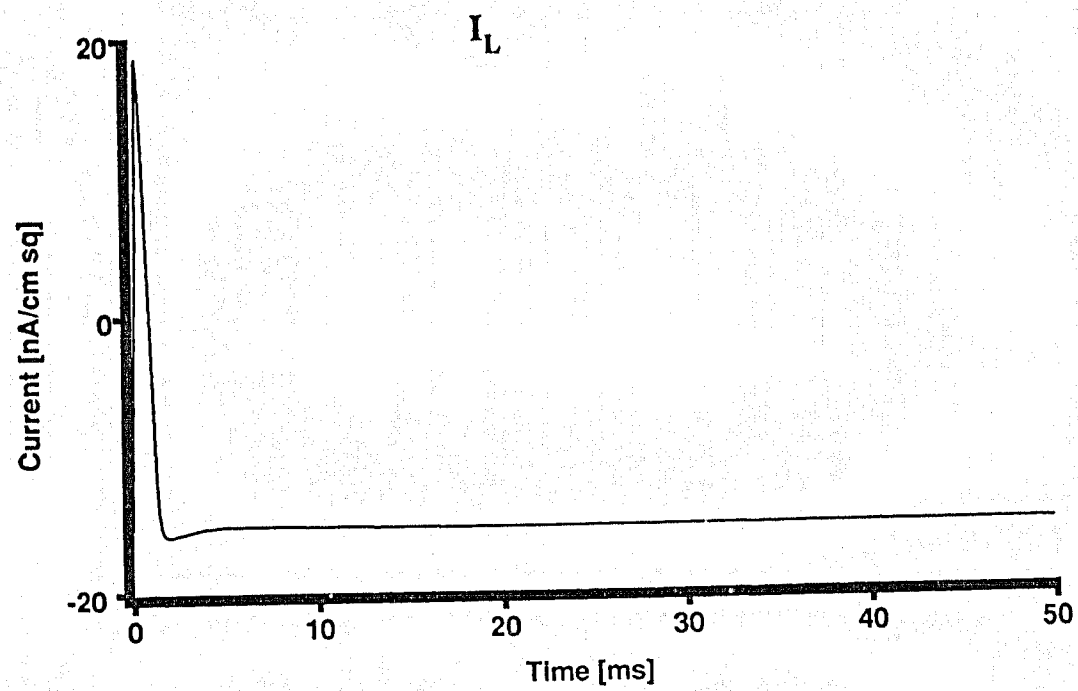


State Variables [n,A,B]



Time course of the leakage current and supernormal period in
CWM model.

FIGURE 5. A plot of the leakage current I_L is shown in the upper trace. It took the shape of the membrane action potential. Shown in the bottom trace is a representation of the excitability determination of the CWM model. The relative thresholds were obtained by dividing the computed threshold by the steady state threshold. A relative threshold of 1, therefore meant the steady state threshold and anything below 1 was supernormal. The notch in the curve showed the supernormal period.



from threshold. The observed SNP lasted for a very long period relative to the time course of the spike.

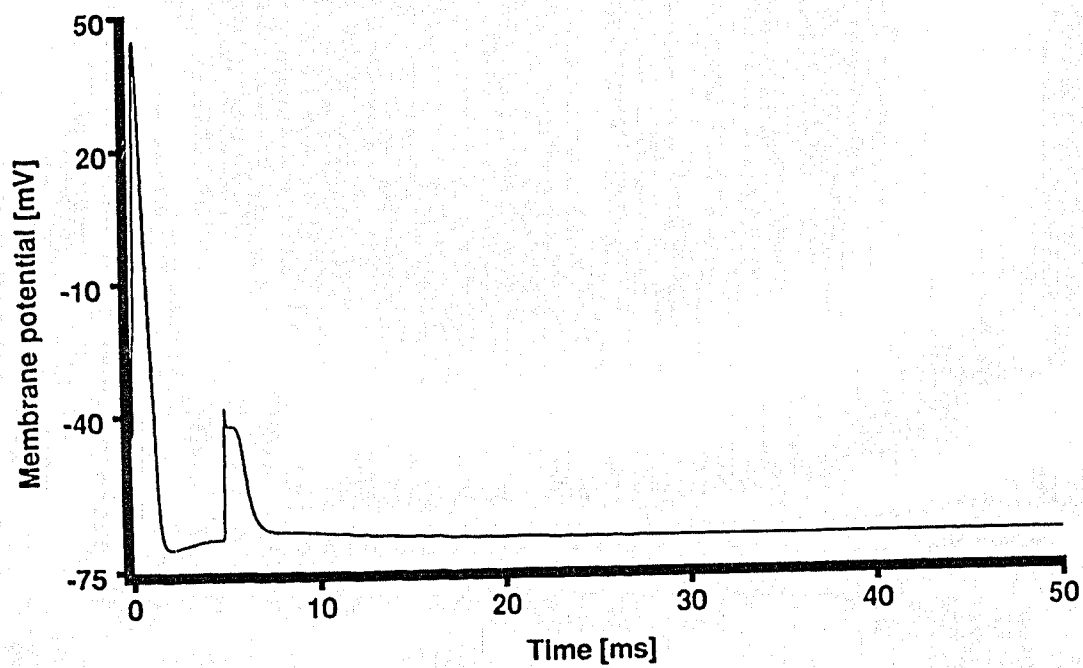
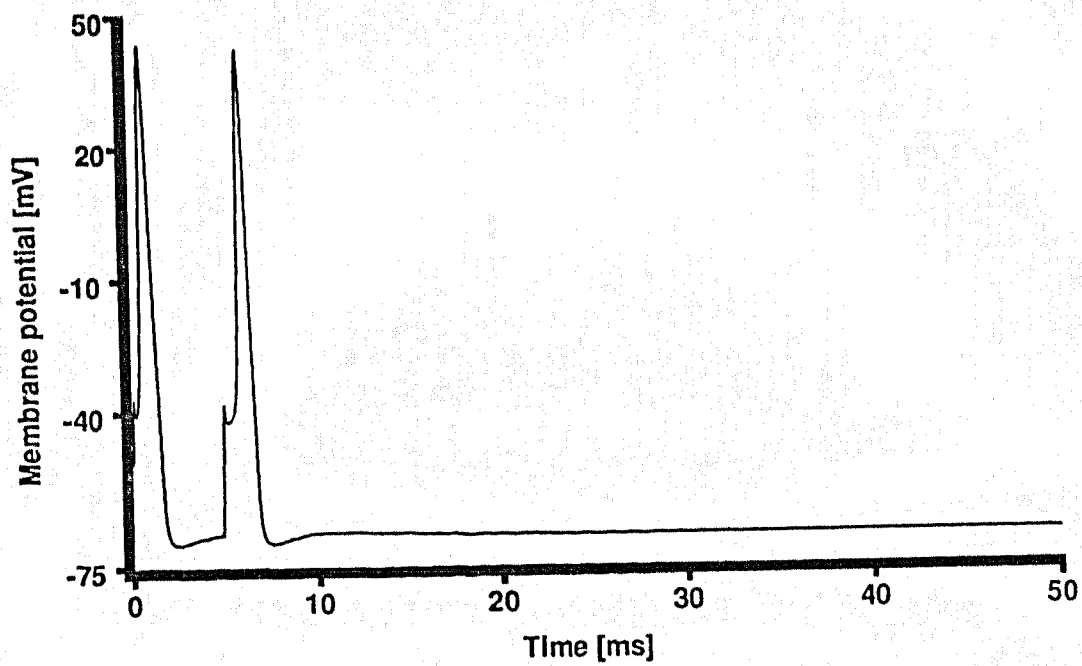
The SNP in the crustacean motor neuron has been described qualitatively as "a few milliseconds following an action potential or a train of spikes" (Zucker, 1974). Furthermore, little is known about the magnitude of the subthreshold stimulus normally used in live preparations. The present results provide an indication of the duration and the relative magnitude of stimulus required during the SNP.

Are the thresholds reported valid for the model? The validity of the criteria employed for threshold test was tested by using the appropriate threshold and stimulus width at 4.5 ms following an action potential. This was done using the program **2ap**. It can be seen from figure 6 that the chosen criteria were valid for the generation of an action potential. Under no circumstance did the computed threshold fail to generate a spike. However, it was observed that slight changes in either the stimulus width or the current failed to elicit a spike (figure 6 bottom trace).

What factors might be involved in the SNP observed in this model? This question was addressed by looking at the threshold while selectively manipulating one of the ionic currents and their state variables. Presented in figure 7 is the extent of supernormality when I_{Na} was set to its steady state 2 ms after the initiation of an action potential. Clearly, the SNP persisted although there is a slight decrease in excitability. The bottom trace shows the threshold curve obtained when I_L was treated as above. Supernormal excitability was enhanced under this condition. The

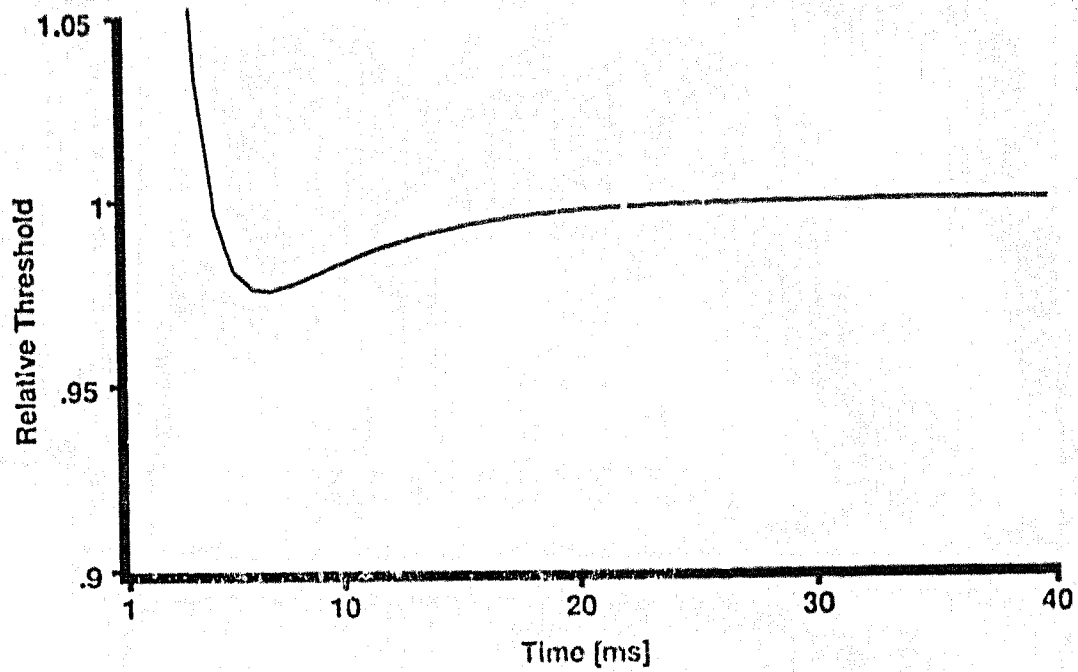
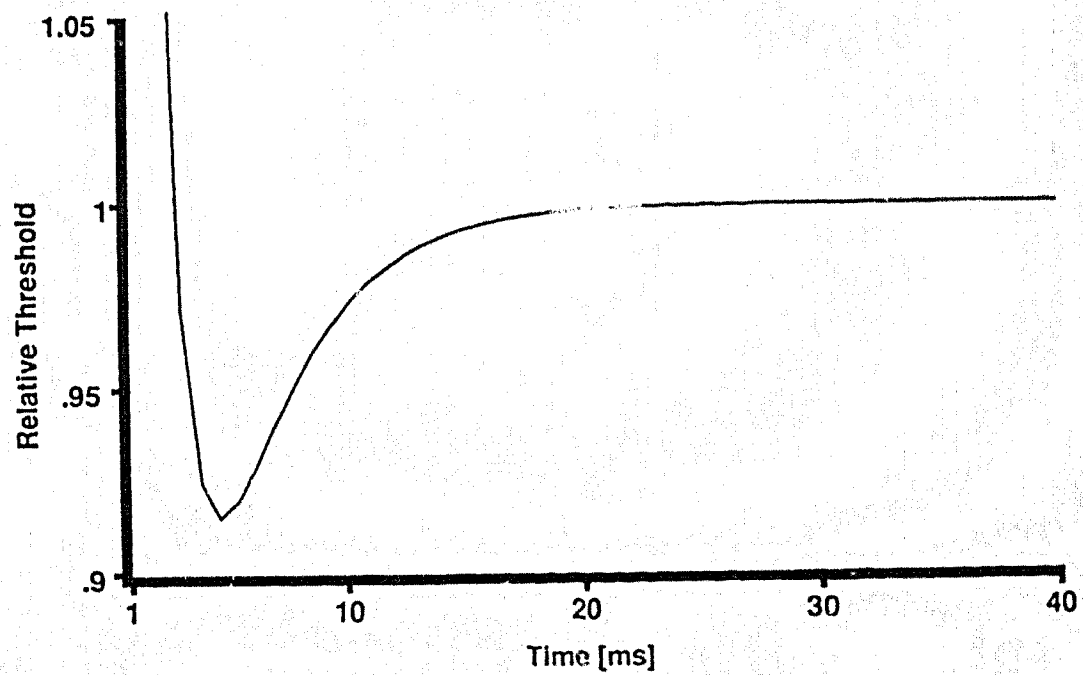
Assessment of the criteria for threshold.

FIGURE 6. The criteria for threshold were assessed by generating a second action potential, using the computed threshold at 4.5 ms following the conditioning action potential. A 0.01% reduction of the stimulus amplitude (bottom trace) failed to generate an action potential.



Effect of the sodium and leakage currents on the SNP.

FIGURE 7. Simulations were run in which, after 1 ms of normal conditions, the sodium (top trace) and the leakage (bottom trace) currents were clamped at their resting values and held there until the time for the threshold test. Under these conditions, the SNP was slightly reduced for the case of I_{Na} and enhanced for I_L .

SNP [CWM I_{r} at steady state]SNP [CWM I_{Na} at steady state]

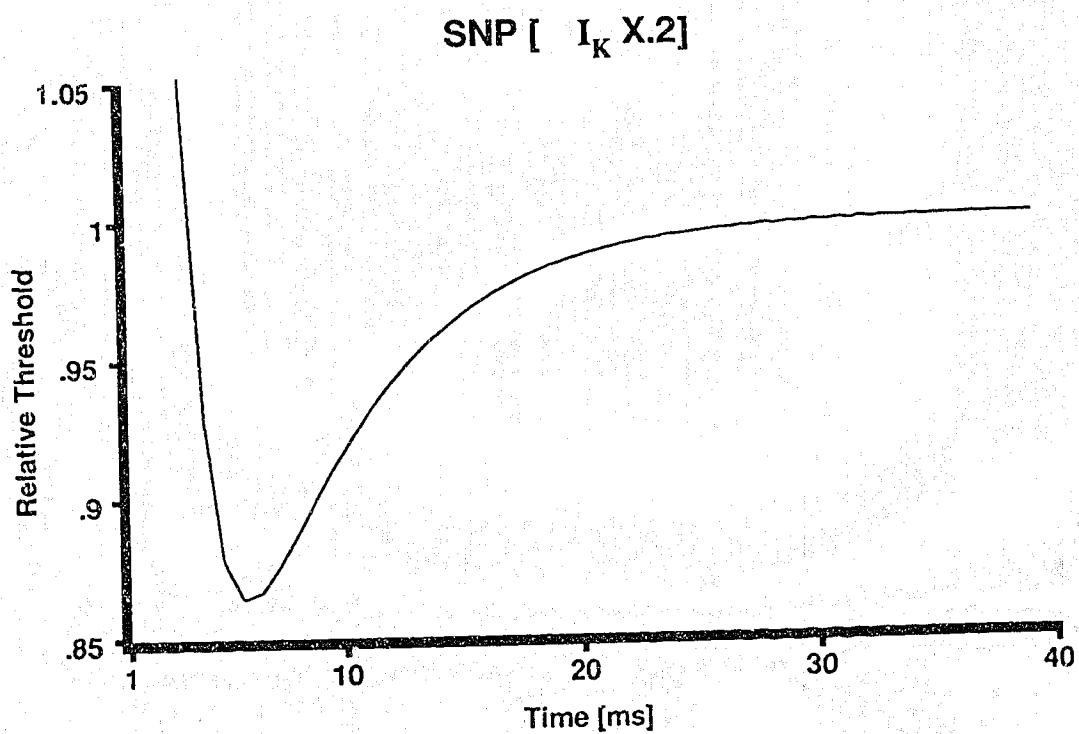
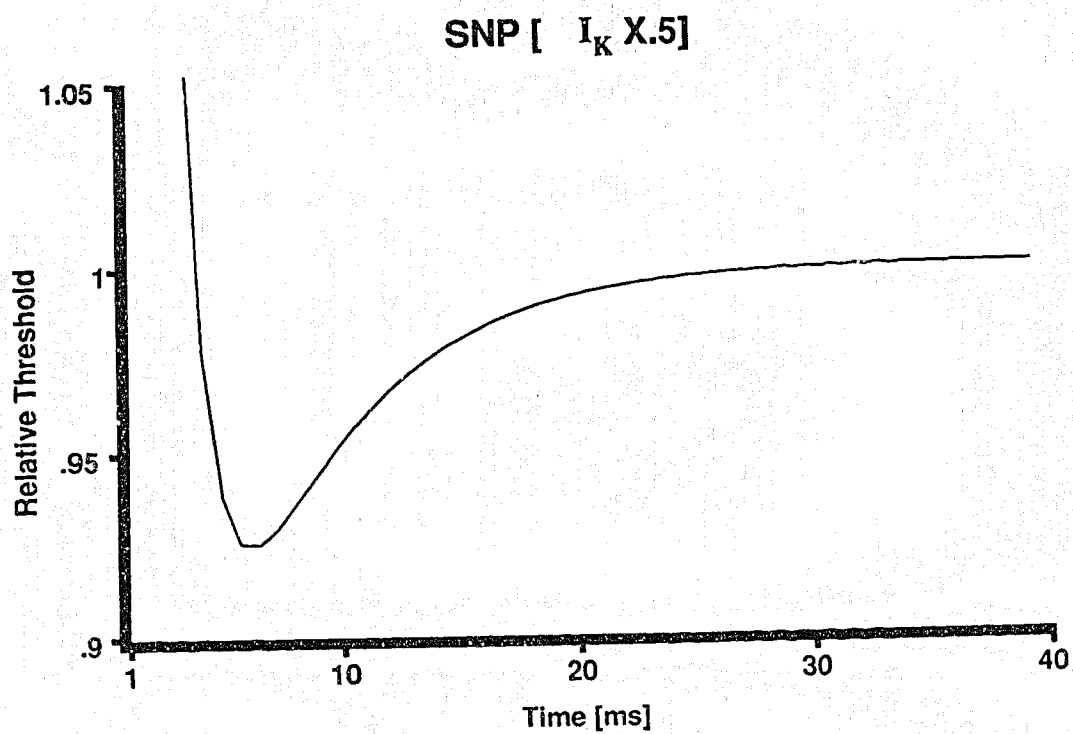
reversal potential of I_L was -17 mV. Hence, at the steady state it was an inward current. Thus although passive, the leakage current enhanced the SNP.

Setting the delayed rectifier current (I_K) to its steady state produced immediate membrane depolarization. This was avoided by multiplying I_K by factors less than 1 but greater than 0.1. Multiplying I_K by a factor of 0.5 and 0.2 (figure 8) enhanced the SNP. When I_K was multiplied by 10, the reverse situation was observed. Figure 9 represents the effect of raising I_K by a factor of 10. Therefore, increasing I_K , an outward current, prevented increased excitability beyond the refractory period.

The SNP was not dependent on the membrane potential because there was no apparent difference between the SNP observed when the membrane potential was set to the resting potential (figure 10 top trace), and the one seen under normal conditions (figure 5 bottom trace). Clamping of the transient potassium current (I_A) to its steady state was avoided since this resulted in spontaneous activity of the model. Instead, the inactivation state variable B was clamped to its steady state. Shown in the bottom trace of figure 10 is the result obtained when B was clamped to the steady state value; the SNP was abolished. Figure 4 shows that it was only the B variable which undershot its resting level and that the time course of the undershoot corresponded to the phase of supernormality. The total conductance of I_A remained below its steady state value for about 30 ms - a time span which also corresponded to the

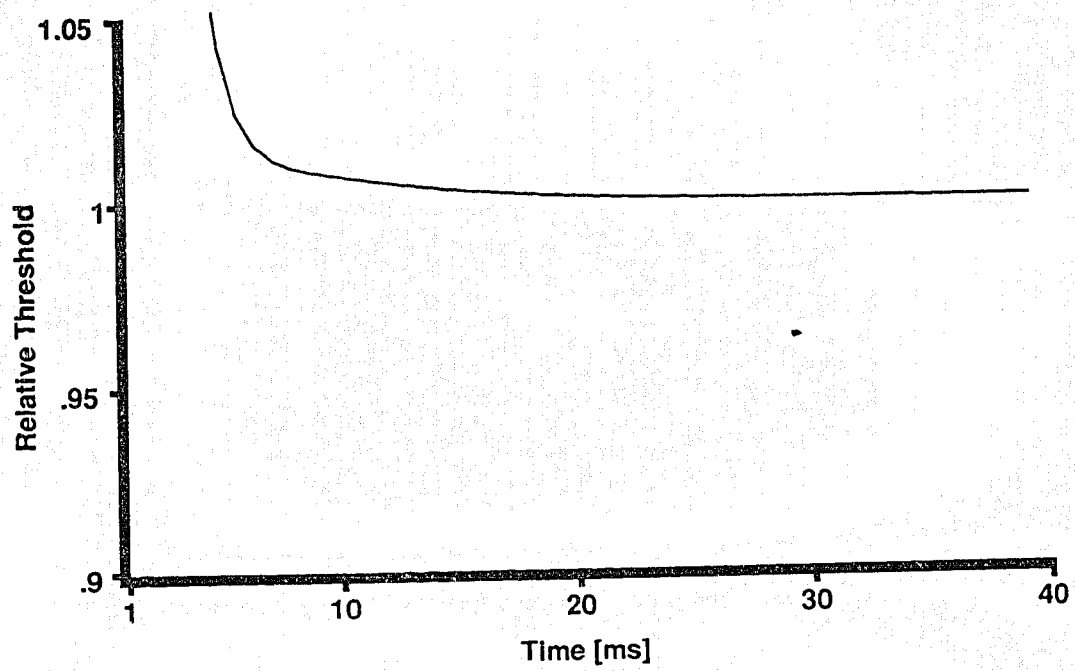
Effects of I_K on supernormal excitability (I).

FIGURE 8. Treating the potassium current I_K like I_{Na} was treated in figure 7 immediately and strongly depolarized the membrane. To keep the membrane potential at rest and yet test for threshold, a series of simulations were run in which I_K was multiplied by factors less than one. This figure shows the results of multiplying I_K by 0.5 (top trace) and by 0.2 (bottom trace). The SNP was monotonically enhanced under such conditions. Multiplication of I_K by a factor less than 0.2 perturbed the resting membrane potential.



Effects of I_K on supernormal excitability (II).

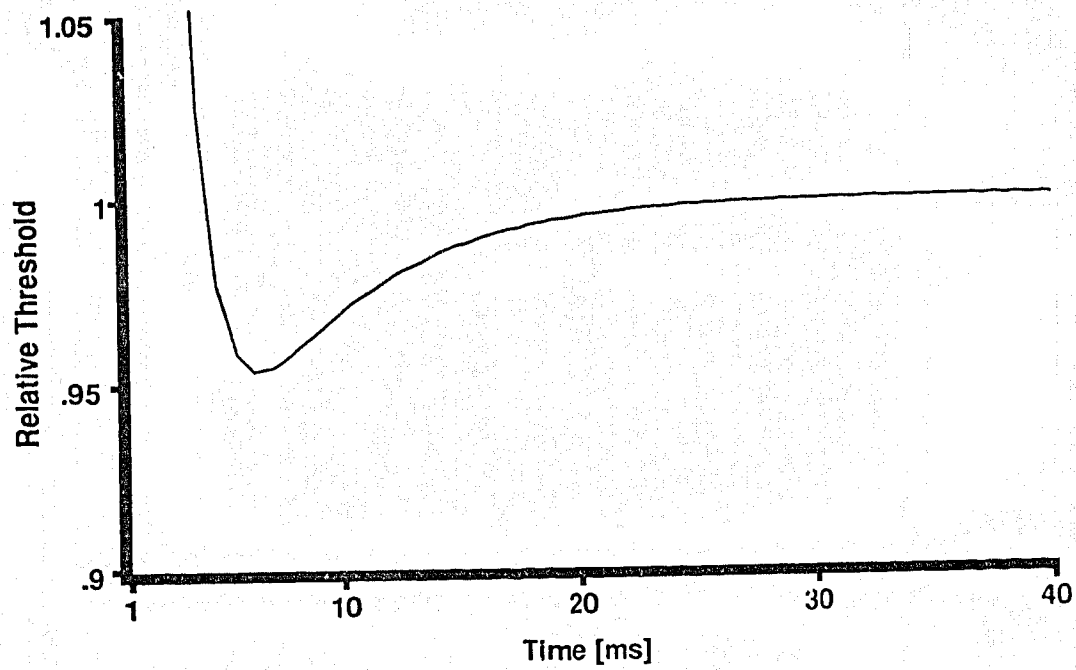
FIGURE 9. A similar simulation to that described in figure 8 was performed with I_K multiplied by 10. The SNP was abolished. Thus I_K seemed to counter supernormality.



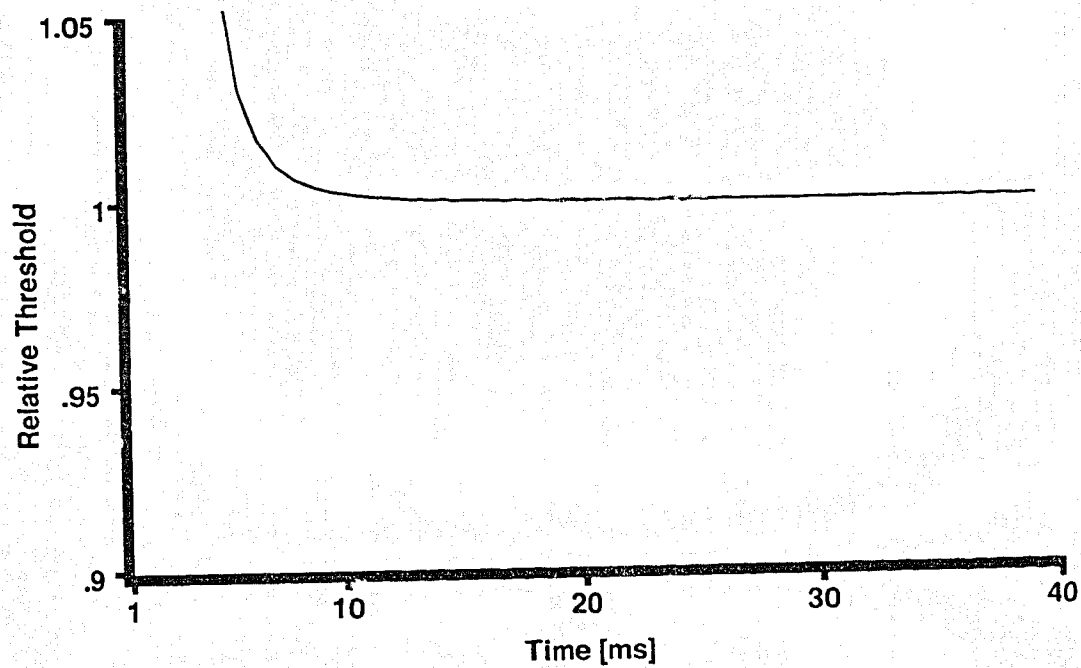
Elimination of B undershoot removed supernormality.

FIGURE 10. The membrane potential was allowed to proceed normally for 1 ms. After that, it was clamped to the resting potential and held there until the threshold test was applied. The SNP persisted under such conditions (top trace). The bottom trace shows the result when the variable **B** was set to its steady state after 1 ms. This procedure completely eliminated the SNP.

SNP [V_m set to rest]



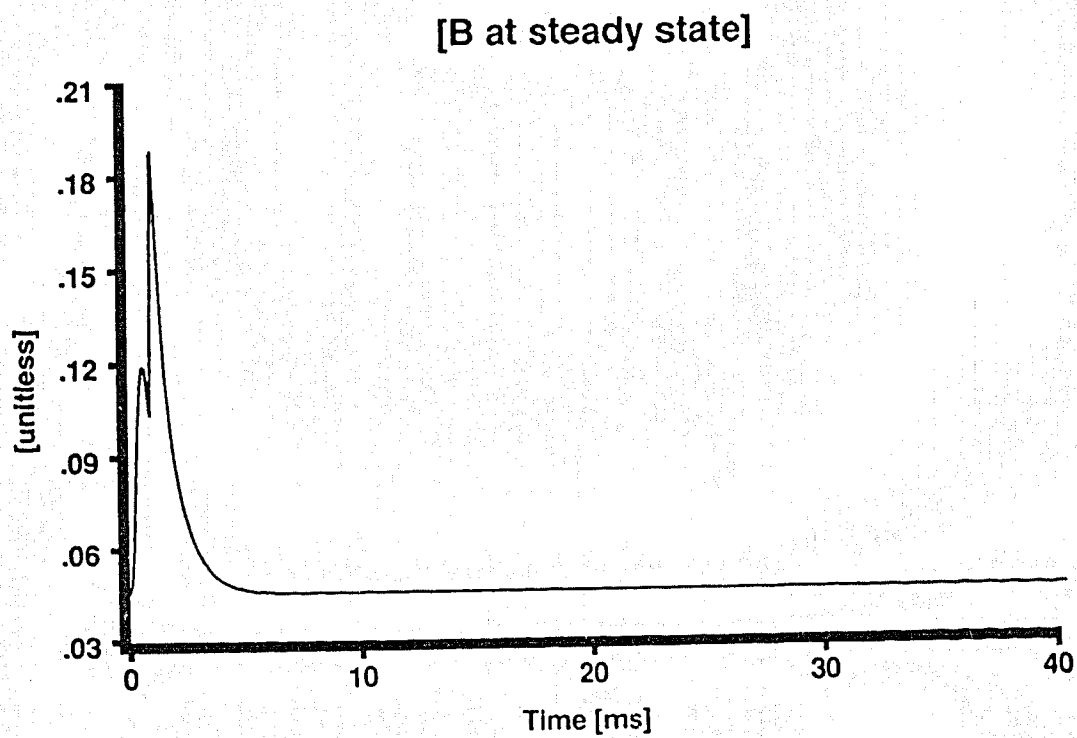
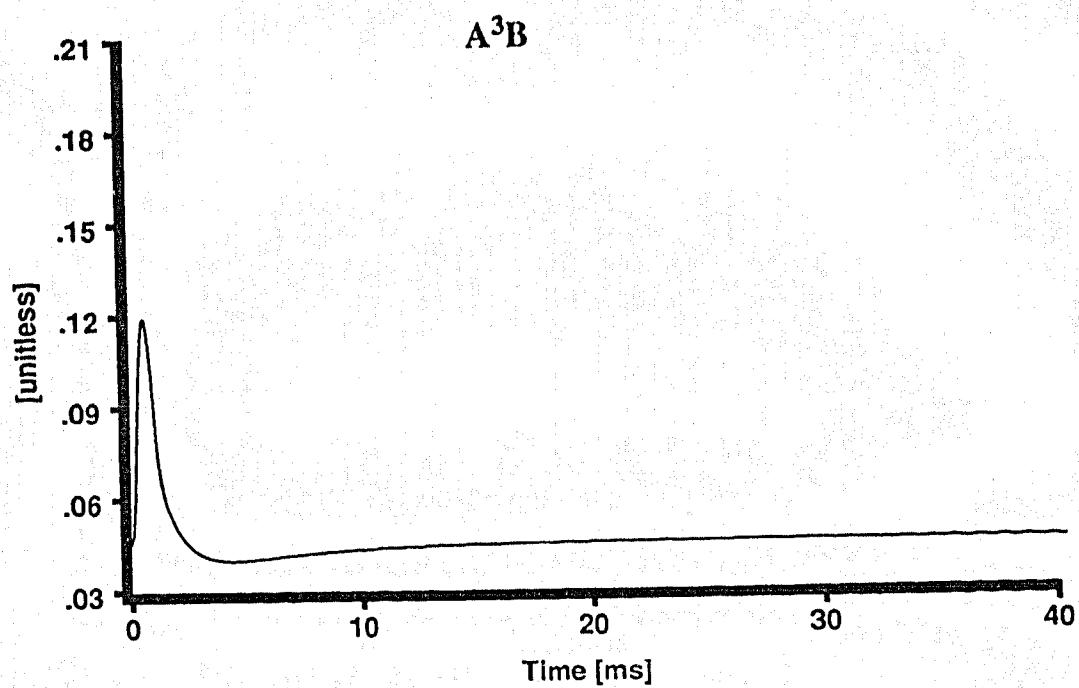
B set to steady state.



supernormal period. Presented in figure 11 (top trace) is the conductance of I_A under normal conditions. This undershoot was abolished when B was clamped to its steady state during the threshold test (bottom trace of figure 11). A reduction in the conductance of the outward current at a period when the inward current was at its steady state reduced the current needed to produce another action potential.

Effect of B undershoot on the conductance of I_A :

FIGURE 11. The conductance of I_A is proportional to the product A^3B . A^3B undershot its steady state value (top trace) after an action potential. However, this undershoot was completely eliminated when B was held at its steady state value after 1 ms of stimulation. This is shown in the lower trace. Note that removal of B undershoot eliminated supernormality.



2. Effect of repetitive firing on supernormal period

Does repetitive stimulation affect the extent of supernormality?

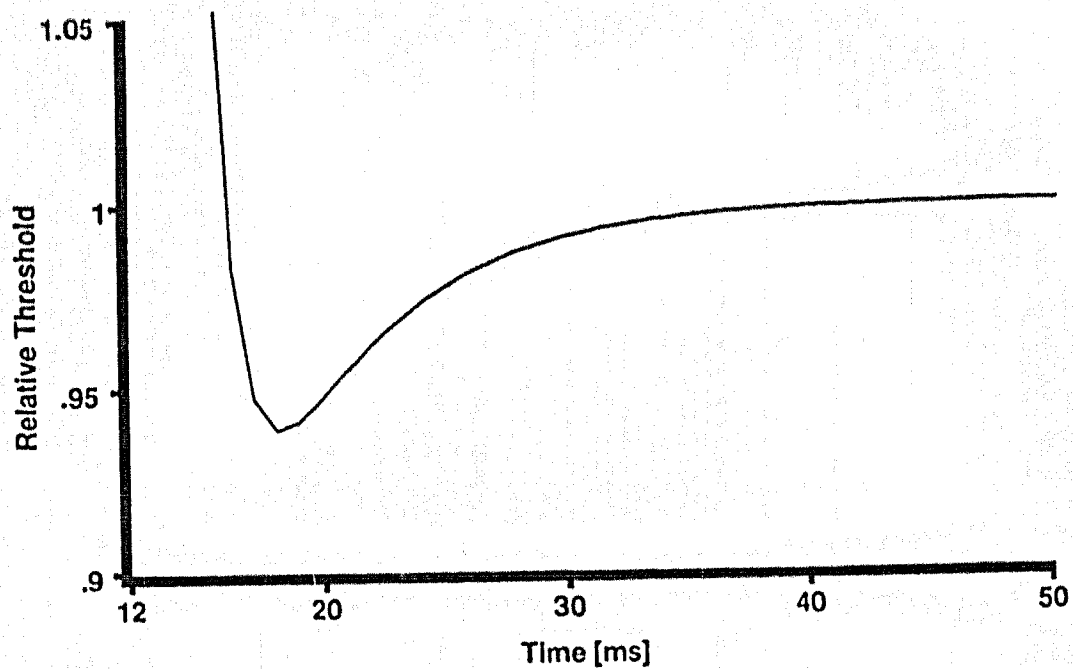
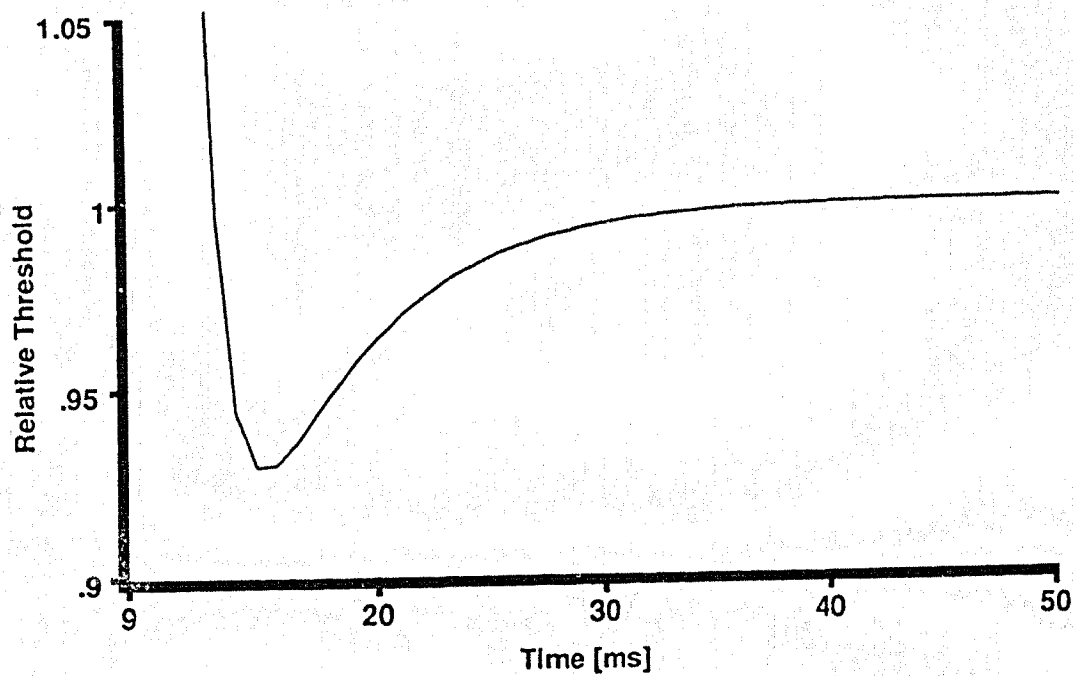
This question was addressed by using the program thn.c. Figures 12 and 13 illustrate cases where the threshold test was initiated subsequent to the generation of four impulses with varying interstimulus intervals. Clearly, repetitive firing enhanced the SNP. A decrease in interstimulus interval also potentiated supernormal excitability.

It should be noted that when action potentials were generated at 1 ms intervals in these conditioning trains, a larger stimulus was required to generate the action potentials following the first spike. This was necessary since the membrane was in the refractory phase 1 ms following the action potential.

With a constant interstimulus interval but varying number of spikes, the excitability of the membrane increased as the number of conditioning action potentials was increased, as shown in figures 14 and 15. Little further increase in excitability was seen with more than five conditioning action potentials.

Effect of varying interstimulus intervals on the SNP (I).

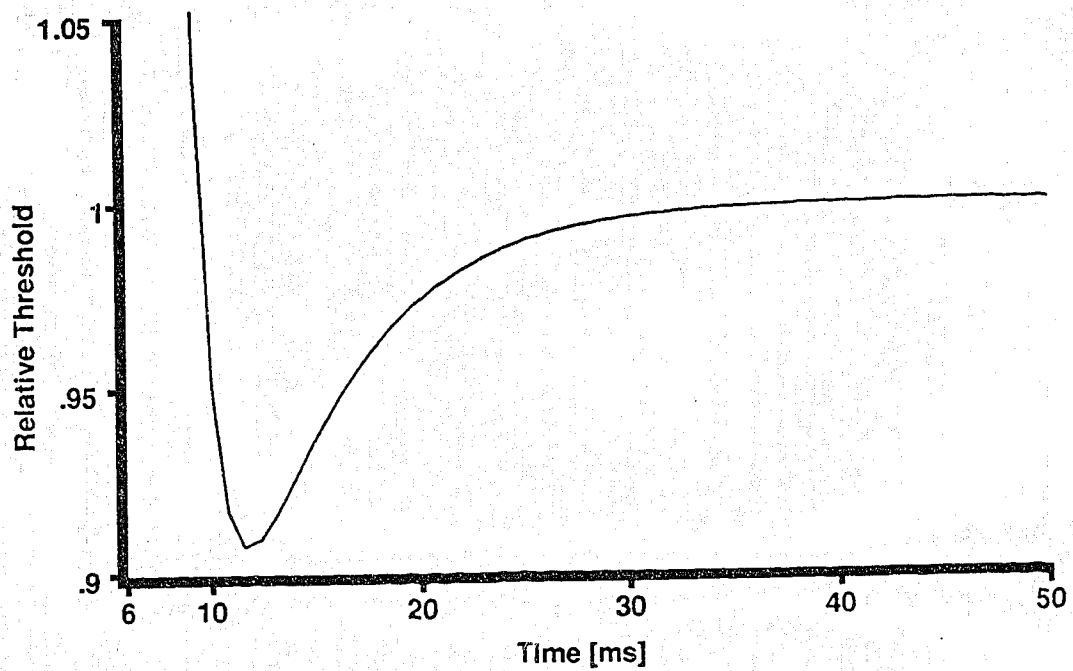
FIGURE 12. A series of simulations were run in which four conditioning action potentials were generated with various interstimulus intervals. The SNP observed with four and three milliseconds interstimulus intervals are shown in the top and bottom traces respectively.

SNP [After 4 Impulses at 4 ms intervals].**SNP [After 4 impulses at 3 ms intervals].**

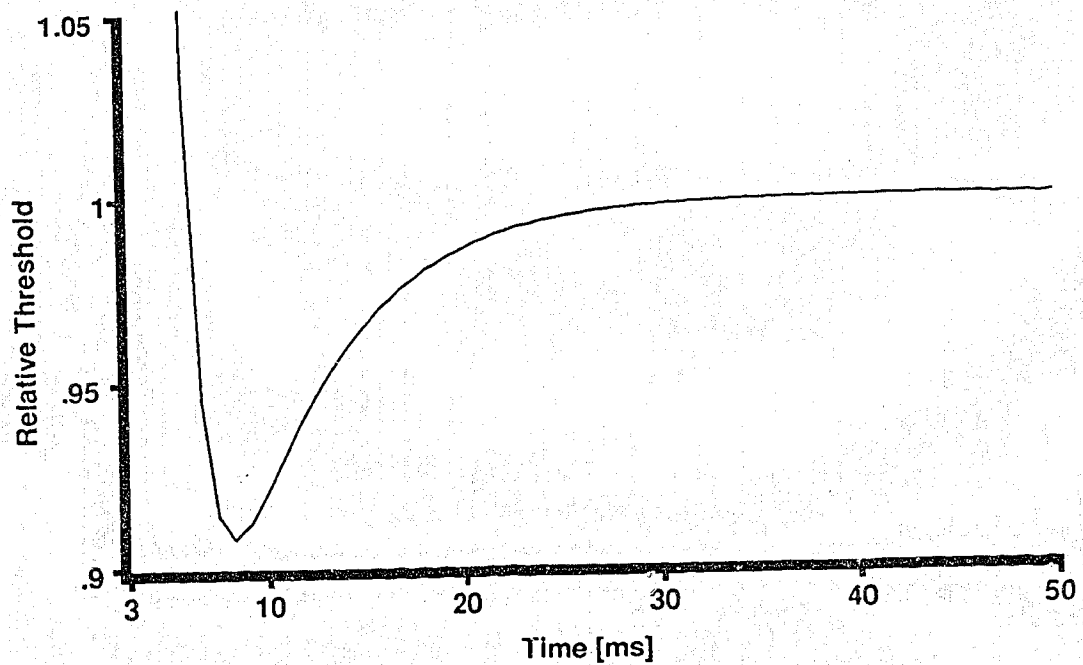
Effect of varying interstimulus intervals on the SNP (II).

FIGURE 13. The same procedure as described in figure 12 was used here. The top trace shows the result with 2 ms interstimulus intervals. The bottom trace shows the SNP observed with 1 ms interstimulus intervals. In the latter case, a higher stimulus had to be applied during the conditioning train.

SNP [After 4 impulses at 2 ms interval]

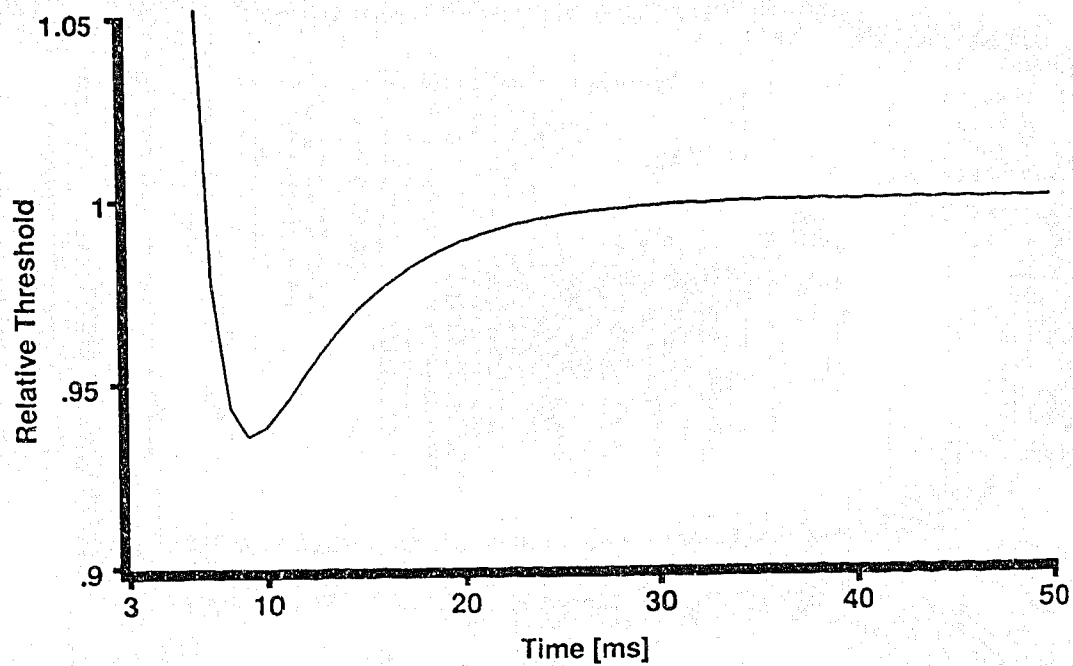
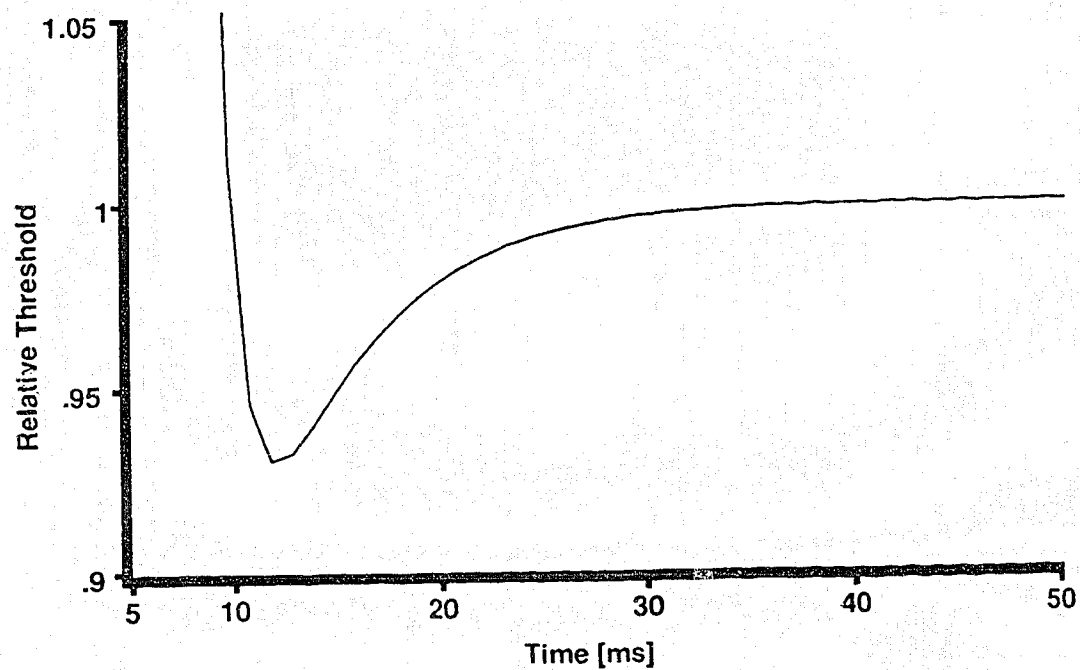


SNP [After 4 impulses at 1 ms intervals].



Repetitive firing and the SNP (I).

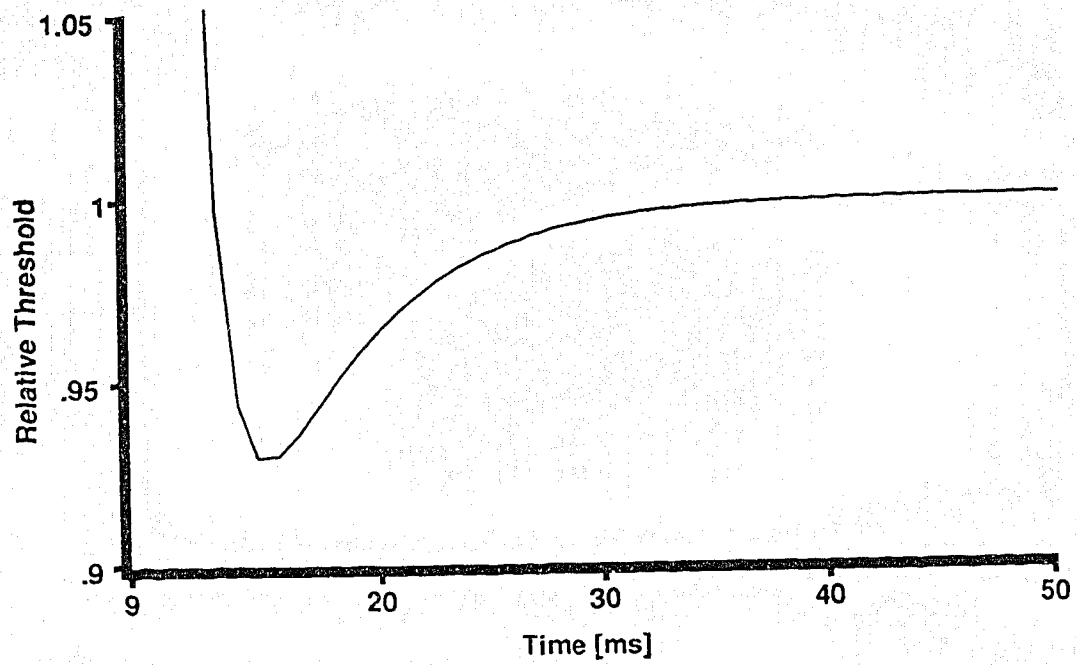
FIGURE 14. The results of repetitive stimulation with a constant interstimulus intervals (3 ms) are shown for two action potentials (top trace) and three action potentials (bottom trace). An increase in the number of action potentials slightly increased supernormal excitability.

SNP [After 2 impulses at 3 ms intervals].**SNP [After 3 impulses at 3 ms intervals].**

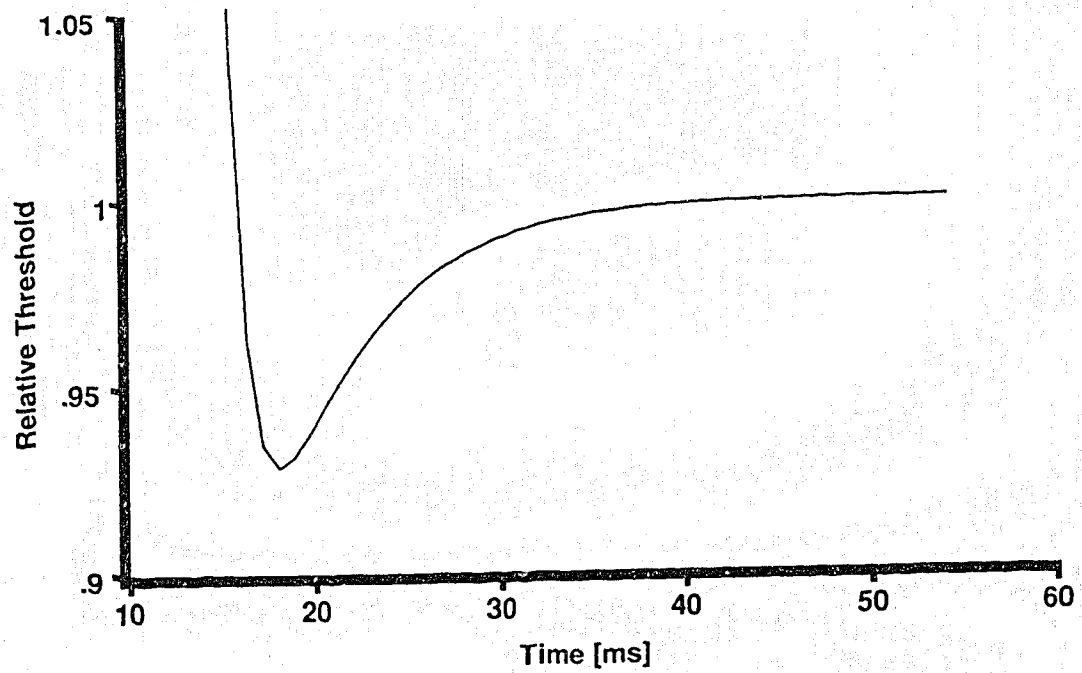
Repetitive firing and the SNP (II).

FIGURE 15. Increasing the number of conditioning action potentials from four (top trace) to five (bottom) did not produce a significant increase in the SNP.

SNP [After 4 impulses at 3 ms intervals].



SNP [After 5 impulses at 3 ms intervals].



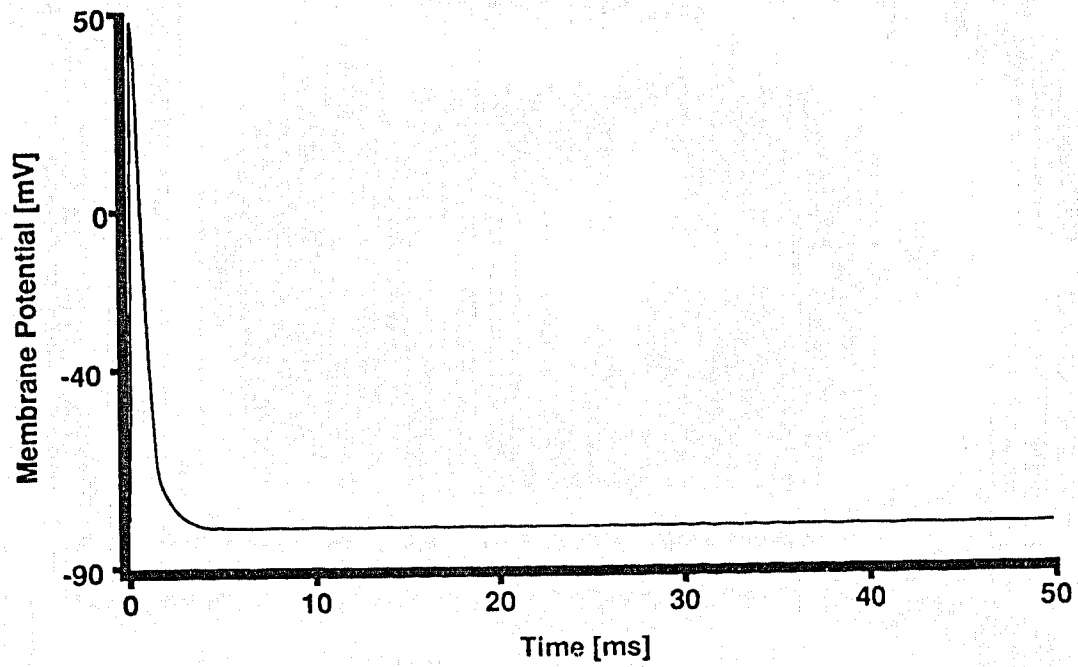
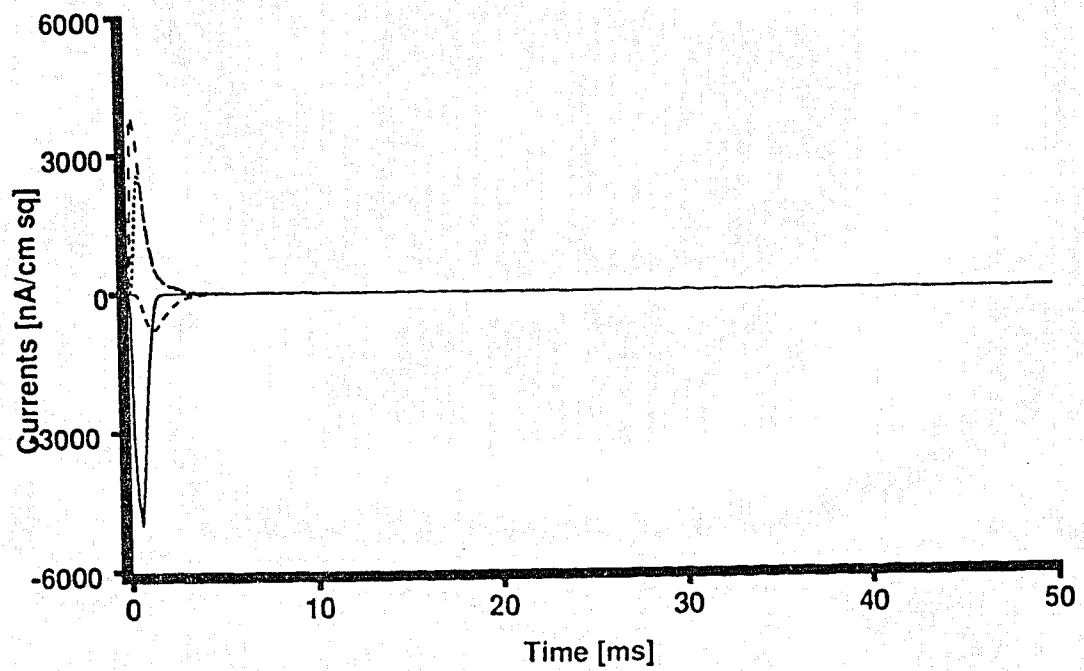
B. FH Model

The FH model for myelinated nerves of the frog was implemented in the same fashion as the CWM model. In the FH model, however, permeabilities of the ion channels are used instead of conductances. This model does not have an I_A current. Instead, a non specific current (I_P) carried mainly by potassium is added to the sodium (I_{Na}), potassium (I_K , delayed rectifier) and the leakage (I_L) currents. Presented in figure 16 (50 ms time scale) and 17 (10 ms time scale) are the action potentials (top traces) and currents (bottom traces) for the FH model. A test for the threshold following the action potential showed that this model does not produce supernormality (figure 18).

Action potential and the membrane currents of the FH model.

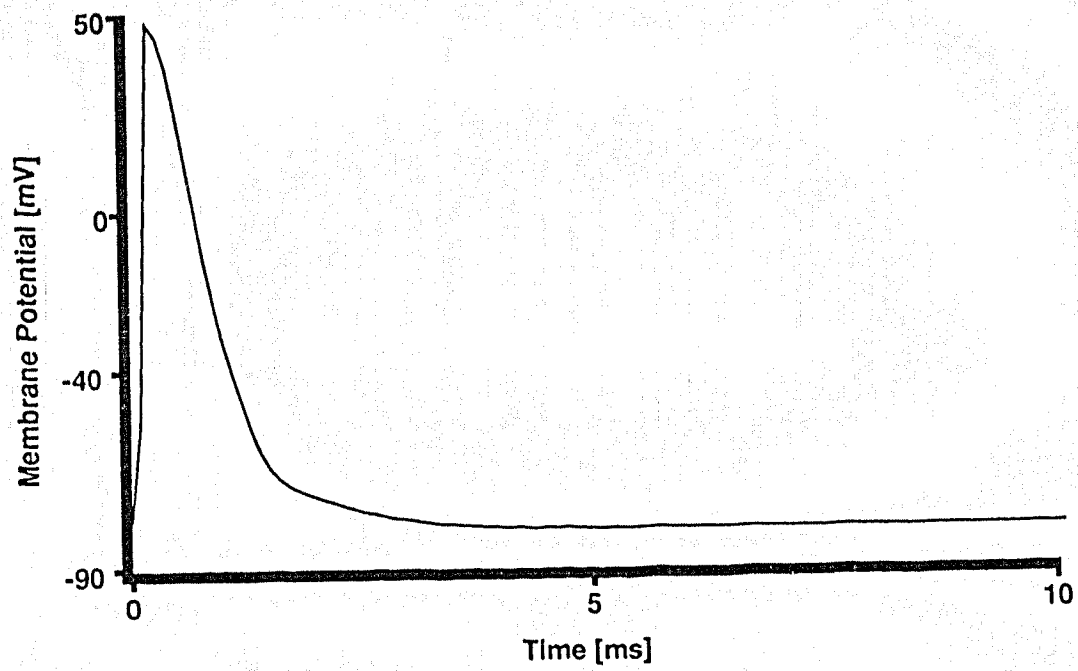
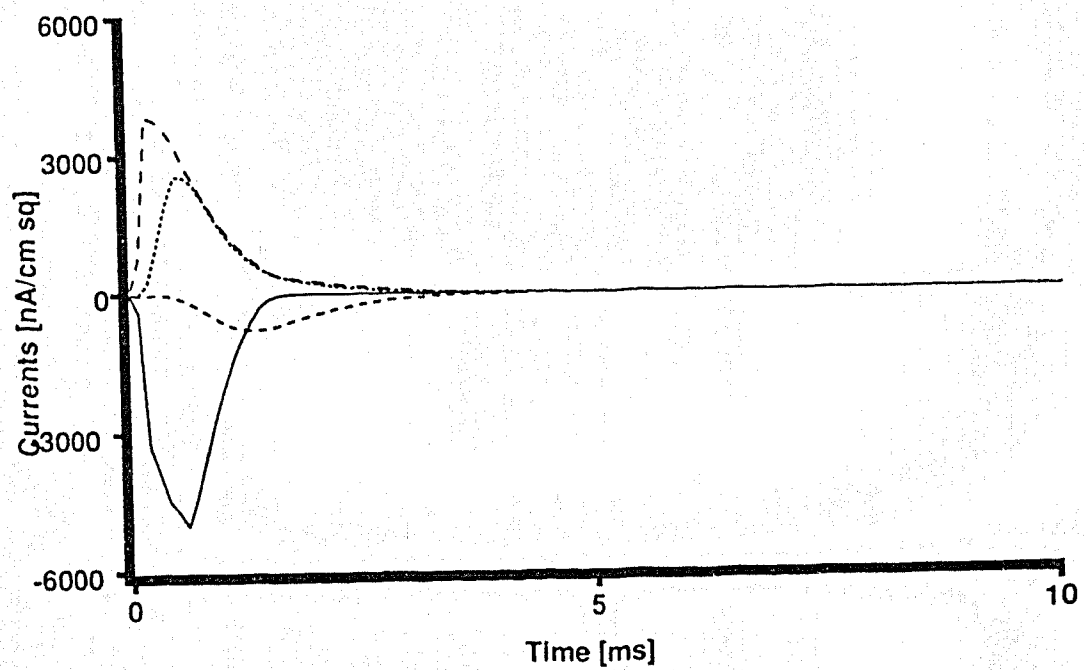
FIGURE 16. The top trace shows the time course of the membrane action potential computed from the equations of the Frankenhaeuser and Huxley model for frog myelinated nerves. The resting membrane potential was -80 mV and the amplitude of the action potential was about 120 mV. The bottom trace shows the currents responsible for the generation of the action potential: sodium current I_{Na} (solid line), potassium current I_K (fine dashed line), a nonspecific current I_p (coarser dashed line) and the leakage current I_L (coarsest dashed line).

Action Potential [fh]

Currents I_{Na} I_K I_P 

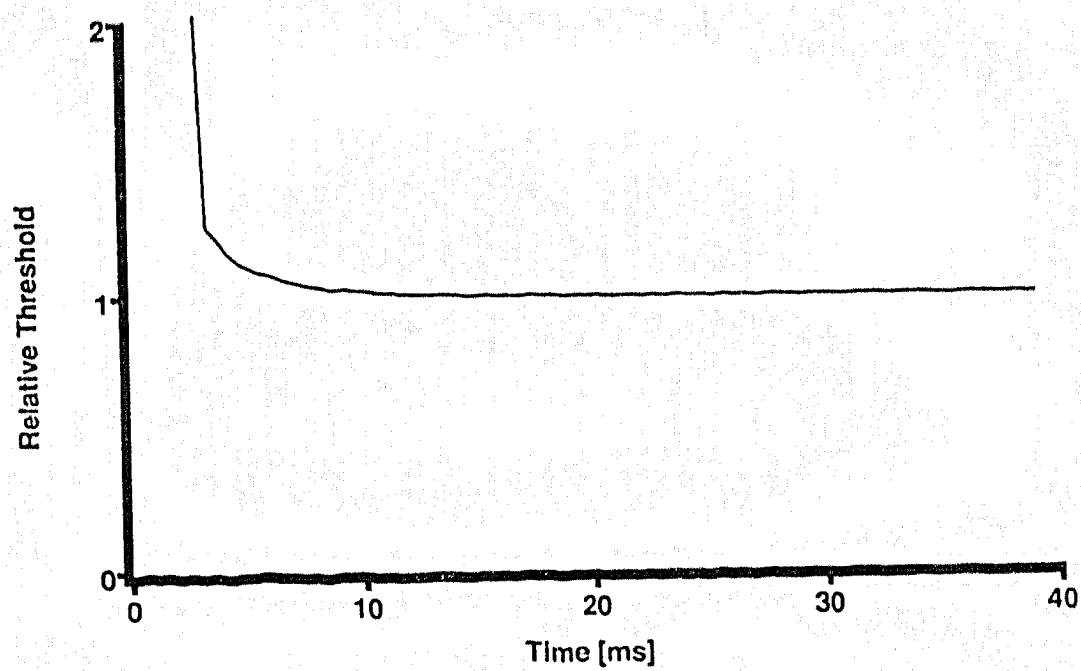
Action potential of the FH model and the membrane currents-
detail representation.

FIGURE 17. Figure 16 is reproduced using an expanded time scale.

Action Potential [FH]**Currents I_{Na} I_K I_P** 

FH model does not exhibit supernormality.

FIGURE 18. A normal action potential was allowed to proceed for 1 ms and a threshold test with a stimulus width of 0.1 ms was run until 40 ms. The graph indicates that the FH model does not demonstrate supernormal excitability.

Threshold Test [No SNIP]

C. BR Model

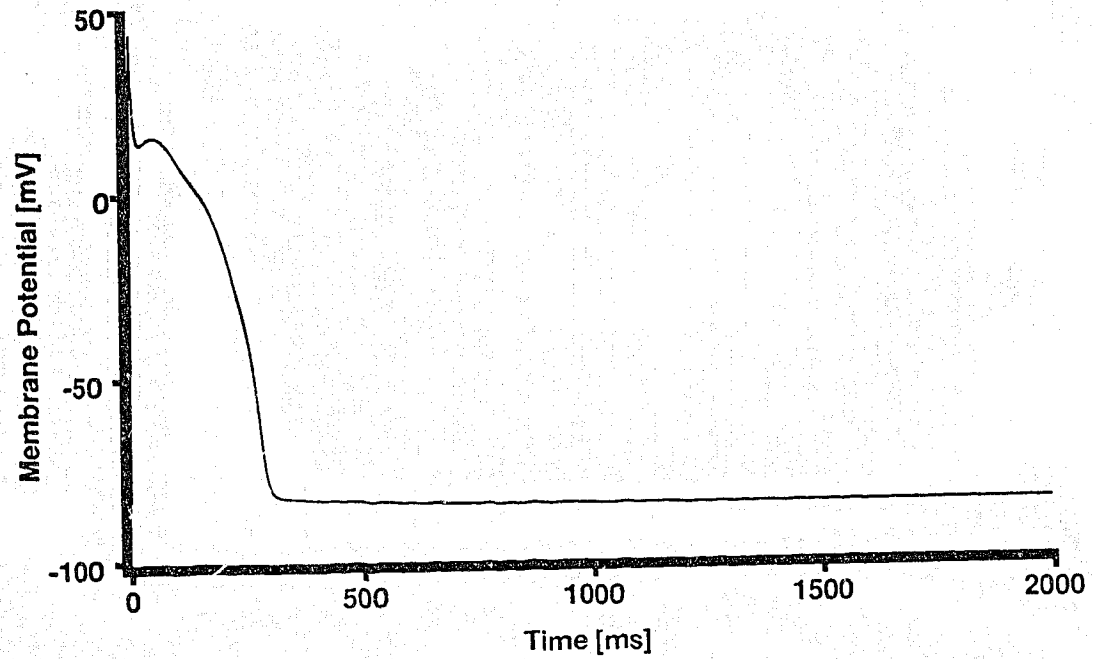
The top trace of figure 19 presents the standard action potential of a ventricle computed from the BR model. The shape and duration of the simulated action potential was identical to that shown in Beeler and Reuter's figure 4. The resting potential was -84.57 mV. The action potential had a slight afterdepolarization and this is illustrated in more detail at the bottom trace of figure 19. The result of the excitability determination is depicted on the top trace of figure 20. The threshold values obtained for each time were normalized and treated in the same manner as for the CWM and FH models. A SNP was observed from 340-1568 ms. The steady state threshold was 49.63 nA/cm² with a stimulus duration of 0.5 ms. The lowest threshold was (48.22 nA/cm²). Presented in figure 20 (bottom trace) is the validation for the criteria for defining an action potential in the threshold test. The amplitude of the second spike was a bit lower than that of the first because of residual inactivation of inward currents and, possibly, faster activation of potassium currents.

The currents responsible for the generation of the action potential were: two outward currents, I_{x_1} (time and voltage dependent potassium current) and I_{K_1} (time independent potassium current) and two inward currents, I_{Na} and I_s , which are sodium and calcium currents

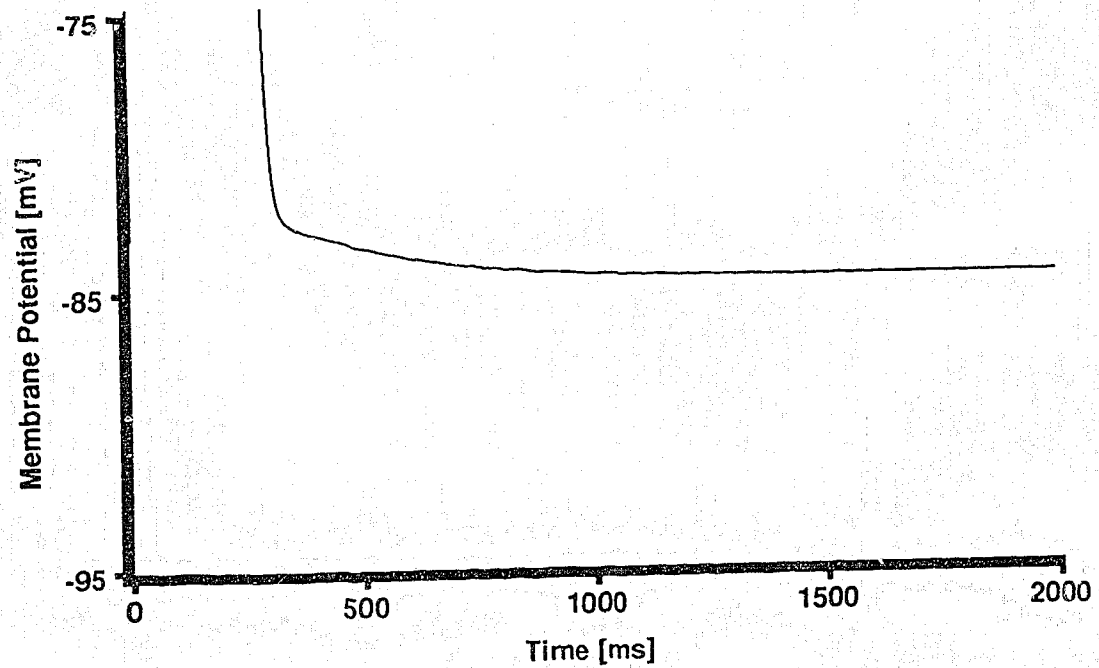
Action potential of the BR model.

FIGURE 19. The shape and time course of a computed action potential for guinea pig ventricular myocardial trabeculum (top trace) is similar to that in the Beeler and Reuter (1977) paper. There is a period of afterdepolarization which is depicted in more detail in the bottom trace.

Ventricular action potential [BR]

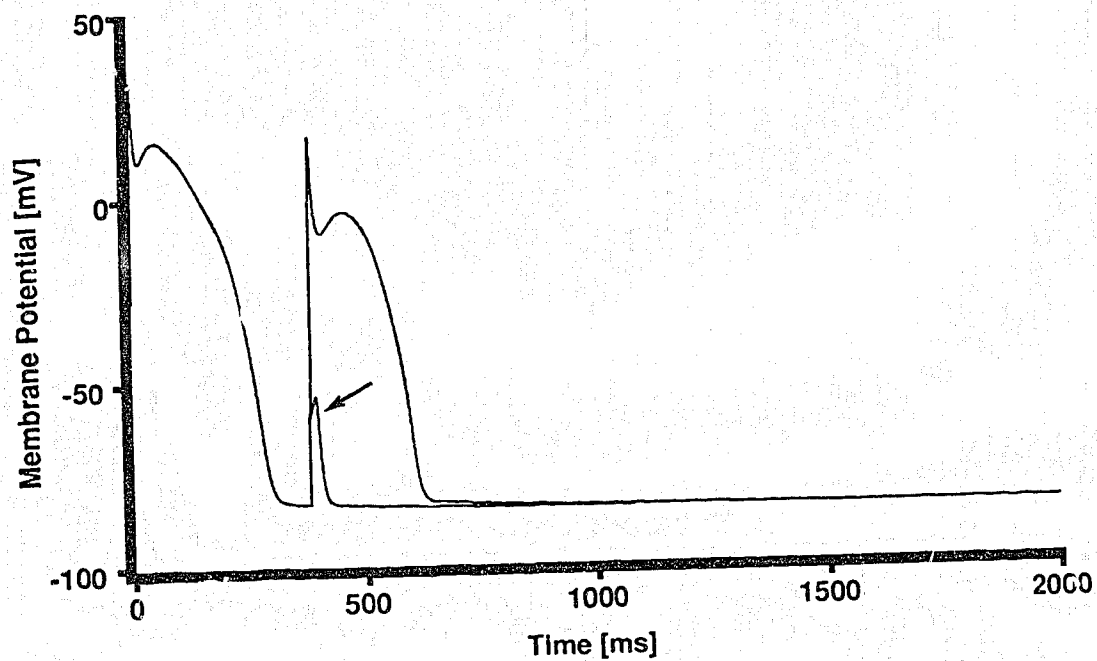
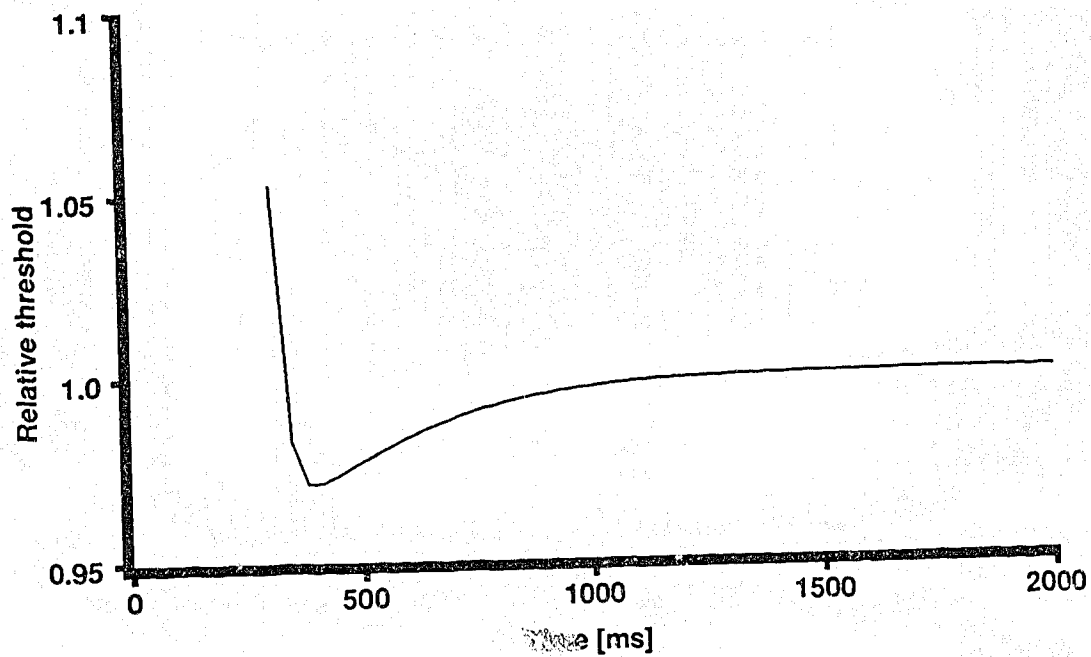


Afterdepolarization



Supernormality in the BR model and assessment of computed threshold.

FIGURE 20. This figure (top trace) represents the excitability of the membrane beginning at 270 ms after a normal membrane action potential has been initiated. The method for obtaining relative threshold is described in the legend for figure 5. The SNP in the **BR** model for the ventricular myocardium lasts for about 1228 ms (340-1568 ms). The validity of the criteria used for the threshold test was examined by using the computed threshold at 380 ms following a conditioning membrane action potential (bottom trace). Reduction of the computed threshold by 0.0001% failed to generate an action potential. The decrease in amplitude of the second action potential resulted from inactivation of inward currents.



respectively. Figure 21, top and bottom traces, illustrates the time course of these currents.

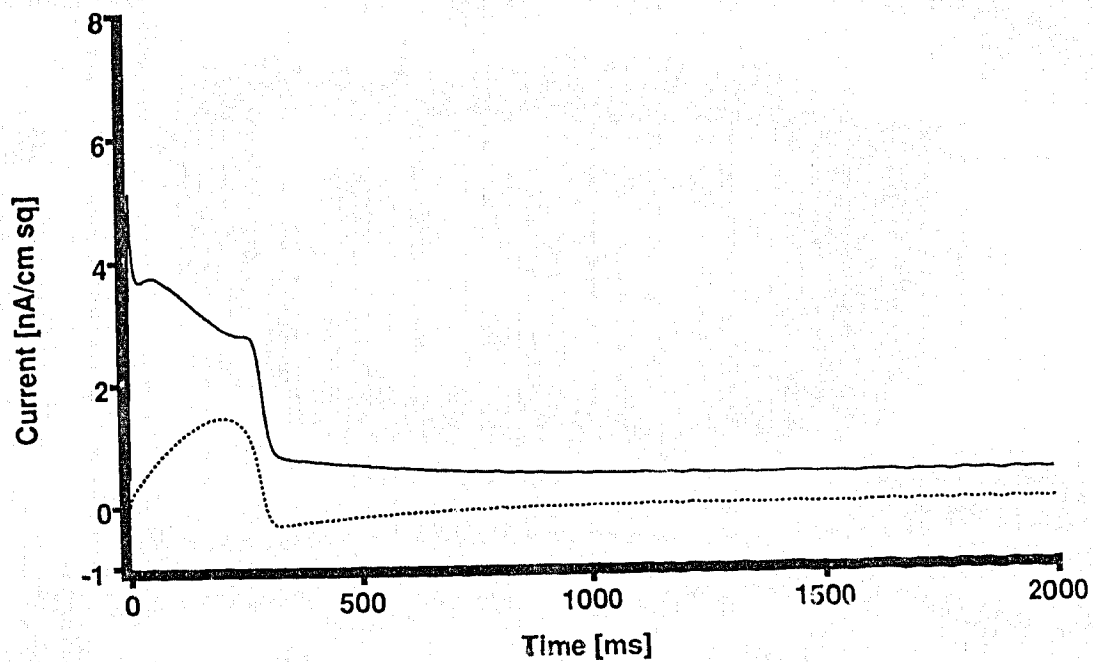
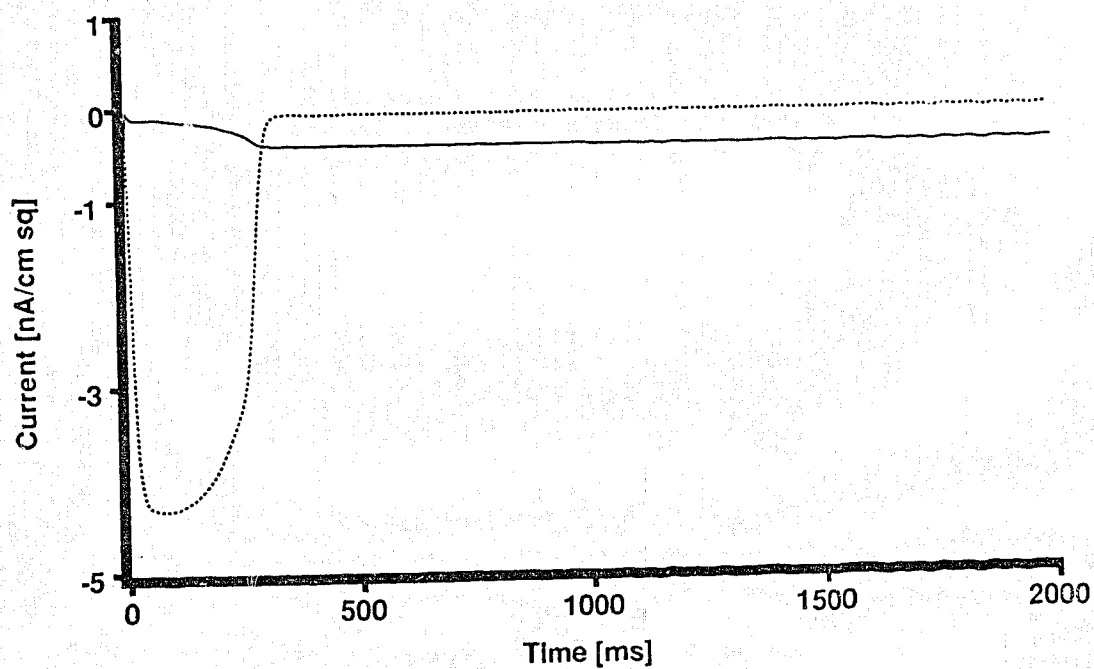
To ascertain which of the currents was responsible for the SNP, individual currents were clamped to their steady state values until the time of the threshold test. Treating I_{Na} or I_s as mentioned above did not abolish the SNP as shown in figure 22. The potassium current I_{x1} undershot its steady state value at 292 ms before it gradually rose to its resting value. One would expect that the undershoot of I_{x1} would enhance membrane excitability. However, SNP was eliminated when I_{x1} was clamped to its resting value (figure 23, top trace). Not only was the SNP abolished but the afterdepolarization following the action potential was also removed.

It is possible, then, that the SNP in this model results directly from undershoot in I_{x1} . On the other hand, a cause-effect relationship might be operating between the membrane potential and the potassium current. Therefore, the threshold was tested while the membrane potential was forced to its resting value. Presented in figure 23, bottom trace, is the result, which shows the elimination of the SNP. However, the undershoot in I_{x1} persisted under resting-potential-clamped conditions (figure 24, top trace). If setting the membrane potential to the resting level independently eliminated the SNP without affecting the undershoot of I_{x1} , then, the afterdepolarization alone was responsible for SNP.

How is the membrane potential related to the threshold current?

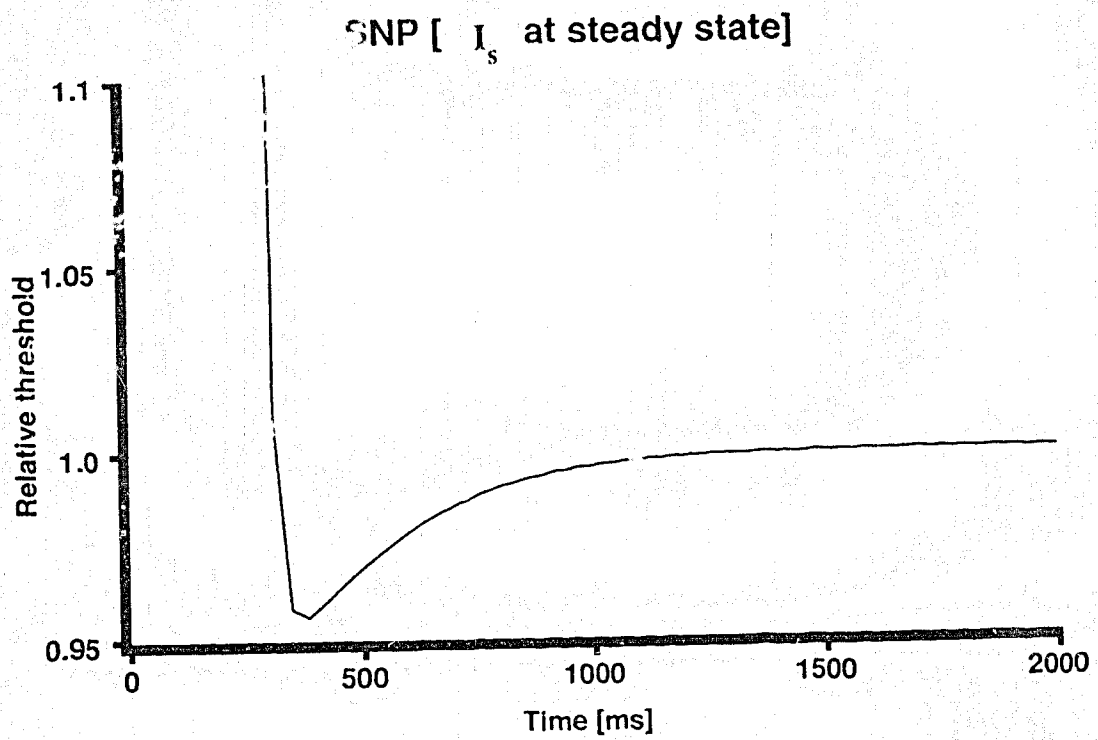
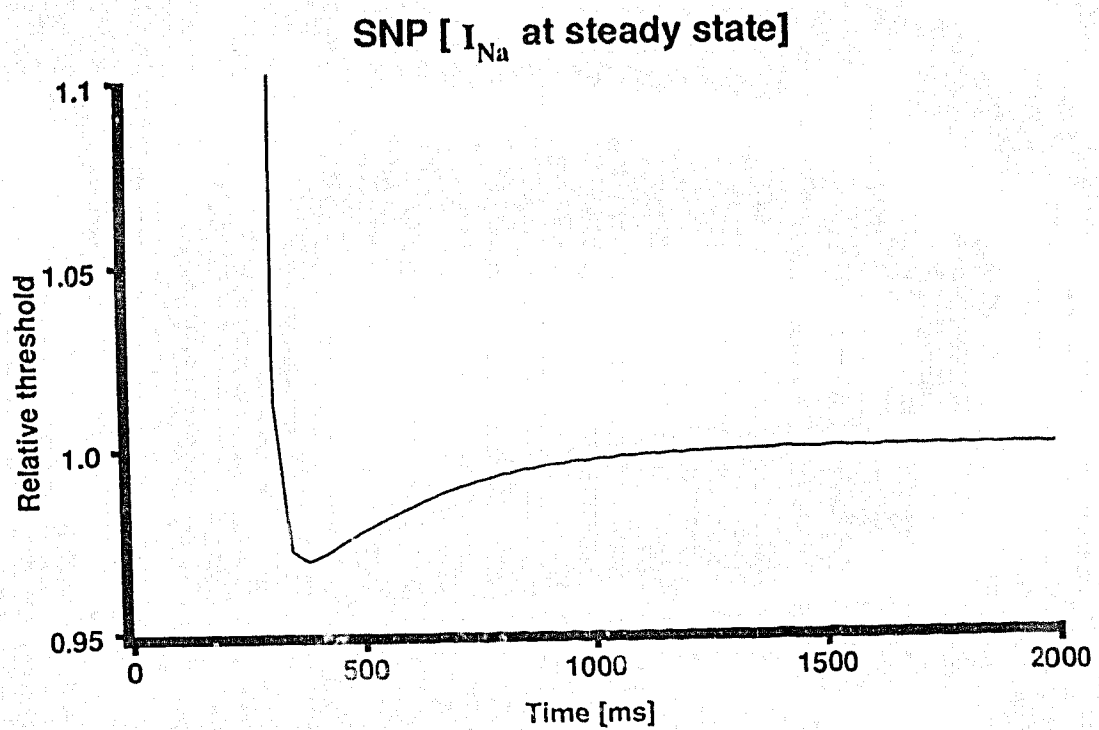
Ionic currents in the BR model.

FIGURE 21. The figure shows the time courses of computed ionic currents. The top trace shows the voltage dependent potassium current, I_{K_1} (solid line) and the voltage and time dependent potassium current, I_{x_1} (dashed line). I_{x_1} underwent its steady state value before it gradually recovered. The bottom trace shows the sodium current, I_{Na} (solid line) and the calcium current, I_s (dashed line).

Currents I_{K1} I_{X1} [BR]Currents I_{Na} I_{si} [BR]

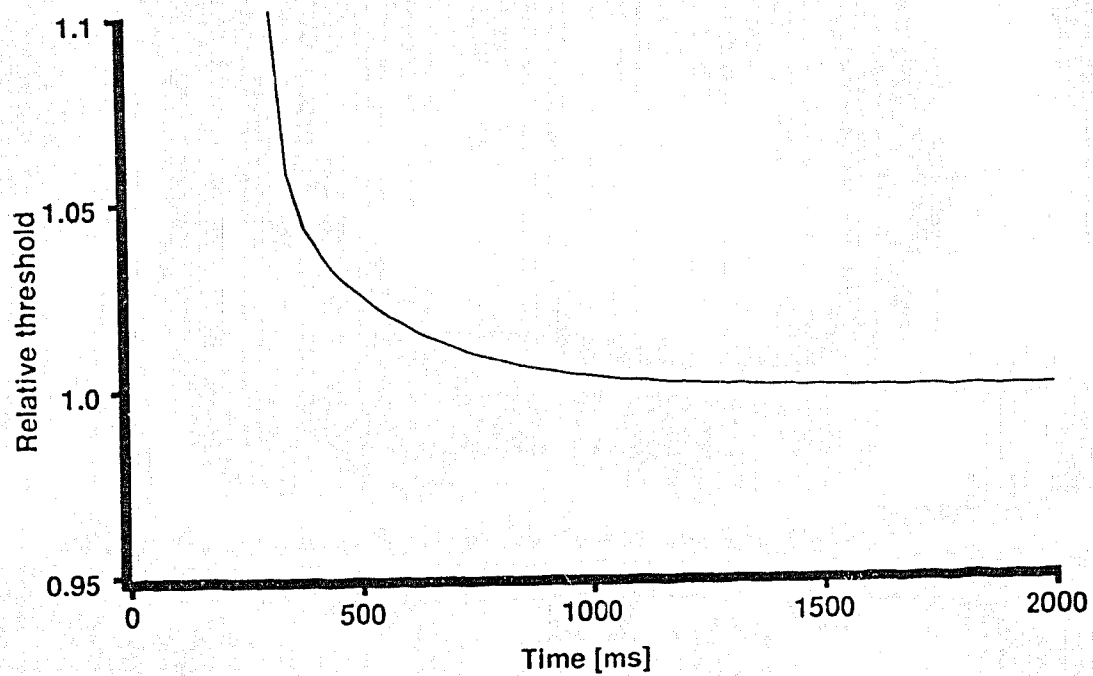
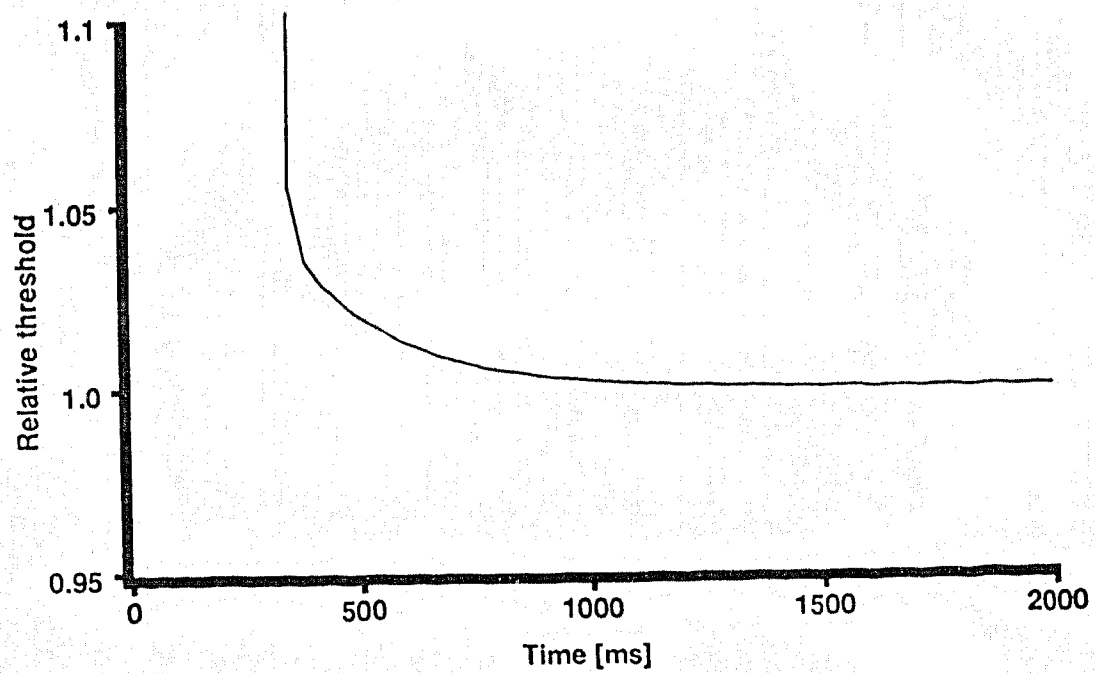
Effects of I_{Na} and I_s on the SNP.

FIGURE 22. A series of simulations were run in which the membrane action potential was allowed to proceed normally until 250 ms. Beyond this time, one current was clamped at its steady state until time to test for the threshold. When I_{Na} (upper trace) or I_s (lower trace) was tested in this fashion, the SNP persisted. In fact, in both cases the SNP was slightly enhanced.



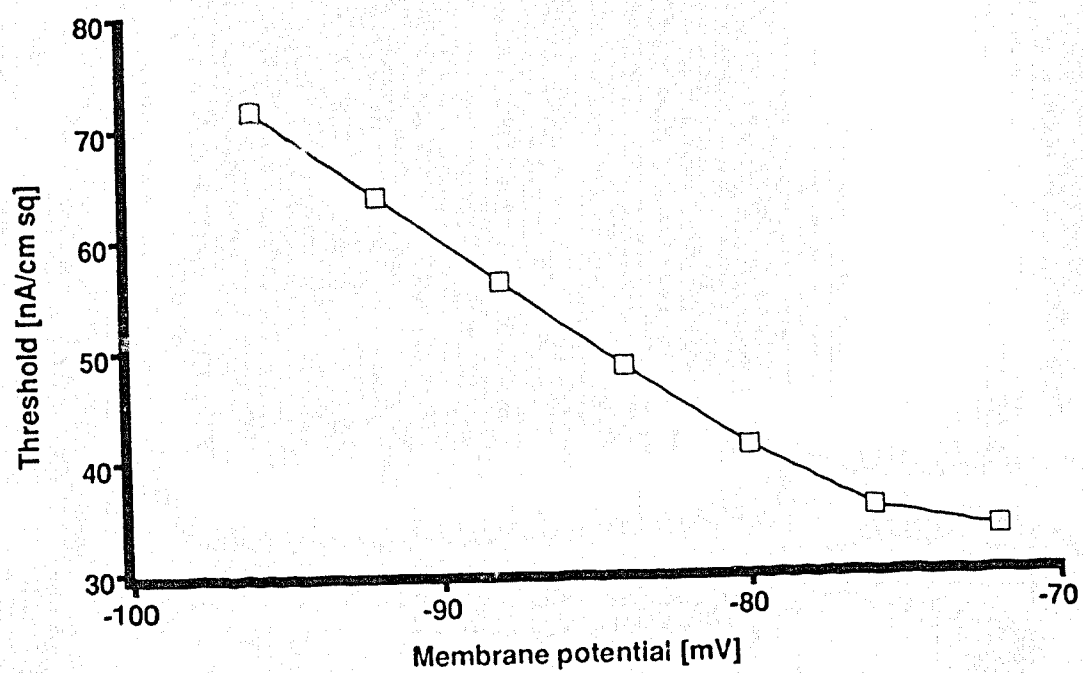
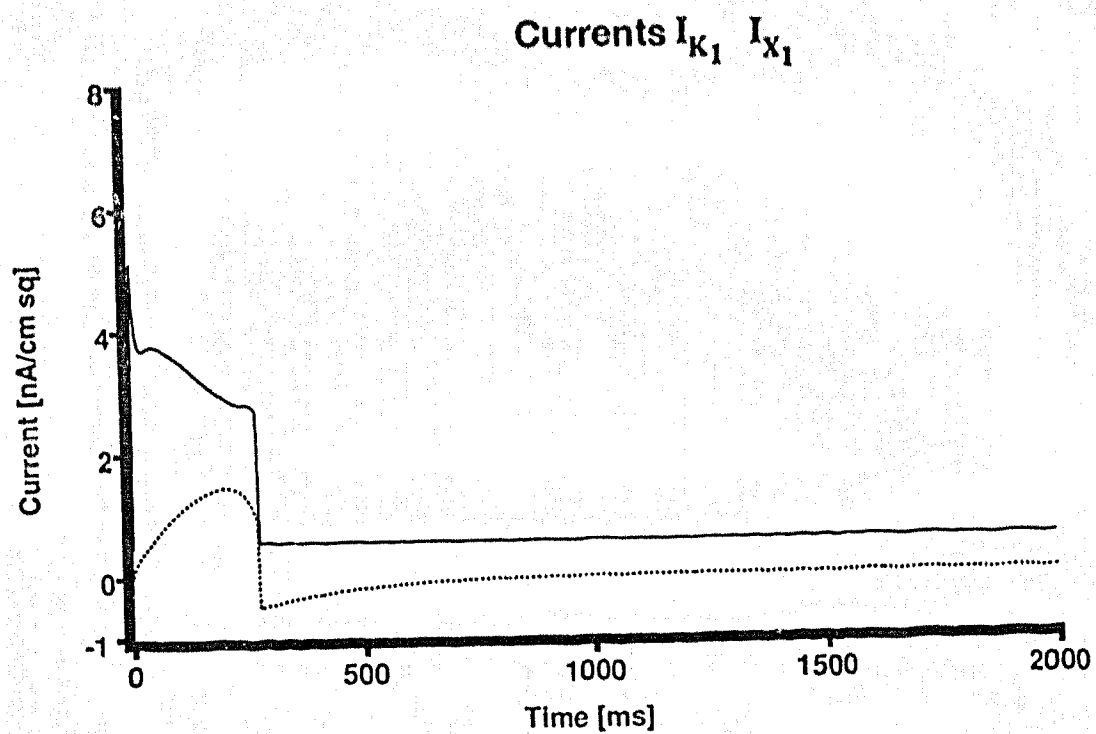
Effect of I_{x_1} and V_m on supernormality.

FIGURE 23. The same procedure as described in figure 22 was adopted here to examine I_{x_1} (top trace) and the membrane potential (bottom trace). The threshold test indicated that under both conditions the SNP was entirely eliminated. Setting I_{x_1} to its steady state abolished the afterdepolarization as well (not shown).



Afterdepolarization causes supernormality in the BR model.

FIGURE 24. The top trace of this figure shows a plot of I_{K_1} (solid line and I_{x_1} (dashed line) when the membrane potential was set to its resting value (-84 mV) at 270 ms. Even under these conditions the undershoot of I_{x_1} persisted. This indicates that the undershoot of I_{x_1} was not directly responsible for the SNP. Rather, the undershoot of I_{x_1} causes the afterdepolarization. It is the afterdepolarization which subsequently causes the SNP. The bottom trace illustrates the linear relationship between the threshold and the membrane potential.



Simulations were performed in which the steady state threshold was determined at different membrane potentials. The bottom trace of figure 24 shows that threshold current was linearly related to the membrane potential. Therefore, an undershoot of I_{x_1} resulted in afterdepolarization, which in turn caused supernormal excitability in the BR model.

D. MNT Model

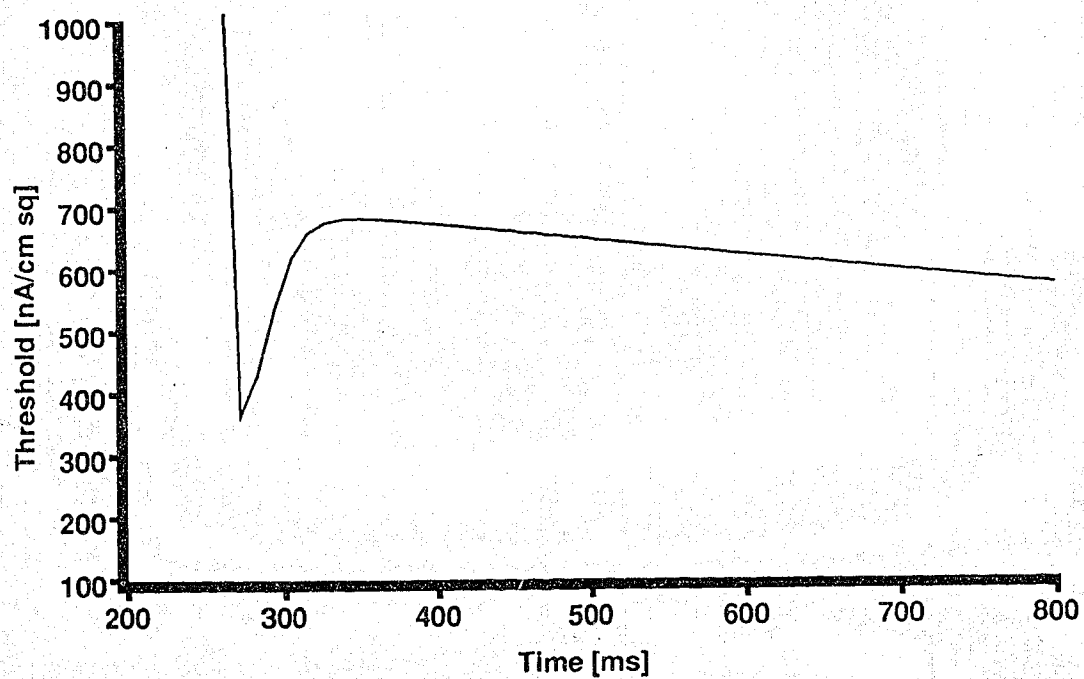
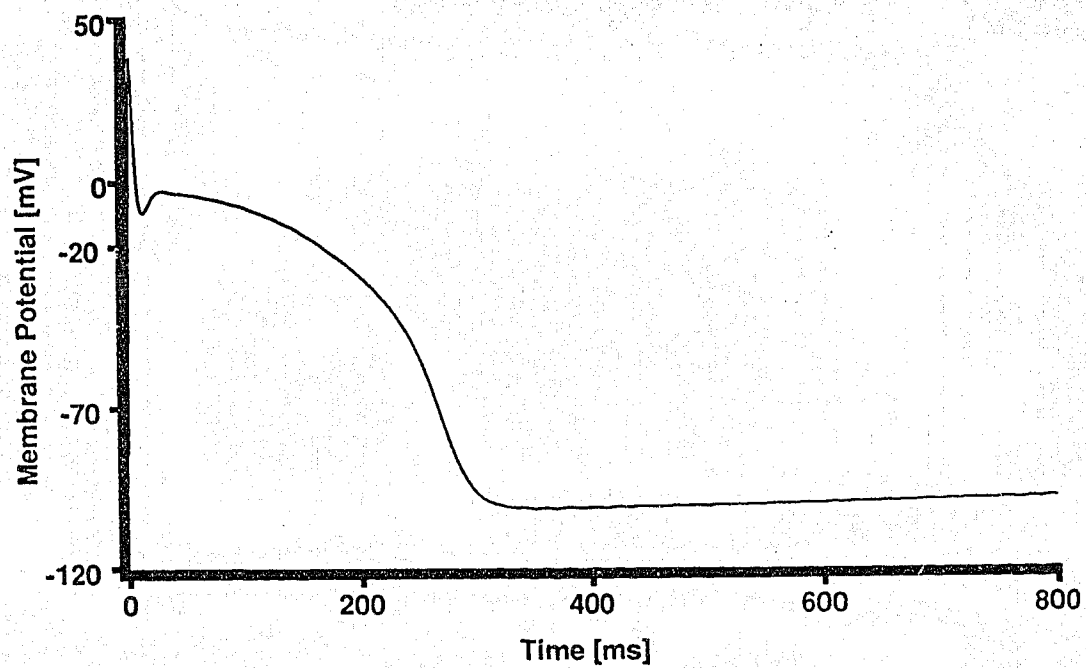
The MNT model for the Purkinje fiber action potential, as presented in the top trace of figure 25, looks similar to the published action potential (figure 4 of McAllister *et al.*, 1975). However, the MNT model is normally spontaneously active, and since no meaningful threshold test could be made in a spontaneously active membrane, $\overline{g_{Na,b}}$ was adjusted to maintain a stable resting membrane potential of -80 mV. There was still a long lasting afterhyperpolarization which is typical of *in vivo* recordings of Purkinje fiber action potentials (Draper & Weidmann, 1951) and the normal MNT model. $\overline{g_{Na,b}}$ was altered because a leakage current cannot possibly cause supernormal excitability.

A threshold test on the model (figure 25, bottom trace) showed that a period of increased excitability occurred between 272-340 ms.

Action potential of the MNT model and the period of relative excitability.

FIGURE 25. The top trace shows a computed membrane action potential for a Purkinje fiber using the MacAllister, Noble and Tsien (1975) model. The shape looks very much like the one in their 1975 paper. The spontaneous activity of this model was prevented by altering the conductance of the leakage current $I_{Na,b}$. There was a long period of afterhyperpolarization. The bottom trace shows the results of a threshold test initiated 250 ms after a normal action potential. Within the relative refractory period, there was a period of increased excitability even though it is not supernormal. This notch of relative excitability was observed from 272-340 ms.

Purkinje fiber action potential



682.13 nA/cm² while the steady state is 106.70 nA/cm². However, the notch observed in the excitability curve means that there is a region of lowered threshold within the refractory period. An effort was made to account for this phase of increased excitability.

Depicted in figure 26, top and bottom traces, are the currents which constitute the model. I_{qr} (chloride current) was back to its steady state as early as 250 ms and was therefore removed from the list of possible currents that might be causing this phase of increased excitability. No other current could be eliminated in this way. The remaining currents were either set to their steady state values or removed entirely if removal (at the notch phase) did not have any effect on the shape of the action potential.

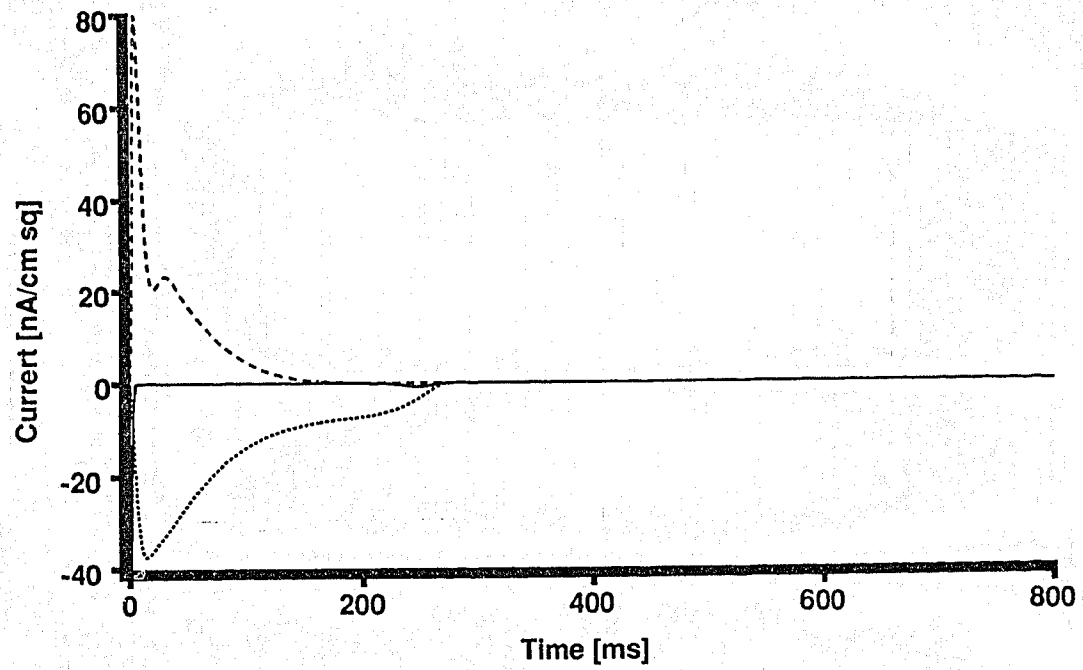
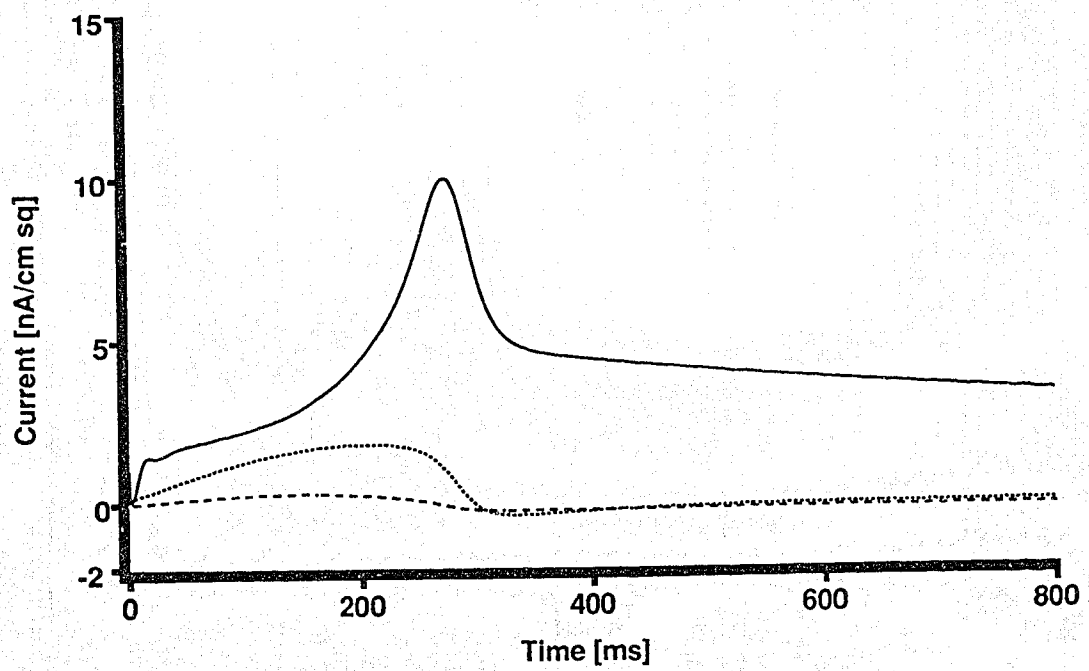
Figure 27 shows the effect of clamping the outward currents I_{x1} (top trace) and I_{x2} (bottom trace) to their steady state values. The phase of increased excitability remained essentially unchanged. Even though these two currents undershot their steady state values, they did not have any causal effect on the changes in the excitability of the membrane.

A profound increase in excitability was observed following the setting of I_{K2} to its steady state (figure 28, top trace). This was expected since, I_{K2} - an outward current - peaks within the time span of study. Hence reducing I_{K2} to its resting value increases the membrane excitability.

Since removal of the two inward currents, I_{si} and I_{Na} , at 250 ms

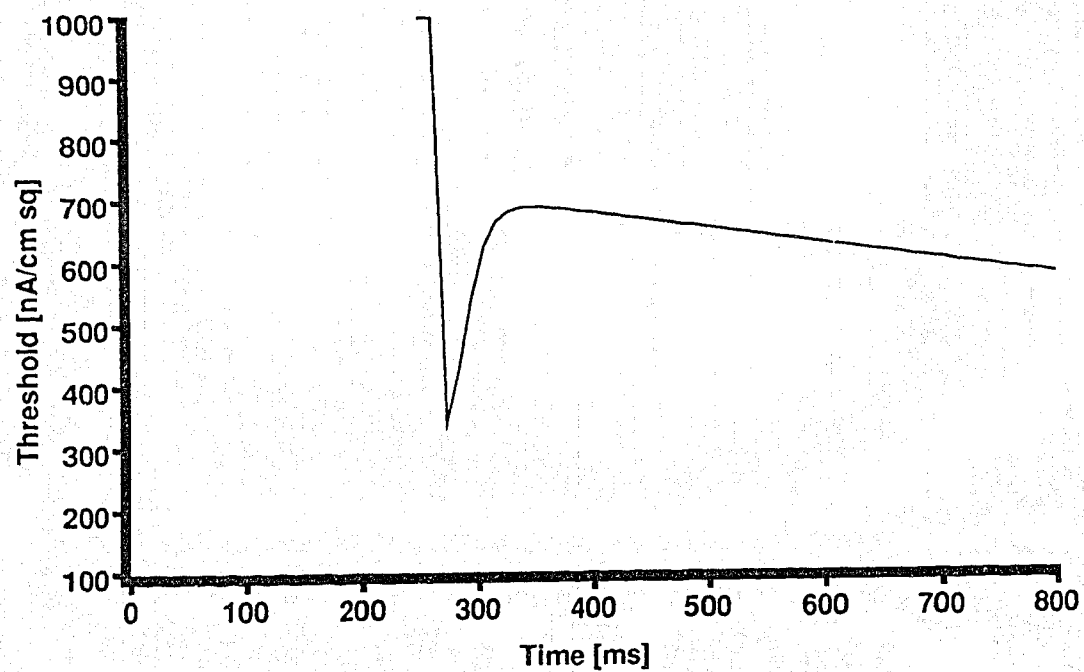
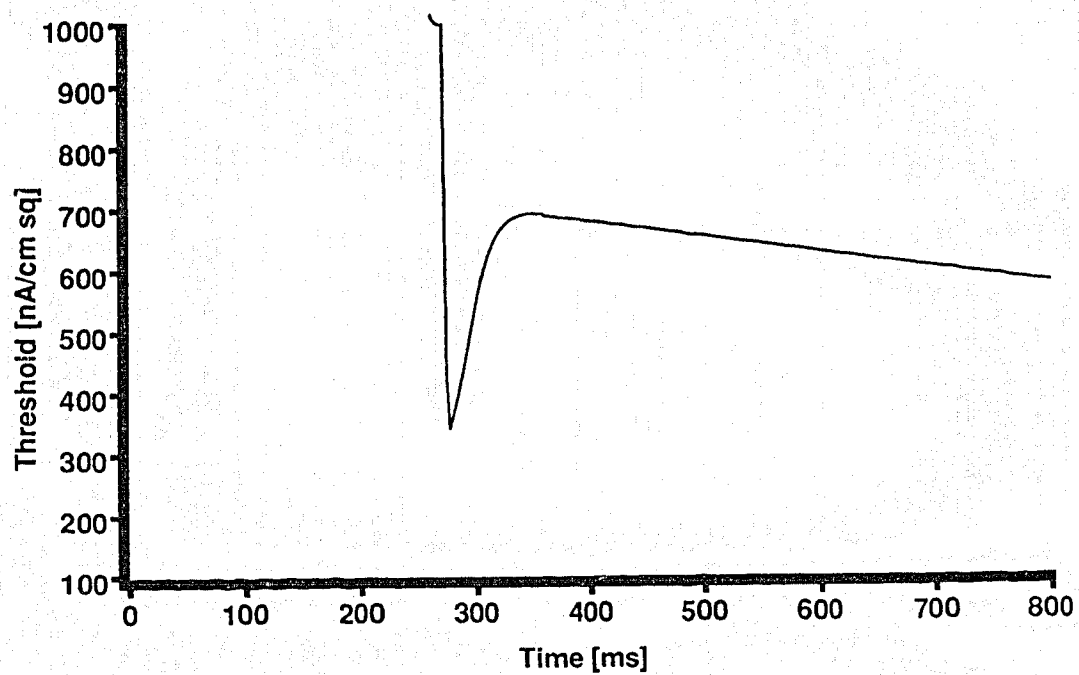
Time course of the ionic currents in the MNT model.

FIGURE 26. The figure shows the time courses of the ionic currents responsible for the action potential of Purkinje fibers. The upper trace depicts the sodium current, I_{Na} (solid line), calcium current, I_{si} (fine dashed line) and chloride current, I_{qr} (coarse dashed line). Note that there was a slight increase in I_{Na} from about 250-350 ms. The lower trace shows I_{K_2} (solid line), I_{x_1} (fine dashed line) and I_{x_2} (coarse dashed line). All three of these currents are carried by potassium.

Currents I_{Na} I_{si} I_{qr} Currents I_{K2} I_{X1} I_{X2} 

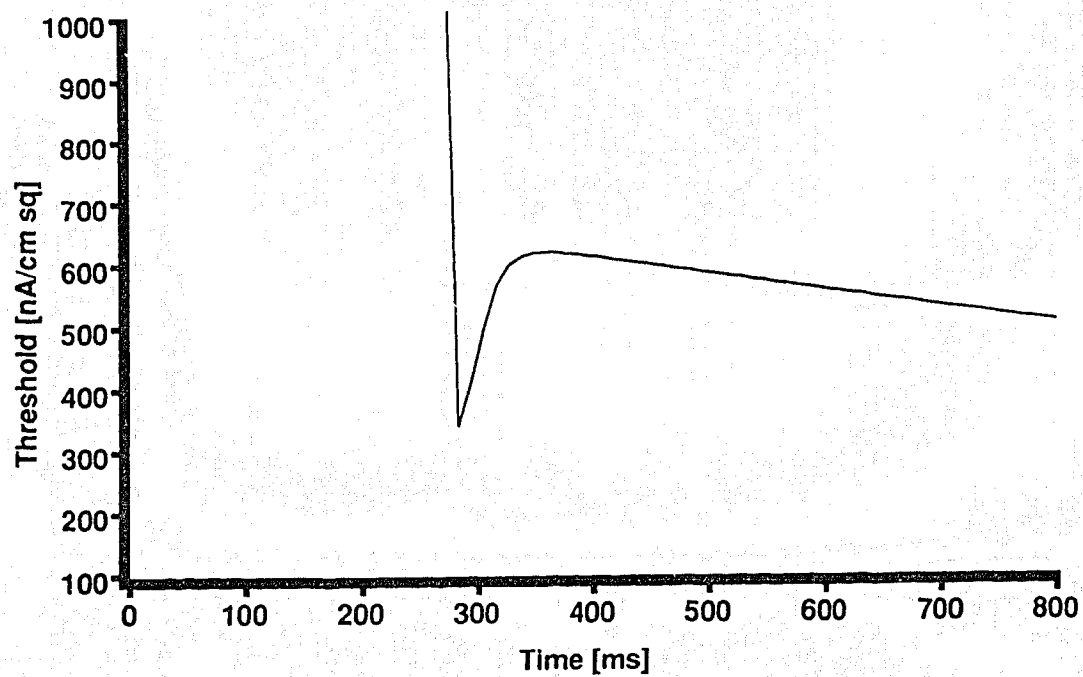
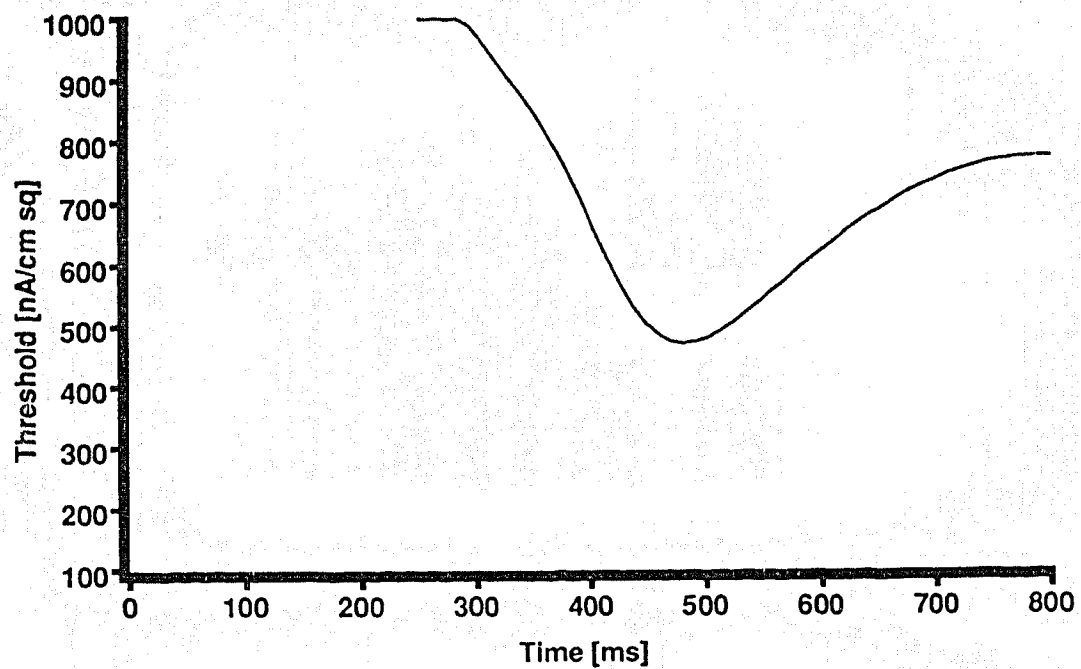
Effect of I_{x_1} and I_{x_2} on membrane excitability.

FIGURE 27. As tested in the other models I_{x_1} (upper trace) and I_{x_2} (bottom trace) were set to their steady state values beyond 250 ms following the initiation of a normal action potential. The threshold test was also begun at 250 ms. The excitability phase was not affected in any way.



Effect of I_{K2} and I_{si} on membrane excitability.

FIGURE 28. The notch in the excitability curve was enhanced when I_{K2} was treated as previously described (top trace). Setting I_{si} to zero at 250 ms had no effect on the shape of action potential (not shown) but slightly reduced the notch in the excitability curve (bottom trace).



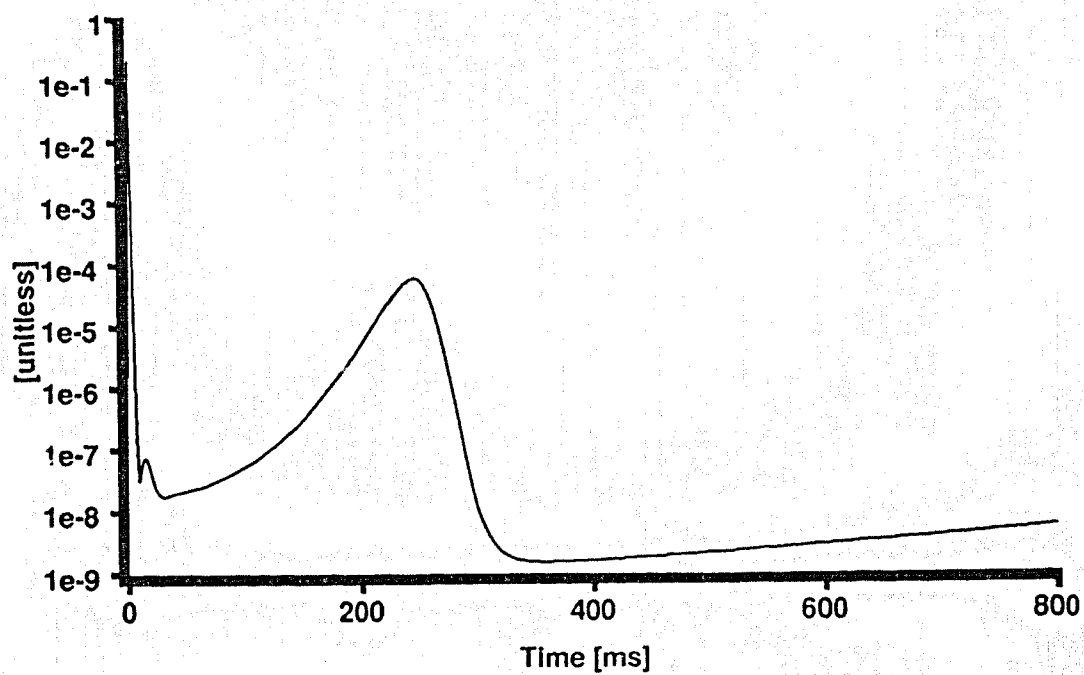
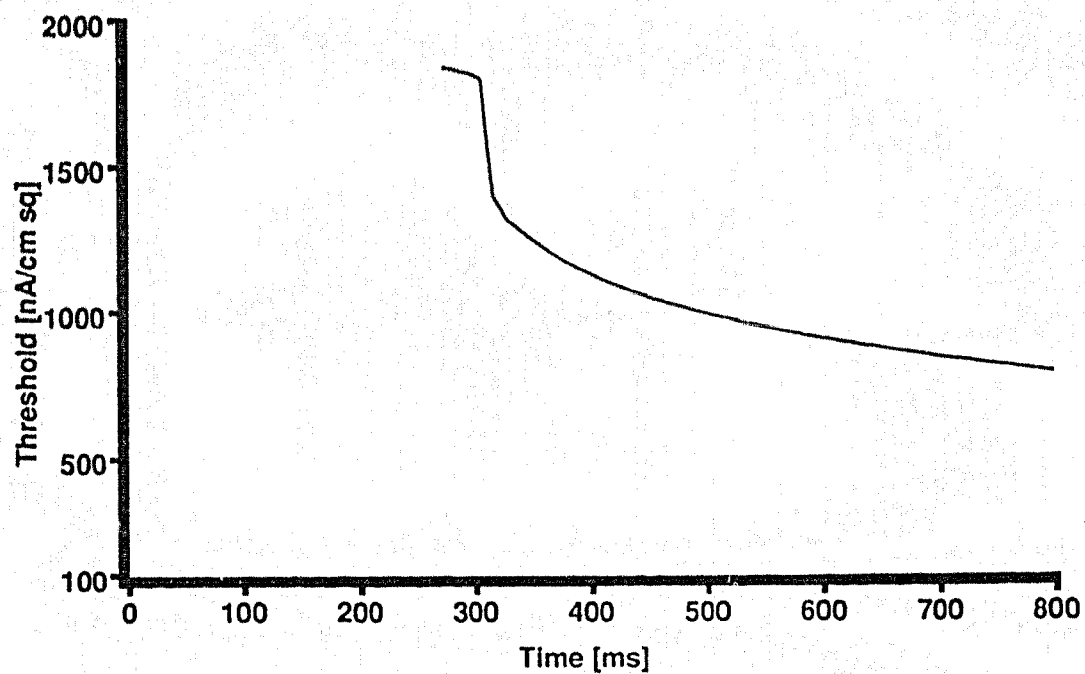
excitability.

Since removal of the two inward currents, i_{si} and I_{Na} , at 250 ms did not have any significant effect on the shape of the action potential, their values were set to zero at 250 ms. Elimination of I_{si} at 250 ms left the excitable phase virtually undisturbed, as shown in the lower trace of figure 28.

In contrast, removal of I_{Na} at this time abolished the excitability notch. *How did the sodium current affect the excitability notch?* The conductance of the I_{Na} is given by $m^3h\overline{g_{Na}}$. When m^3h was plotted against time (figure 29, bottom trace), it was noted that the conductance of I_{Na} peaked for a second time before returning to its steady state. The second increase in the conductance began before and lasted beyond the peak phase of I_{K2} . Hence a 'push-and-pull' phenomenon between inwardly directed sodium and outwardly directed potassium currents prevailed at this time and the phase of enhanced excitability was observed when the depolarizing effect of I_{Na} overcame the hyperpolarizing effect of I_{K2} .

The relative excitability in the MNT model resulted from an increased sodium conductance.

FIGURE 29. Removal of I_{Na} at 250 ms removed the notch observed in the refractory period of the MNT model for the Purkinje fiber action potential. In general, the excitability of the membrane was decreased under these conditions (upper trace). The lower trace shows that m^3h peaked for the second time after the initial spike. The time span during which the sodium current outweighed the opposing I_{K2} corresponded to the notch in the excitability curve.



IV. DISCUSSION

A. Supernormal period in the CWM model

Recently, Stockbridge (1988) has shown that the supernormal period in the Hodgkin and Huxley (1952) model for squid the giant axon results from slow potassium kinetics during the repolarization phase of the action potential. In this model it was observed that the conductance of the delayed rectifier fell below its steady state value during the SNP at a time when the inward current (I_{Na}) was back to its steady state. As a result there was a larger net inward current during this phase and application of a relatively smaller stimulus could bring the membrane to threshold (Stockbridge, 1988). The present project was undertaken to test the hypothesis that supernormal excitability in other neuron models occurs by a similar mechanism.

The present project demonstrated that the SNP in the crustacean motor neuron resulted from another potassium current, the transient potassium current. Here, the undershoot of the inactivation state variable, B , resulted in a decreased conductance of I_A following the action potential. Consequently, the cell remained more excitable compared to the steady state. The sequence used in this deduction follows:

- (1) The sodium current transiently peaked again during the falling phase of the action potential before gradually settling

to its steady state.

- (2) Sodium current was not responsible for the SNP because setting it to its steady state had little effect on the supernormal period.
- (3) The reversal potential of the leakage current was -17 mV, which made it an inward current when the membrane was close to the resting potential.
- (4) The leakage current did not play an active role in the SNP. However, it enhanced the SNP when set to its resting value since it behaved as an inward current during this phase of the action potential.
- (5) The delayed rectifier (I_K) neither overshoot nor undershot its steady state value during the repolarization phase of the action potential.
- (6) The delayed rectifier enhanced supernormality when multiplied by a factor less than 1 and it abolished the SNP when multiplied by 10. Under normal circumstances, therefore, this current opposed supernormal excitability.
- (7) The transient potassium current inactivation variable, B , undershot its resting value during the afterhyperpolarization. Furthermore, the activation variable, A , decreased from its peak during this phase. As a result, the conductance of the current undershot its resting value during the afterhyperpolarization.
- (8) Preventing B from its undershoot entirely eliminated the

undershoot in I_A and the supernormal excitability.

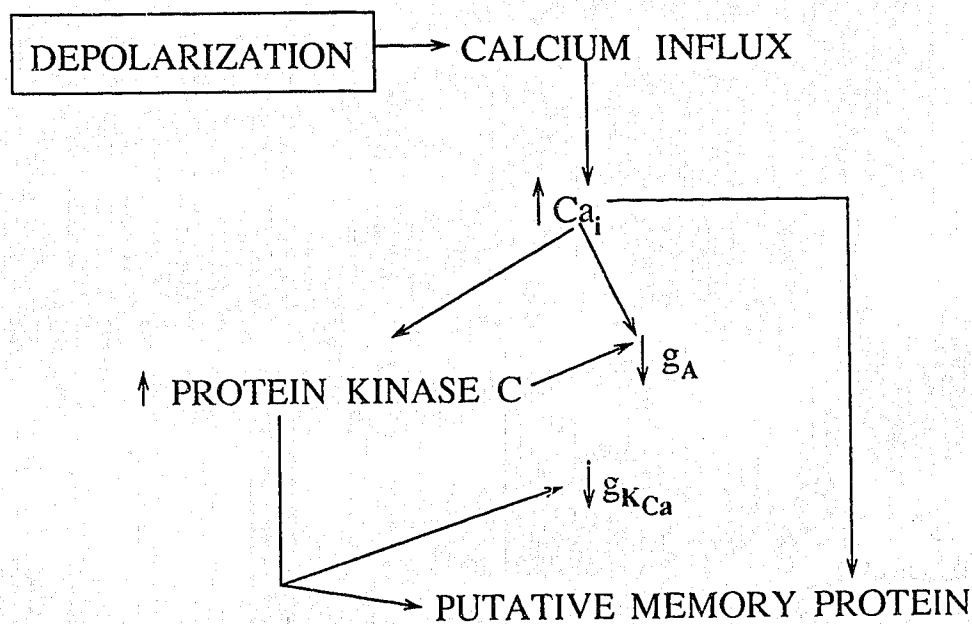
Thus, the sodium current did not have any significant influence on the SNP while the delayed rectifier opposed it. Supernormality resulted from the reduced outward current as a consequence of the undershoot of the conductance of the transient potassium current. With less outward current to overcome compared to the steady state, a stimulus less than the steady state threshold value was able to bring the membrane to the firing level.

The present observation supports the general hypothesis that supernormality results from an outward current remaining smaller than its steady state value for a period of time when the membrane potential and inward currents have returned to their resting states (Stockbridge, 1988). However, it differed from the Hodgkin-Huxley model in which potassium current was responsible for supernormality.

The reduction of the conductance of potassium currents following a spike may have a mechanistic role for the process of memory acquisition. Evidence obtained from studies on *Hermisenda crassicornis* indicates that depolarization of type B photoreceptors with light leads to a gradual reduction of the transient and calcium sensitive potassium currents (Alkon *et al.*, 1982; Alkon, 1986; West *et al.*, 1982). More importantly, it has been shown that this reduction of potassium currents is highly correlated with associative learning (Alkon, 1984; Alkon & Sakakibara, 1985). Calcium and other second messenger systems, *e.g.* protein kinase C (Sakakibara *et al.*, 1986b; Alkon & Rasmussen, 1988) might be involved in mediating these changes. However, the evidence is

preliminary. A reduction in potassium current should enhance calcium influx. Calcium, either directly or through the action of another second messenger system, can effect changes in the conductive properties of the potassium channel. Furthermore, calcium and second messengers may turn on genes responsible for the transcription of putative memory proteins (Alkon, 1987; Alkon & Rasmussen, 1988). Below is a diagram which shows how calcium can effect reduction in potassium currents.

Membrane depolarization results in calcium influx. Transient increase in intracellular calcium activates second messengers and enzymes e.g. protein kinase c. Through the action of calcium itself or the second messengers, the conductance of the potassium channels are reduced which results in increase excitability. It is believed that the above sequence of events may enhance the synthesis of putative memory proteins. KEY: ↓ Decrease; ↑ Increase.



In what way can we enhance the excitability or reduce potassium currents? The next discussion may give some glimpse of how this could be accomplished.

B. Repetitive Stimulation and SNP

How are transient changes in the intracellular concentration of calcium altered in response to different stimulus paradigms? Calcium influx is enhanced if the potassium current is delayed or if potassium currents are blocked by channel blockers (Llinas, 1982; Simon & Llinas, 1985).

In this project it has been shown that repetitive firing enhances supernormality. It has also been shown that supernormality arises as a consequence of potassium current reduction. Though not shown, it was found that the enhanced supernormality observed with repetitive stimulation was directly correlated with potassium current reduction. Thus the profound potassium current reduction which follows repetitive stimulation may enhance transient calcium influx to cause synaptic facilitation. Since many calcium-mediated activities depend on transient calcium influx one would expect that the bolus of calcium which enters the cell during the SNP following repetitive stimulation would be more effective than the calcium influx during a single action potential.

C. FH Model

One of the main motives in carrying out threshold tests on published mathematical models of excitable cells is to determine their validity in terms of the observed *in vivo* phenomena. Given this goal, the model should not only be consistent with the observed data but should be predictive as well. Failure to predict some of the *in vivo* phenomena would support suggestions that some of these models, especially the FH model, need to be modified to account for recent data (Hille, 1973). The results presented here showed that the inward current I_{Na} did not overshoot its steady state following a spike. Neither the delayed rectifier nor the nonspecific current showed any significant change in conductance which could be responsible for an enhancement of excitability. Although the nonspecific current decreased during the repolarization phase of a spike, this was not enough to remove the refractoriness of the membrane. It follows that supernormality was not predicted in the FH model.

What are the possible defects in this model? The FH model was based on certain assumptions, among which is the independence principle which is used in calculating the reversal potentials of ionic currents using Goldman-Hodgkin-Katz equations (Goldman, 1943; Hodgkin & Katz, 1949). Hille (1973) clearly showed that the potassium channels in the node of Ranvier of the frog are not entirely potassium selective and that

the reversal potential for I_K in this model may have to be reconsidered. Although the nonspecific current is attributed to potassium, calcium and sodium, the reversal potential used for this model is that of potassium alone. Other recent data (Hille, 1973, 1984) relates to the interpretation of the nonspecific current, which was extracted from the tail current of the delayed rectifier (FH, 1964; Hille, 1973, Armstrong & Hille, 1972). Hille (1973) suggested that the equation describing the delayed rectifier should be modified to account for its tail features rather than having a separate equation to describe it. Thus, one can appreciate why this model may be insufficient to account for all the observed properties of the frog myelinated nerves. The present results complement the suggestions by Hille (1973) and Armstrong & Hille (1972) that the FH model may not be a complete representation of the electrical activities of the frog myelinated nerve.

Axial current flow may alter the interpretation of the factors responsible for the SNP. If that were true, then a cable model would be the appropriate tool to study the SNP in myelinated nerves. For this reason, this work has not yet been extended to deal with recent a more recent myelinated nerve membrane model (Chiu *et al.*, 1979).

D. BR Model

The BR model was used to demonstrate that the SNP in the

ventricle resulted from the afterdepolarization which occurred following repolarization phase of the action potential. The afterdepolarization was caused by the undershoot of the outward potassium current I_{K1} . The reasoning used in our deduction was as follows:

- (1) The sodium current returned to the steady state condition before the initiation of the supernormal period. Thus, clamping the sodium current to its steady state did not alter supernormality.
- (2) The calcium current cannot have cause the SNP since no significant change in the supernormal notch was observed when it was set to its steady state.
- (3) The potassium current (I_{K1}) remained below its steady state value during the afterdepolarization phase of the action potential.
- (4) Removal of the undershoot of the potassium current abolished the afterdepolarization as well as supernormality. *Which of these causes supernormality: potassium current undershoot or afterdepolarization?* If the SNP resulted from the undershoot of potassium current alone, then clamping the membrane to the resting potential should not affect supernormality. On the other hand, if, upon clamping the membrane to the resting potential, supernormality were to be abolished without perturbing the potassium current undershoot, then the SNP was caused by afterdepolarization.

- (5) Forcing the membrane potential to the resting value during the threshold test eliminated the SNP while the undershoot of the potassium current persisted.
- (6) Over a broad range, the threshold current was linearly related to the membrane potential.

The cause of the SNP in the BR model is this: The undershoot of the potassium current results in the afterdepolarization. Consequently the membrane potential is brought closer to the threshold potential and a current less than the steady state value can elicit an action potential.

E. MNT Model

While the BR model exhibited supernormality, the MNT model did not. Instead, the latter showed a phase of increased excitability in the refractory period. Although the membrane excitability was not enough to be called supernormality, it was a time when an action potential could be more easily generated than it could earlier or later, and its etiology was investigated. This period of increased excitability resulted from an increase in sodium conductance as shown by the following:

- (1) Setting the outward currents (I_{x_1} and I_{x_2}) to their steady state values did not have any appreciable effects on the excitability notch. Therefore, the possible modulation of the SNP by these two currents was excluded.

(2) I_{K_2} , another outward current, reached its peak during the excitability phase. Being an outward current, it could not increase the excitability of the membrane at its peak. Rather, setting I_{K_2} to its steady state resulted in a profound increase in the excitability notch. Thus the factor responsible for this notch is in a 'push and pull' state with I_{K_2} .

(3) Both the inward currents, I_{Na} and I_{si} have not fully recovered from depolarization of the membrane at this phase of refractoriness, and yet removing these currents at this phase did not change the shape of the action potential. Elimination of I_{si} reduced the notch slightly. However, removal of I_{Na} abolished the excitability notch entirely.

(4) A plot of m^3h revealed that there was a second increase in the sodium conductance within the time span of the increased excitability.

Thus the period of relative excitability in the refractory phase of the MNT model action potential occurred as a result of the increase in the sodium conductance during this phase. The peak of the second sodium conductance increase did not coincide exactly with the time of minimum threshold because of the effect of the outward current I_{K_2} . As I_{K_2} fell from its peak, there was a time window in which the effect of I_{Na} outweighed the I_{K_2} effect. This was when the increase in the excitability in the refractory period occurred.

To what extent do these findings explain the mode of action of clinically used antiarrhythmic drugs? The class 1C antiarrhythmic drugs are sodium channel blockers (Harrison, 1985). In the presence of clinical doses of these drugs, the number of sodium channels blocked during an action potential must be increased. Consequently, a premature stimulus occurring at or near the end of membrane repolarization will encounter fewer activatable sodium channels in the presence of these drugs - making it less likely to elicit a premature action potential. The effectiveness of these drugs is correlated with their ability to prolong the effective refractory period (Campbell, 1983) relative to the action potential duration by delaying the recovery of the sodium channels from inactivation.

Another antiarrhythmic drug is quinidine - a potassium channel blocker (Hermann & Gorman, 1984; Iwatsuki & Petersen, 1985; Findley *et al.*, 1985; Kurachi *et al.*, 1987; Arena *et al.*, 1987). Presumably, the antiarrhythmic action of quinidine is a direct consequence of the elimination of supernormality - by removing the potassium current undershoot.

Arrhythmogenic agents such as the cardiac glycosides inhibit the electrogenic sodium-potassium pump. This results in membrane depolarization which make it more likely to initiate an abnormal beat.

F. Future studies

It may be possible to test for the basis of supernormal excitability in a space-clamped biological preparation. The sequence of steps would be (1) Develop a kinetic description of the cell's potassium conductance based on voltage clamp experiments, (2) to block these potassium currents using either ionic substitution or specific blockers such as 4-aminopyridine or tetraethylammonium, and (3) to current clamp using a waveform which is the sum of a depolarizing stimulus current and the expected potassium current based on the kinetic description previously obtained. Any undershoot in the supplied 'potassium conductance' then could be eliminated by a method analogous to the one employed in these models studies.

A similar approach, though not exactly the same, has been used to study synaptic transmission (Llinas, 1984). A recording of the calcium current in the squid presynaptic terminal was stored in a computer. Following that, calcium ions in the preparation medium were removed, the stored current was played back into the cell and calcium was injected into the synaptic through a microelectrode to study calcium evoked transmitter release.

G. Conclusion

This study demonstrated that: (i) Supernormality was predicted by the crustacean motor neuron and mammalian ventricular models. Supernormality in these models resulted from direct (crustacean neuron) or indirect (ventricle) consequences of slow potassium kinetics. The undershoot of the potassium conductance and the resulting increase in membrane excitability observed in the present studies further supports the hypothesis put forth by Stockbridge (1988) that supernormality results from slow potassium kinetics. (ii) Supernormality was not present in the frog myelinated axon and the Purkinje fiber models. The MNT Purkinje fiber model, however, exhibited a period of enhanced excitability resulting from an increased sodium conductance. This result is not consistent with Stockbridge's hypothesis.

VI. REFERENCES

Adrian, E. D. 1921. The recovery process of excitable tissues. Part 11. *J. Physiol.* **55**: 193-225.

Adrian, E. D & Lucas, K. 1912. On the summation of propagated disturbances in nerve and muscle. *J. Physiol.* **44**: 68-124.

Agha, A. S., Castillo, C. A., Castellanos, A., Myerburg, R. J., Tessler, M. P., 1972. Supernormal conduction in the human atria. *Circulation* **66**: 522-527.

Alkon, D. L., 1987. Memory traces in the brain. Cambridge Univ. Press New York. pp 87-108.

Alkon, D. L., 1986. Changes of membrane currents and calcium-dependent phosphorylation during associative learning. In *Neural mechanisms of conditioning*, Ed. D. L. Alkon and C. D. Woody. Plenum Press: New York & London. pp 3-18.

Alkon, D. L., 1984. Calcium-mediated reduction of ionic currents: A biophysical memory trace. *Science* **226**:1037-1045.

Alkon, D. L., Lederhendler, I., & Shoukimas, J. J., 1982. Primary changes of membrane currents during retention of associative learning. *Science* 215: 693-695.

Alkon, D. L., & Rasmussen, H., 1988. A spatial-temporal model of cell activation. *Science* 239: 998-1005.

Alkon, D. L. & Sakakibara, M. 1985. Calcium activates and inactivates a photoreceptor soma potassium current. *Biophys. J.* 48: 983-95.

Arena, A. P., McArdle, J. J., Argentieri, M. T., 1987. Antiarrhythmic-like actions of the smooth muscle spasmolytic agent, cinnamedrine, on action potentials of mammalian ventricular tissue. *Pharmacology* 34: 286-295.

Armstrong, C. M. & Hille. B. 1972. The inner quaternary ammonium ion receptor in potassium channels of the node of Ranvier. *J. Gen. Physiol.* 59: 388-400.

Arnsdorf, F. M. 1977. Membrane factors in arrhythmogenesis: concept and definitions. *Prog. Cardiovas. Dis.* 19: 413-429.

Bartesaghi, R. 1987. Supernormal excitability of fibers of the dorsal hippocampal commissure. *Exp. Neurol.* 96: 208-213.

Barrett, E. F. & Barrett, J. N. 1982. Intracellular recording from

vertebrate myelinated axons: mechanism of the depolarizing afterpotential. *J. Physiol.* **323**: 117-144.

Beeler, G. W. & Reuter, H. 1977. Reconstruction of the action potential of ventricular myocardial fibers. *J. Physiol.* **268**: 547-577.

Campbell, T. J. 1983. Kinetics of onset of rate-dependent effect of class I antiarrhythmic drugs are important in determining their effect on refractoriness in guinea-pig ventricle, and provide a theoretical basis for their subclassification. *Cardiovas. Res.* **17**: 344-352.

Chang, M-S., Milles, W. M., Prystowsky, E.N. 1987. Supernormal conduction in accessory atrioventricular connections. *Am. J. Cardiol.* **59**: 852-856.

Childers, R. W. Merideth, J & Moe, G. K. 1968. Supernormality in Bachmann's bundle: an *in vitro* and *in vivo* study in the dog. *Cir. Res.* **22**: 363-370.

Chiu, S. Y., Ritchie, J. M., Rogart, R. B., & Stagg, D. 1979. A quantitative description of membrane currents in rabbit myelinated nerve. *J. Physiol.* **292**: 149-166.

Chung, S. H., Raymond, S.A. & Lettvin, J.Y. 1970. Multiple meaning in single visual units. *Brain Behav. Evol.* **3**: 72-101.

Connor, J. A., Walter, D. & McKown, R. 1977. Neural repetitive firing: modification of the Hodgkin-Huxley axon suggested by experimental results from crustacean axons. *Biophys. J.* **18**: 81-102.

Cranfield, P. F. 1977. Action potential, afterpotentials, and arrhythmias. *Circ. Res.* **41**: 415-423.

Cranefield, P.F., Hoffman, B.F., & Siebens, A. A. 1957. Anodal excitation of cardiac muscle. *Am. J. Physiol.* **190**: 383-390.

DiFrancesco, D. & Noble, D. 1985. A model of cardiac electrical activity incorporating ionic pumps and concentration changes. *Phil. Trans. R. Soc. Lond. B* **307**: 353-398.

Domich, L., Delhay-Bouchaud, N. & Laget, P. 1986. Alterations of the functional properties of the parallel fibers in the cerebellum of the "scrapie mouse". *Arch. Ital. Biol.* **124**: 27-41.

Draper, M. H., & Weidmann, S. 1951. Cardiac resting and action potentials recorded with an intracellular electrode. *J. Physiol.*, **115**: 74-94.

Drouhard, J-Up & Roberge, F. A. 1986. Revised formulation of the Hodgkin-Huxley representation of the sodium current in cardiac cells. *Comp. Biomed. Res.* **20**: 333-350.

Drury, J., & Andrus, E. C. 1924. The influence of hydrogen-ion concentration upon conduction in the auricle of the perfused mammalian heart. *Heart* **11**: 389-403.

Eng, D. L., & Kocsis, J. D. 1987. Activity dependent changes in extracellular potassium and excitability in turtle olfactory nerve. *J. Neurophysiol.* **57**: 740-54.

Ferreira-Moyano, H. & Cinelli, A.R. 1986. Axonal projection and conduction properties of olfactory peduncle neurons in the armadillo. *Exp. Brain Res.* **64**: 527-534.

Findlay, I., Dunne, M. J., Ullrich, S., Wollheim, C. B. & Petersen, O. H. 1985. Quinine inhibits Ca^{2+} -independent K^{+} channels whereas tetraethylammonium inhibits Ca^{2+} -activated K^{+} channels in insulin-secreting cells. *FEBS Lett.* **185**: 4-8.

Fozzard, H. A. 1977. Cardiac muscle: Excitability and passive electrical properties. *Prog. Cardiovas. Dis.* **19**: 343-359.

Frankenhaeuser, B. & Huxley, A. F. 1964. The action potential in the myelinated nerve fiber of *Xenopus Laevis* as computed on the basis of voltage clamp data. *J. Physiol.* **171**: 302-315.

Fuchs, P. A. & Getting, P. A. 1980. Ionic basis of presynaptic inhibitory potential at crayfish claw opener. *J. Neurophysiol.* **43**: 1547-57.

Gardner-Medwin, A. R. 1971. An extreme supernormal period in cerebellar parallel fibers. *J. Physiol.* **224**: 357-371.

Goldman, D. E. 1943. Potential, impedance, and rectification in membranes. *J. Gen Physiol.* **27**: 37-60.

Goto, M. 1986. Depolarization-induced automaticity in the myocardium: its ionic mechanisms and relation to excitability changes. *Japan. J. Physiol.* **36**: 1-14.

Harrison, C. D. 1985. Antiarrhythmic drug classification: *New science and practical application.* **56**: 185-189.

Hermann, A. & Gorman, A. L. F. 1984. Action of quinidine on ionic currents of molluscan pacemaker neurons. *J. Gen. Physiol.* **83**: 919-940.

Hille, B. 1973. Potassium channels in myelinated nerve. Selective permeability to small cations. *J. Gen. Physiol.* **61**: 669-686.

Hille, B. 1984. *Ionic channels of excitable membranes.* Sinauer Assoc. Inc. Massachusetts. pp 69-242.

Hodgkin, A. L. & Huxley, A. F. 1952. A quantitative description of membrane current and its application to excitation and conduction in nerve. *J. Physiol.* **117**: 500-544.

Hodgkin, A. L. 1948. The local electrical changes associated with repetitive action in a non-medullated axon. *J. Physiol.* **107**: 165-181.

Hodgkin, A. L. & Katz, B. 1949. The effect of sodium ions on the electrical activity of the giant axon of the squid. *J. Physiol.* **108**: 37-77.

Hoff, H. E. & Nahum, L. H. 1938. The supernormal period in the mammalian ventricle. *Am J. Physiol.* **124**: 591-595.

Hoffman, B. F. & Cranefield, P. F. 1976. Electrophysiology of the heart. Futura Publishing Co. New York. pp 211-256.

Hoffman, B. F. & Rosen, R. M. 1981. Cellular mechanism for cardiac arrhythmias. *Cir. Res.* **49**: 1-15.

Iwatsuki, N. & Petersen, O. H. 1985. Inhibition of Ca^{2+} -activated K^{+} channels in pig pancreatic acinar cells by Ba^{2+} , Ca^{2+} , quinine and quinidine. *Biochim. Biophys. Acta* **819**: 249-257.

Joyner, W. R. & Capelle, F. J. L. 1986. Propagation through electrically coupled cells. *Biophys. J.* **50**: 1157-1164.

Sharp, G. H. & Joyner, W. R. 1980. Simulated propagation of cardiac action potential. *Biophys. J.* **31**: 403-424

Kocsis, J. D., Swadlow, H. A., Waxman, S. G. & Brill, M. H. 1979. Variation in conduction velocity during the relative refractory and supernormal periods: a mechanism for impulse entrainment in central axons. *Exp. Neurol.* **65**: 230-386.

Kocsis, J.D., & VanderMaelen, C.P. 1979. A supernormal period in central axons following single cell stimulation. *Exp. Brain Res.* **36**: 381-386.

Llinas, R.R. 1982. Calcium in synaptic transmission. *Sci. Am.* **247**: 56-65.

Lueken, B., & Schutz E. 1938. Die Relativerefraktarphase des Herzens, 3. Mitteilung: Reversibilitat und Antagonismus. *Z. Biol.* **99**: 186-197.

Mark, I., & Langendorf, R. 1950. Factors influencing the time of appearance of premature systoles (Including a demonstration of cases with ventricular premature systoles due to re-entry but exhibiting variable coupling). *Circulation.* **1**: 910

McAllister, R.E., Noble, D. Tsien, R. W. 1975 Reconstruction of the electrical activity of cardiac Purkinje fibers. *J. Physiol.*, **251**: 1-59.

McHenry, P. L., Knoebel, S. B., Fisch, C. 1966 The Wolff-Parkinson-White (WPW) syndrome with supernormal conduction through the anomalous bypass. *Circulation* 34: 734-739.

Merrill, E. G., Wall, P. D. & Yaksh, T. L. 1978. Properties of two unmyelinated fiber tracts of the central nervous system: lateral Lissauer tract and parallel fibers of the cerebellum. *J. Physiol.* 284: 127-145.

Moe, G. K. & Anzelevitch, CH. 1987. Reflection as a mechanism of reentrant cardiac arrhythmias. *Physiol. Bohem.* 36: 243-253.

Moe, G. K. Childers, R. W & Merideth, J. 1968. An appraisal of 'supernormal' A-V conduction. *Circulation.* 38: 5-28.

Noble, D. 1984. The surprising heart: a review of recent progress in cardiac electrophysiology. *J. Physiol.* 353: 1-50.

Owen, D. G., Segel, M. & Barker, J. L. 1986. Voltage-clamp analysis of a calcium- and voltage-dependent chloride conductance in cultured mouse spinal neurons. *J. Neurophysiol.* 55: 1115-1135.

Paleev, N. R., Kovaleva, L. I. & Nikiforova, T. B. 1986. Mechanism of occurrence of ventricular bigeminy. *Kardiologia.* 26: 40-44.

Rompere, P. Up & Miliaressis, E. 1987. Behavioral determination of

refractory periods of the brainstem substrates of self-stimulation. *Behav. Brain. Res.* **23**: 205-219.

Sakakibara, M., Alkon, D. L., Neary, J. T., Heldman, E., & Gould R. 1986b. Inositol triphosphate regulation of photoreceptor membrane currents. *Biophys. J.* **50**: 797-803.

Schmitt, F. O. & Erlanger, J. 1928. Directional differences in the conduction of the impulse through heart muscle and their possible relation to extrasystolic and fibrillary contractions. *Am. J. Physiol.*, **87**: 326-347.

Sharp, G. W. & Joyner. R. W. 1980. Simulated propagation of cardiac action potentials. *Biophys. J.* **31**: 403-424.

Simon, S. M. & Llinas, R. R. 1985. Compartmentalization of the submembrane calcium influx and its significance in transmitter release. *Biophys. J.* **48**: 485-98.

Spear, J.F. & Moore, E. N. 1974. Supernormal excitability and conduction in the His-Purkinje system of the dog. *Circ. Res.* **35**: 782-792.

Stein, R. B. 1966. The frequency of nerve action potentials generated by applied currents. *Proc. R. Soc. B.* **167**: 64-86.

Stockbridge, N. & Stockbridge, L. L. 1988. Differential conduction at

axonal bifurcations: effect of electrotonic length. *J. Neurophysiol.* **59**: 1277-1285.

Stockbridge, N. 1988. Differential conduction at axonal bifurcations: II. theoretical basis. *J. Neurophysiol.* **59**: 1286-1294.

Stockbridge, N. 1988. Etiology of supernormal period. *Biophysical. J.* (accepted for publication).

Swadlow, H.A. & Waxman, S.G 1976. Variations in conduction velocity and excitability following single and multiple impulses of visual callosal axons in the rabbit. *Exp. Neurol.* **53**: 128-150.

Swadlow, H.A. 1985. Physiological properties of individual cerebral axons studied *in vivo* for as long as one year. *J. Neurophysiol.* **54**:1346-1362.

West, A., Barnes, E. S., & Alkon, D. L. 1982. Primary changes of voltage responses during retention of associative learning. *J. Neurophysiol.* **48**: 1243-55.

Weidmann, S. 1955b. Effects of calcium ions and local anesthetics on electrical properties of Purkinje fibers. *J. Physiol.* **127**: 568-582.

Zucker, P. S., Lando, L. & Forgelson, A. 1986. Can presynaptic depolarization release transmitter without calcium influx? *J. de Physiol.*

(*Paris*) **81**: 237-245.

Zucker, R. S. 1973. Crayfish neuromuscular facilitation activated by constant presynaptic action potentials and depolarizing pulses. *J. Physiol.* **241**: 69-89.

Zucker, R. S. 1974. Excitability changes in crayfish motoneurons terminals. *J. Physiol.* **241**: 111-126.

V. APPENDIX

A. Outline of Map Program

The Map program began with an initiation step which involved computation of voltage dependent parameters. These values were stored in a table.

Given the current membrane potential, values in the table were taken to further the solution for the next time step.

An approximation was made for the integration of the differential equations using Runge Kutta method.

The individual currents were computed and the sum of all the currents, together with capacitance used to compute the voltage change.

B. Equations for CWM model

$$I_m = I_{Na} + I_K + I_A + I_L$$

$$I_{Na} = \overline{g_{Na}} m^3 h (V_m - E_{Na})$$

$$\frac{dm}{dt} = \alpha_m(1-m) + \beta_m$$

$$\alpha_m = \frac{-.1(V_m+29.7)}{e^{-.1(V_m+29.7)}-1}$$

$$\beta_m = 4 \frac{e^{-(V_m+54.7)}}{18}$$

$$\frac{dh}{dt} = \alpha_h(1-h) + \beta_h$$

$$\alpha_h = 0.07 \frac{e^{-(V_m+48)}}{20}$$

$$\beta_h = \frac{1}{e^{-.1(V_m+18)}+1}$$

$$I_K = \overline{g_K} n^4 (V_m - E_K)$$

$$\frac{dn}{dt} = \alpha_n(1-n) + \beta_n$$

$$\alpha_n = \frac{-.01(V_m+45.7)}{e^{-.1(V_m+45.7)}-1}$$

$$\beta_n = .125 \frac{e^{-(V_m+55.7)}}{80}$$

$$I_A = \bar{g}_A A^3 B (V_m - E_A)$$

$$A_\infty = \left[0.0761 \frac{e^{(V_m+94.22)/31.84}}{1+e^{(V_m+1.17)/28.93}} \right]^{1/3}$$

$$\tau_A = 0.3632 + \frac{1.158}{1+e^{(V_m+55.96)/20.12}}$$

$$B_\infty = \frac{1}{\left[1+e^{(V_m+53.3)/14.54} \right]^4}$$

$$\tau_B = 1.24 + \frac{2.678}{1+e^{(V_m+50)/16.027}}$$

$$I_L = g_L (V_m - E_L)$$

C. Equations for FH model

$$I_m = I_{Na} + I_K + I_p + I_L$$

$$I_{Na} = \overline{g_{Na}} m^3 h F_{Na}$$

$$\alpha_m = \frac{.36(V_m - 22)}{1 - e^{(22 - V_m)/3}}$$

$$\beta_m = \frac{.4(13 - V_m)}{1 - e^{(V_m - 13)/20}}$$

$$\alpha_h = \frac{.1(-10 - V_m)}{1 - e^{(V_m + 10)/6}}$$

$$\beta_h = \frac{4.5}{1 + e^{(45 - V_m)/10}}$$

$$F_{Na} = P_{Na}(EF^2)/(RT)(Na_o - Na_i) \frac{e^{(EF)/(RT)}}{1 - e^{(EF)/(RT)}}$$

$$I_K = \overline{g_K} n^2 F_K$$

$$\alpha_n = \frac{.02(V_m - 35)}{1 - e^{(35 - V_m)/10}}$$

$$\beta_n = \frac{.05(10 - V_m)}{1 - e^{(V_m - 10)/10}}$$

$$F_K = P_K(EF^2)/(RT)(K_o - K_i) \frac{e^{(EF)/(RT)}}{1 - e^{(EF)/(RT)}}$$

$$I_p = \overline{g_p} p^2 F_p$$

$$\alpha_p = \frac{.006(V_m - 40)}{1 - e^{(40 - V_m)/10}}$$

$$\beta_p = .09 \frac{(-25 - V_m)}{1 - e^{(V_m + 25)/20}}$$

$$F_P = P_P(EF^2)/(RT)(P_o - P_i) \frac{e^{(EF)/(RT)}}{1 - e^{(EF)/(RT)}}$$

D. Equations for BR model

$$I_m = I_{Na} + I_{K_1} + I_{x_1} + I_s$$

$$I_{Na} = \overline{g_{Na}} m^3 h j + g_{NaC} (V_m - E_{Na})$$

$$\alpha_m = \frac{-(V_m + 47)}{e^{-.1(V_m + 47)} - 1}$$

$$\beta_m = 40e^{-.056(V_m + 72)}$$

$$\alpha_h = .126e^{-.25(V_m + 77)}$$

$$\beta_h = \frac{1.7}{e^{-.082(V_m + 22.5)} + 1}$$

$$\alpha_j = .055 \frac{e^{-.25(V_m + 78)}}{e^{-.2(V_m + 78)} + 1}$$

$$\beta_j = \frac{.3}{e^{-.1(V_m + 32)} + 1}$$

$$I_s = \overline{g_s} df(V_m - E_s)$$

$$\alpha_f = .012 \frac{e^{-.008(V_m + 28)}}{e^{.15(V_m + 28)} + 1}$$

$$\beta_f = .0065 \frac{e^{-.02(V_m + 30)}}{e^{-.2(V_m + 30)} + 1}$$

$$\alpha_d = .095 \frac{e^{-.01(V_m-5)}}{e^{-.072(V_m-5)} + 1}$$

$$\beta_d = .07 \frac{e^{-.017(V_m+44)}}{1 + e^{.05(V_m+44)}}$$

$$I_{K_1} = .35 \left[\frac{(4e^{.04(V_m+85)} - 1)}{e^{.08(V_m+53)} + e^{.04(V_m+53)}} + \frac{.2(V_m+23)}{1 - e^{-.04(V_m+23)}} \right]$$

$$i_{x_1} = \bar{i}_{x_1} x_1$$

$$\alpha_{x_1} = .0005 \frac{e^{.083(V_m+50)}}{e^{.057(V_m+50)} + 1}$$

$$\beta_{x_1} = .0013 \frac{e^{-.06(V_m+20)}}{e^{-.04(V_m+20)} + 1}$$

$$\bar{i}_{x_1} = .8 \frac{e^{.04(V_m+77)} - 1}{e^{.04(V_m+35)}}$$

E. Equations for MNT model

$$I_m = I_{Na} + I_{si} + I_{qr} + I_{K_2} + I_{x_1} + I_{x_2} + I_{K_1} + I_{Na_b} + I_{Cl_b}$$

$$I_{Na} = \overline{g_{Na}} m^3 h (V_m - E_{Na})$$

$$\alpha_m = \frac{V_m + 47}{1 - e^{-.1(V_m + 47)}}$$

$$\beta_m = 9.86 e^{-(V_m + 47)/17.86}$$

$$\alpha_h = 1.13 \times 10^{-7} e^{-(V_m + 10)/5.43}$$

$$\beta_h = \frac{2.5}{e^{-(V_m + 10)/12.2} + 1}$$

$$I_{si} = \overline{g_{si}} df(V_m - E_{si}) + g'_{si}(V_m - E_{si}) d'$$

$$\alpha_d = .002 \frac{V_m + 40}{1 - e^{-(V_m + 40)}}$$

$$\beta_d = .02 e^{-(V_m + 40)/11.26}$$

$$\alpha_f = .000253 e^{-.04(V_m + 26)}$$

$$\beta_f = \frac{.02}{e^{-(V_m + 26)/11.49} + 1}$$

$$d' = \frac{1}{1+e^{-0.15(V_m+40)}}$$

$$I_{qr} = \overline{g_{qr}}qr(V_m - E_{Cl})$$

$$\alpha_q = .008 \frac{V_m}{1-e^{-.1V_m}}$$

$$\beta_q = .08e^{-V_m/11.26}$$

$$\alpha_r = 2.08 \times 10^5 e^{-.04(V_m+26)}$$

$$\beta_r = \frac{.02}{1+e^{-(V_m+26)/11.49}}$$

$$I_{K_2} = \overline{I_{K_2}}s$$

$$\overline{I_{K_2}} = 2.8 \frac{e^{.04(V_m+110)} - 1}{e^{.08(V_m+60)} + e^{.04(V_m+60)}}$$

$$\alpha_s = .001 \frac{V_m+52}{1-e^{-.2(V_m+52)}}$$

$$\beta_s = 5 \times 10^{-5} e^{-(V_m+52)/14.93}$$

$$I_{x_1} = \overline{I_{x_1}}x_1$$

$$\alpha_{x_1} = .0005 \frac{e^{.083(V_m+50)}}{.057e^{-(V_m+50)} + 1}$$

$$\beta_{x_1} = .0012 \frac{e^{-(V_m+20)/16.67}}{e^{-.04(V_m+20)} + 1}$$

$$I_{x_2} = \overline{I_{x_2}} x_2$$

$$\alpha_{x_2} = \frac{1.27 \times 10^{-4}}{1 + e^{-.2(V_m+19)}}$$

$$\beta_{x_2} = 3 \times 10^{-4} \frac{e^{-(V_m+20)}}{1 + e^{-.04(V_m+20)}}$$

$$I_{K_1} = (\overline{I_{K_2}}/2.8) + .2(V_m+30)/(1 - e^{-.04(V_m+30)})$$

$$I_{Na,b} = \overline{g_{Na,b}}(V_m - E_{Na})$$

$$I_{Cl,b} = \overline{g_{Cl,b}}(V_m - E_{Cl})$$